98030

WORLD BANK GROUP

ESMAP
Energy Sector Management Assistance Program

Solar Resource Mapping in Zambia

SOLAR MODELING REPORT

November 2014

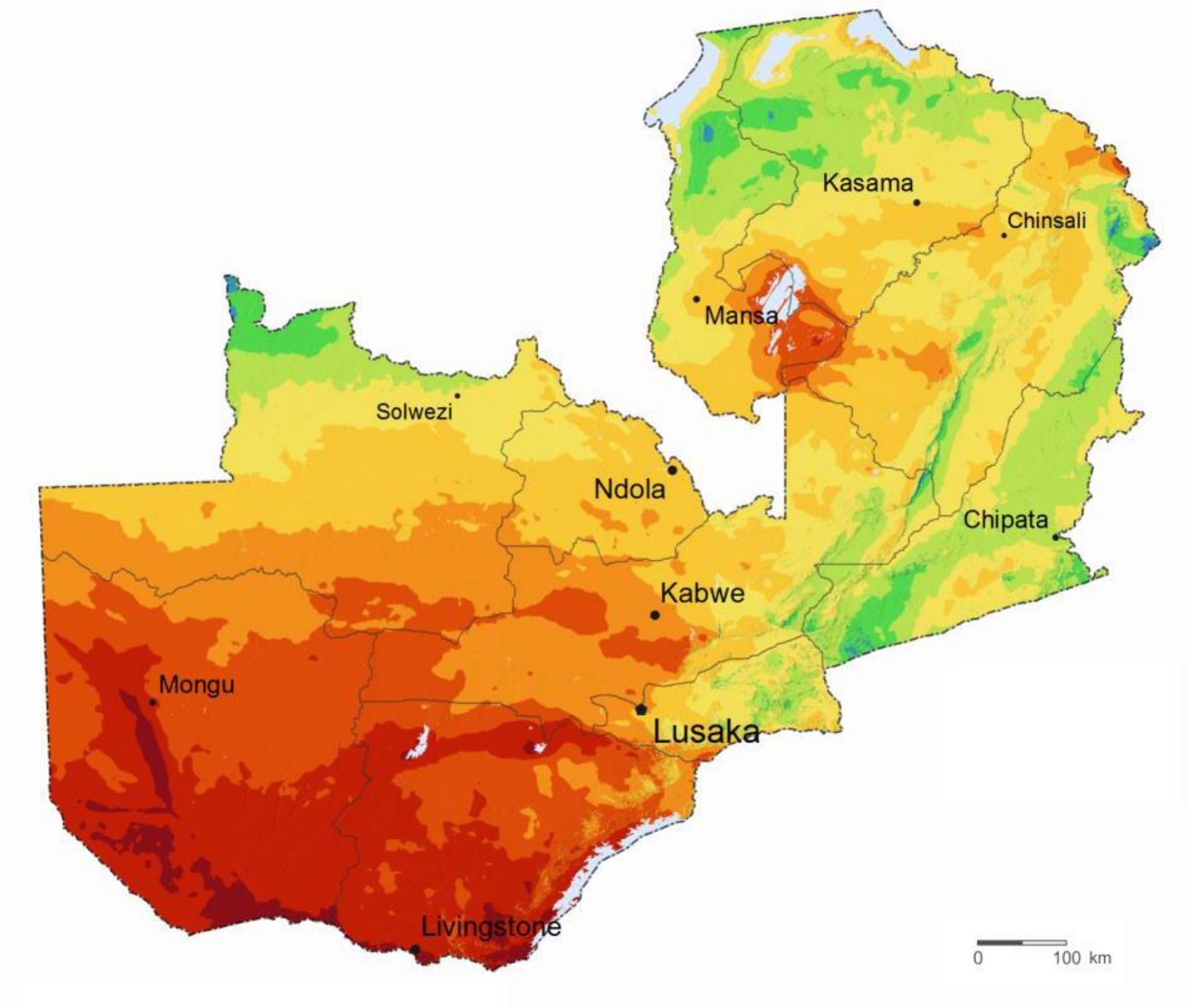

This report was prepared by Marcel Suri, Nada Suriova, Tomas Cebecauer, Artur Skoczek, Juraj Betak and Branislav Schnierer, GeoModel Solar (http://geomodelsolar.eu), under contract to the World Bank Group (WBG).

It is one of several outputs from the solar resource mapping component of the activity '*Renewable Energy Resource Mapping and Geospatial Planning – Zambia* [Project ID: P145271]. This activity is funded and supported by the Energy Sector Management Assistance Program (ESMAP), a multi-donor trust fund administered by the World Bank, under a global initiative on Renewable Energy Resource Mapping. Further details on the initiative can be obtained from the ESMAP website at http://www.esmap.org/.

This document is an **interim output** from the above-mentioned project, and the maps and visualizations presented are **preliminary and unvalidated**. Users are strongly advised to exercise caution when utilizing the information and data contained, as this has not been subject to full peer review. The final, validated, peer reviewed output from this project will be a Zambia Solar Atlas, which will be made available once the project is completed.

ESMAP Solar Resource Mapping for Zambia

Interim Solar Modelling Report

Renewable Energy Resource Mapping and Geospatial Planning – Zambia [P145271]

November 2014

GeoModel Solar, Pionierska 15, 831 02 Bratislava, Slovakia

http://geomodelsolar.eu

Reference No. (GeoModel Solar): 128-01/2014

TABLE OF CONTENTS

ACRONYMS

AERONET	The AERONET (AErosol RObotic NETwork) is a ground-based remote sensing network dedicated to measure atmospheric aerosol properties. It provides a longterm database of aerosol optical, microphysical and radiative parameters.
AOD	Aerosol Optical Depth at 670 nm. This is one of atmospheric parameters derived from MACC database and used in SolarGIS. It has important impact on accuracy of solar calculations in arid zones.
CFSR	Climate Forecast System Reanalysis. The meteorological model operated by the US service NOAA.
CPV	Concentrated PhotoVoltaic systems, which uses optics such as lenses or curved mirrors to concentrate a large amount of sunlight onto a small area of photovoltaic cells to generate electricity.
DIF	Diffuse Horizontal Irradiation, if integrated solar energy is assumed. Diffuse Horizontal Irradiance, if solar power values are discussed.
DNI	Direct Normal Irradiation, if integrated solar energy is assumed. Direct Normal Irradiance, if solar power values are discussed.
ECMWF	European Centre for Medium-Range Weather Forecasts is independent intergovernmental organisation supported by 34 states, which provide operational medium- and extended-range forecasts and a computing facility for scientific research.
GFS	Global Forecast System. The meteorological model operated by the US service NOAA.
GHI	Global Horizontal Irradiation, if integrated solar energy is assumed. Global Horizontal Irradiance, if solar power values are discussed.
GTI	Global Tilted (in-plane) Irradiation, if integrated solar energy is assumed. Global Tilted Irradiance, if solar power values are discussed.
MACC	Monitoring Atmospheric Composition and Climate – meteorological model operated by the European service ECMWF (European Centre for Medium-Range Weather Forecasts)
Meteosat MFG and MSG	Meteosat satellite operated by EUMETSAT organization. MSG: Meteosat Second Generation; MFG: Meteosat First Generation
NOAA NCEP	National Oceanic and Atmospheric Administration, National Centre for Environmental Prediction
NOCT	The Nominal Operating Cell Temperature, is defined as the temperature reached by open circuited cells in a module under the defined conditions: Irradiance on cell surface = 800 W/m^2, Air Temperature = 20°C, Wind Velocity = 1 m/s and mounted with open back side.
PVOUT	Photovoltaic electricity output, often presented as percentage of installed DC power of the photovoltaic modules. This unit is calculated as a ratio between output power of the PV system and the cumulative nominal power at the label of the PV modules (Power at Standard Test Conditions).
RSR	Rotating Shadowband Radiometer
STC	Standard Test Conditions, used for module performance rating to ensure the same measurement conditions: irradiance of 1,000 W/m^2, solar spectrum of AM 1.5 and module temperature at 25°C.
TEMP	Air Temperature at 2 metres

GLOSSARY

AC power output of a PV power plant	Power output measured at the distribution grid at a connection point.
Aerosols	Small solid or liquid particles suspended in air, for example clouds, haze, and air pollution such as smog or smoke.
All-sky irradiance	The amount of solar radiation reaching the Earth's surface is mainly determined by Earth-Sun geometry (the position of a point on the Earth's surface relative to the Sun which is determined by latitude, the time of year and the time of day) and the atmospheric conditions (the level of cloud cover and the optical transparency of atmosphere). All-sky irradiance is computed with all factors taken into account
Bias	Represents systematic deviation (over- or underestimation) and it is determined by systematic or seasonal issues in cloud identification algorithms, coarse resolution and regional imperfections of atmospheric data (aerosols, water vapour), terrain, sun position, satellite viewing angle, microclimate effects, high mountains, etc.
Clear-sky irradiance	The clear sky irradiance is calculated similarly to all-sky irradiance but without taking into account the impact of cloud cover.
Fixed-mounted modules	Photovoltaic modules assembled on fixed bearing structure in a defined tilt to the horizontal plane and oriented in fixed azimuth.
Frequency of data (15 minute, hourly, daily, monthly, yearly)	Period of aggregation of solar data that can be obtained from the SolarGIS database.
Installed DC capacity	Total sum of nominal power (label values) of all modules installed on photovoltaic power plant.
Longterm average	Average value of selected parameter (GHI, DNI, etc.) based on multiyear historical time series. Longterm averages provide a basic overview of solar resource availability and its seasonal variability.
PV electricity production	AC power output of a PV power plant expressed as percentual part of installed DC capacity.
Root Mean Square Deviation (RMSD)	Represents spread of deviations given by random discrepancies between measured and modelled data and is calculated according to this formula: $$RMSD = \sqrt{\frac{\sum_{k=1}^{n}(X^{k}{}_{measured} - X^{k}_{modeled})^{2}}{n}}$$ On the modelling side, this could be low accuracy of cloud estimate (e.g. intermediate clouds), under/over estimation of atmospheric input data, terrain, microclimate and other effects, which are not captured by the model. Part of this discrepancy is natural - as satellite monitors large area (of approx. 3 x 4 km), while sensor sees only micro area of approx. 1 sq. centimetre. On the measurement side, the discrepancy may be determined by accuracy/quality and errors of the instrument, pollution of the detector, misalignment, data loggers, insufficient quality control, etc.
Solar irradiance	Solar power (instantaneous energy) falling on a unit area per unit time [W/m^2]. Solar resource or solar radiation is used when considering both irradiance and irradiation.
Solar irradiation	Amount of solar energy falling on a unit area over a stated time interval [Wh/m^2 or kWh/m^2].

Spatial grid resolution	In digital cartography the term applies to the minimum size of the grid cell or in the other words minimal size of the pixels in the digital map
Uncertainty	Is a parameter characterizing the possible dispersion of the values attributed to an estimated irradiance/irradiation values. In this report, uncertainty assessment of the solar resource estimate is based on a detailed understanding of the achievable accuracy of the solar radiation model and its data inputs (satellite, atmospheric and other data), which is confronted by an extensive data validation experience. The second important source of uncertainty information is the understanding of quality issues of ground measuring instruments and methods, as well as the methods correlating the ground-measured and satellite-based data. In this study, the range of uncertainty assumes 80% probability of *occurrence* of values. Thus, the lower boundary (negative value) of uncertainty represents 90% probability of *exceedance*, and it is also used for calculating the P90 value.
Water vapour	Water in the gaseous state. Atmospheric water vapour is the absolute amount of water dissolved in air.

1 SUMMARY

Context

This Interim Modelling Report presents results of the World Bank's ESMAP Solar Resource Mapping project. The project in its Phase 1, conducts preliminary modelling of solar resources in the Republic of Zambia. These services are part of a technical assistance in renewable energy development, implemented by the World Bank in Zambia. They are being undertaken in close coordination with the Ministry of Energy and Water Development of Zambia, Department of Energy, the World Bank's primary country counterpart for this project.

The project is funded by the Energy Sector Management Assistance Program (ESMAP), a global knowledge and technical assistance program administered by the World Bank and supported by 11 bilateral donors. It is part of a major ESMAP initiative in support of renewable energy resource mapping and geospatial planning across multiple countries.

Objective and method

The objective of the project, in Phase 1, is to increase the knowledge of solar resource potential for solar energy technologies by producing a comprehensive data set based on satellite and meteorological modelling.

In Phase 1, SolarGIS model is used for preliminary mapping. Satellite-based and meteorological models are used for computing solar resource and meteorological data. These data are validated with ground measurements, available in a wider region.

Primary focus is on solar resources: Global Horizontal Irradiation (GHI) and Global Tilted Irradiation (GTI), used for an assessment of photovoltaic (PV) technology and on Direct Normal Irradiation (DNI), which is fuel for Concentrated Solar Power (CSP) and Concentrated Photovoltaics (CPV) technologies. Meteorological parameters, such as air temperature, wind and humidity are also delivered, as they have an impact on solar power plant operation and efficiency. In addition, photovoltaic (PV) power potential is calculated.

Geospatial data are delivered in a format suitable for Geographical Information Systems (GIS), and also as digital maps. For eleven sites, representing different geographic regions in Zambia, we delivered site-specific time series and TMY (Typical Meteorological Year) data. Methodology and results of the model validation are presented in the *Model Validation Report 128-02/2014.*

Data delivery

The following data products are delivered within this Interim Solar Modelling Report:

1. **GIS data and digital maps** for the whole territory of the Republic of Zambia, representing longterm monthly and yearly averages:
    - Raster digital data layers for Geographical Information System (GIS)
    - High resolution digital maps for poster printing
    - Medium resolution digital maps for presentations
    - Digital image maps for Google Earth and GIS
    - Support maps in vector data format for GIS
2. **Site specific data** at hourly resolution are prepared for 11 representative sites:
    - Time series, for detailed solar resource analysis
    - Typical Meteorological Year (TMY), for use in solar energy simulation software.

The deliveries for Phase 1 are designed to help effective development of solar energy strategies and projects in their first stages. The innovative features of the delivered data are:

- High-resolution, harmonized solar, meteorological and geographical data computed by the best available methods and input data sources;
- The data represent a continuous history of last 20 years (1994 to 2013);
- The models used are extensively validated by GeoModel Solar and by external organizations.

The data is supported by two expert reports:

- *Solar Modelling Report* (128-01/2014, this report), describing the methods and results of Phase 1 activities;
- *Solar Model Validation Report* (128-02/2014), describing the methods and results of data validation.

Phase 1 delivers data based on running the SolarGIS model without any support of region measurements. It is considered to follow up with this project, with two phases:

- Phase 2 will deploy and operate approximately six solar measuring stations in Zambia to collect high-quality site-specific solar and meteorological time series for adaptation or solar and meteorological models and for detailed analysis of solar climate at representative sites. This Phase is planned for at minimum 24 months;
- Phase 3 aims to combine site measurements with models, and to deliver a new version of the modelled data with reduced uncertainty.

Results

Interim Solar Modelling Report is divided into twelve chapters.

Solar radiation basics and collection of solar radiation data from different sources are described in Chapter 2. Characteristics and challenges of using modelled and ground-measured solar parameters are compared in Chapter 3.

Chapter 4 describes measurement and modelling approaches for developing reliable meteorological data at any site. Chapter 5 provides a link between solar resource and meteorological parameters and relevant solar technologies. An emphasis is given to photovoltaic (PV) technology, which has high potential for developing utility-scale projects close to larger consumption centres, as well as deployment of roof-top PV systems, off-grid, hybrid systems and minigrid applications for rural electrification.

Chapters 6 to 8 present developed solar resource and meteorological data in the form of maps. Six representative sites are selected to show potential regional geographical differences in the country through tables and graphs. Chapter 6 introduces support geographical data that influence deployment strategies and performance of solar power plants. Chapter 7 summarizes geographical differences and seasonal variability of solar resource in Zambia. Chapter 8 presents PV power generation potential, calculating theoretical specific PV electricity output from the most commonly used PV technology: fixed system with crystalline-silicon (c-Si) PV modules optimally tilted and oriented towards North.

The expected data uncertainty based on the validation exercise is summarized in Chapter 9. The complete methodology and detailed results can be consulted in the *Model Validation Report 128-02/2014*.

The provided solar resource information, evaluated in the context of other location criteria (geographical, demographic, infrastructural, logistic and other constraints and priorities) is a good starting point for building solar energy strategy in Zambia. Chapter 10 outlines the best practices of solar data use in all stages of a project development and operation. Chapters 11 and 12 summarize the technical features of the delivered items.

The Interim Solar Modelling Report, supported by the maps and site data for eleven representative sites, serve as an input for knowledge-based decisions targeting development of solar power. The Phase 1 outcomes show very good potential for exploitation of solar resources in Zambia, indicating good opportunities for photovoltaics but also for concentrated photovoltaics. Even though DNI resource is good, exploitation of solar thermal power plants (CSP) needs further analysis.

2 INTRODUCTION

2.1 Background

Solar electricity offers a unique opportunity, for each country worldwide, to achieve longterm sustainability goals, such as development of modern economy, healthy and educated society, clean environment, and improved geopolitical stability. Solar power plants exploit local solar resources; they do not require heavy support infrastructure, they are scalable, support diversification of power generation capacities, and improve electricity services. Important feature of solar electricity is that it is accessible also in remote locations, without access to electricity, thus giving unprecedented potential for development anywhere.

Solar resources are fuel to solar power plants and local geography and climate determine their operation. Free fuel makes solar technology very attractive; however effective investment and technical decisions require detailed and validated solar and meteorological data. Such data are also needed for the cost-effective operation of solar power plant and for management of solar power in the transmission and distribution grids. High quality solar resource and meteorological data are available today, and they are based on the use of the modern satellite, atmospheric and meteorological models and operational services.

This study describes methods, and outcomes of solar resource mapping, geographical and PV power potential analysis of Zambia.

2.2 Data needs

Solar resource directly determines how much electricity will be generated from solar power plants. Other meteorological parameters determine operating conditions of solar power plants. Thus, they are also important for accurate energy simulation.

A number of data sources are available in the region. These data sources offer heterogeneous information from various models and measurement campaigns. A number of data sources are static (with no regular update), often with limited information about applied methods and accuracy. Such situation poses risk to financing the solar electricity projects and does not encourage investments.

Professional development and operation of solar power plants needs solar resource and meteorological data, which have the following attributes:

- Solar and meteo data are based on the best available and scientifically-proven models, and the most accurate and detailed input data (satellite, atmospheric and meteorological);
- Models are able to deliver harmonized and seamless historical data (for the project development), and systematically updated data (for project operation and for management of electrical grid);
- Historical data should represent long time period, optimally recent 20 or more years;
- Models should provide geographically continuous data, covering the whole territory in high resolution:
    - Temporal resolution of 15 to 30 minutes at the level of a site;
    - Spatial resolution of derived aggregated maps of 4 km or more detailed;
- Standardized site-specific and map products should make the data easy to access and use;
- Systematic operation of the models and measuring stations should be able to deliver data for:
    - Data quality control and model adaptation based on local measurements
    - Monitoring, performance assessment and forecasting of solar power plants and electrical grid

- Data and maps should be supported by technical information and consultancy.

This project aims to deliver the solar resource and meteorological data fulfilling the above listed criteria.

Solar and meteorological data are needed in all stages of development and operation of solar power plants:

1. Prospection, prefeasibility and site selection;
2. Project assessment, engineering, technical design and financing;
3. Monitoring and performance assessment of solar power plants and forecasting of solar power;
4. Quality control of solar measurements.

Tab. 2.1 shows which data are needed in different stages of solar project lifetime, and how they are implemented in solar resource analysis and energy simulation. Solar Resource Mapping in Zambia supports first two stages of solar development (marked by red box). Parameters delivered as map data and site-specific data products for Zambia are specified in Tab. 2.2.

Tab. 2.1: Overview of solar and meteorological data needed in different stages of a solar energy project

		Maps and GIS data		Time series					TMY	
		LTA/monthly	Operational	15' (30')	Hourly	Daily	Monthly	Yearly	P50	P90 and Pxx
1	Prefeasibility	x					x	x		
	Site selection	x					x	x	x	
2	Project first assessment						x	x	x	
	Engineering and project design			x	x				x	x
	Financial modelling			x	x		x	x	x	x
3	Performance assessment	x	x	x	x	x	x			
	Monitoring		x	x	x	x				
	Forecasting		x	x	x					
4	Quality control of solar measurements		x	x	x					

Note: LTA = Longterm averages, P50 = probability of exceedance 50%, P90 = probability of exceedance 90%

Tab. 2.2: Solar and meteorological data parameters delivered for Zambia

Parameter	Acronym	Unit	GIS data and maps	Site-specific time series	Site-specific Typical Meteorological Year
Global Horizontal Irradiation	GHI	W/m^2	x	x	x
Direct Normal Irradiation	DNI	W/m^2	x	x	x
Global Tilted Irradiation	GTI	W/m^2	x	x	-
Diffuse Horizontal Irradiation	DIF	W/m^2	x	x	x
Air Temperature at 2 metres	TEMP	°C	x	x	x
Wet Bulb Temperature	WBT	°C	-	x	x
Relative Humidity	RH	%	-	x	x
Wind Speed at 10 metres	WS	m/s	-	x	x
Wind Direction at 10 metres	WS	°	-	x	x
Atmospheric Pressure	AP	hPa	-	x	x

3 MEASURING AND MODELLING SOLAR RESOURCE

3.1 Solar basics

The interactions of extra-terrestrial solar radiation with the Earth's atmosphere, surface and objects are divided into four groups (Fig. 3.1):

1. Solar geometry, trajectory around the sun and Earth's rotation (declination, latitude, solar angle)
2. Atmospheric attenuation (scattering and absorption) by:
    - 2.1 Atmospheric gases (air molecules, ozone, NO_2, CO_2 and O_2)
    - 2.2 Solid and liquid particles (aerosols) and water vapour
    - 2.3 Clouds (condensed water or ice crystals)
3. Topography (elevation, surface inclination and orientation, horizon)
4. Shadows, reflections from surface or local obstacles (trees, buildings, etc.) and re-diffusion by atmosphere.

The atmosphere attenuates solar radiation selectively: some wavelengths are associated with high attenuation (e.g. UV) and others with a good transmission. Solar radiation called "short wavelength" (in practice, 300 to 4000 nm) is of main interest to solar power technology. The component that is neither reflected nor scattered, and which directly reaches the surface, is called *direct radiation*; this is the component that produces shadows, and can be concentrated with solar concentrator. Component scattered by the atmosphere, and which reaches the ground is called *diffuse radiation*. Small part of the radiation reflected by the surface and reaching an inclined plane is called the *reflected radiation*. These three components together create *global radiation*.

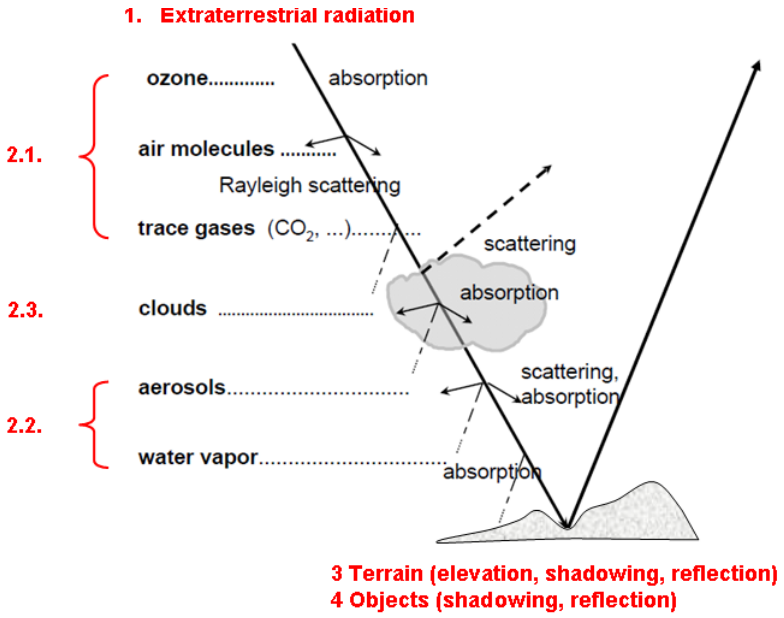

Fig. 3.1: Interaction of solar radiation with the atmosphere and surface.
The red numbers refer to the paragraphs below, in which the corresponding effects are discussed.

Extra-terrestrial radiation (**1**) reaching the top of the Earth's atmosphere above the point on surface depends on the position of the Sun, and varies as a function of the day during the year. This radiation can be accurately calculated using the solar geometry and astronomical equations. In an annual average, extra-terrestrial radiation corresponds approximately to the "solar constant", whose value has been recently estimated at 1362.2 W/m^2 [1]. Solar activity leads to maximum variations of ± 0.5% around this mean value, but in practice these variations are not taken into account.

During its passage through the atmosphere, the radiation is attenuated by components such are gases, liquid and solid particles and clouds. The path length of Sunrays throughout the atmosphere is length is evaluated relatively in dependence on the thickness of the atmosphere above the considered site. This dimensionless relation is called "air mass" or "relative optical air mass". By definition, it has a value of 1 for a sun at zenith (AM1). The air mass "zero" (AM0) is an abstraction commonly used to refer to extra-terrestrial conditions. The air mass varies according to the position of the Sun; it changes during the day and the year. At sunrise and sunset, it reaches its maximum value of ≈36. Due to its dynamic nature and complex interactions, the atmospheric attenuation cannot be modelled precisely at any time.

The so-called uniformly mixed **atmospheric gases** (**2.1**) are the components whose concentration is considerably constant throughout the thickness of the atmosphere. The spatial and temporal variability of these gases (N_2, O_2, N_2O, CH_4, CO, CO_2, etc.) can be considered negligible for all practical purposes. (Even if the CO_2 concentration increases steadily, its effect on the solar radiation of short wavelengths is negligible.) Their optical attenuation can be modelled with a good accuracy. Ozone (O_3) has a variable concentration but it only has a slight influence on broadband solar radiation. On the other hand, effect of ozone is pronounced in the UV, for wavelengths below 300 nm.

The presence of solid and liquid particles determines the atmospheric turbidity, in other words, the optical density of atmosphere caused by the effect of aerosol scattering. This is considerably higher than scattering caused by the Rayleigh effect on gas molecules, which creates the blue colour of the clear sky. An old definition of turbidity (introduced by Linke in 1922) included the effect of absorption of water vapour, for the sake of simplicity. This amalgam of two very different phenomena does not allow precise calculations, and therefore its use is in modern calculations disconnected (in SolarGIS, water vapour and aerosols are treated separately).

The turbidity of the atmosphere is a direct function of its concentration by **aerosols** (**2.2**), which have high temporal and spatial variability. Aerosols are normally concentrated in the lower layers of the atmosphere. Large volcanic eruptions can inject large amounts of aerosols into the upper atmosphere, occasional occurrence of which must be also taken into account. High local concentration of aerosols leads to the "haze" and a gradual reduction of horizontal visibility. In such conditions, the sky (usually blue) has colour closer to white, and takes a milky consistency (it is turbid). Diffuse radiation, which is normally low under a blue sky, is – in the presence of high concentration of aerosols – very intensive. The optical effect of attenuation by aerosol is most often measured by a quantity called "Aerosol Optical Depth" (AOD).

Similarly to aerosols, **water vapour** (**2.2**) is concentrated in the lower layers of the atmosphere, and is very variable in time and space. From a climate perspective, dry regions normally have little water vapour, while humid regions have high concentrations. The quantity of water vapour is measured by "the thickness of condensable water" (Precipitable water, PW). Water vapour is invisible, and its absorption occurs in the infrared, so it cannot be visually detected. This is opposite to the aerosol extinction, which occurs mainly in the visible and UV spectrum.

The maximum direct radiation is reached when the sky is cloudless and the atmosphere is "clean and dry", in other words that it contains little of aerosols and water vapour. Gradually, as their concentration increase, the direct radiation weakens. It also weakens when the air mass increases, so when the Sun is closer to the horizon.

As mentioned above, the interaction between radiation and atmospheric constituents is considerably complex. Some effects, such as Rayleigh molecular diffusion, absorption by mixed gas or ozone, are well known and do not pose a significant problem in modelling. On the contrary, all effects associated with variable attenuation (clouds, aerosols, and – to a lesser extent – water vapour) remain difficult to model accurately due to the lack of reliable observations with sufficient spatial and temporal resolution throughout the world.

Majority of an attenuation effect is usually determined by **clouds** (**2.3**). In operational numerical models, it is simulated by empirical equations using satellite data. In comparison with all the other effects of atmospheric attenuation, the uncertainty (potential error) of the impact of clouds is the most important. The most difficult cases for modelling are those with scattered and intermittent cloud cover.

Radiation that finally reaches the ground is also influenced by local **topography** (**3**). The altitude above sea level determines the relative thickness of the atmosphere, and thus the amount of radiation attenuated by scattering and absorption. The slope and obstructions on the horizon determine access to direct, diffuse and

reflected radiation. On a smaller scale, a similar role is played by **natural or artificial obstacles** such as trees, buildings, etc. (**4**). This type of attenuation can be measured accurately as long as the geometry of these obstacles and their reflectance are known.

According to the generally adopted terminology (project MESoR, IEA SHC Tasks 36 and 46), the two terms are used in the field of radiation of short wavelengths:

- **Irradiance** indicates power (instant energy) per second incident on a surface of 1 m^2 (unit: W/ m^2).
- **Irradiation**, expressed in MJ/ m^2 or Wh/m^2 it indicates the amount of incident solar energy per unit area during a lapse of time (hour, day, month, etc.).

Often, the term *irradiance* is used by the authors of numerous publications in both cases, which can be sometimes confusing.

In **solar energy applications**, the following conventions are commonly used:

- **Direct Normal** Irradiation/Irradiance (DNI): it is the direct solar radiation from the solar disk and the region closest to the sun (circumsolar disk of 5° centred on the sun). DNI is component that is involved in thermal (concentrating solar power, CSP) and photovoltaic concentration technology (concentrated photovoltaic, CPV).
- **Global Horizontal** Irradiation/Irradiance (GHI): sum of direct and diffuse radiation received on a horizontal plane. GHI is a reference radiation for the comparison of climatic zones; it is also essential parameter for calculation of radiation on a tilted plane.
- **Global Tilted** Irradiation/Irradiance (GTI), or total radiation received on a surface with defined tilt and azimuth, fixed or sun-tracking. This is the sum of the scattered radiation, direct and reflected. In the case of photovoltaic (PV) applications, GTI can be occasionally affected by shadow.

Solar resource can be modelled by satellite-based solar models or measured by ground-mounted sensors. **Ground-mounted sensors** are good in providing high frequency and accurate data (for well-maintained, high accuracy measuring equipment) for a given site. **Satellite-based models** provide data with lower frequency of measurement, but representing long history over lager territories. Satellite-models are not capable to produce instantaneous values at the same accuracy as ground sensors, but can provide robust aggregated values.

Chapter 4 summarizes approaches for measuring and computing these parameters, and the main factors and sources of uncertainty. The most effective approach is to correlate multiyear satellite time series with data measured locally over short period of time (at least one year) to reduce uncertainty and achieve more reliable estimates.

3.2 Satellite-based models: SolarGIS approach

Numerical models using satellite and atmospheric data on the input became a standard for calculating solar resource time series and maps. The same models are also used for real-time data deliveries for monitoring and forecasting.

Reliable solar models exist today. A good description of the current approaches can be consulted in [1]. The state-of-the-art approaches have the following features:

- Use of modern models based on sound theoretical grounds, which are consistent and computationally stable;
- Use of modern input data: satellite and atmospheric. These input data are systematically quality-controlled and validated;
- Models and input data are integrated and regionally adapted to perform reliably at a wide range of geographical conditions.

Satellite-based irradiance models range from physically rigorous to purely empirical. At the one end, physical models attempt to explain observed earth's radiance by solving radiative-transfer equations. **Physical models** require precise information on the composition of the atmosphere and also depend on accurate calibration from the satellite sensors. At the other end **empirical models** may consist of a simple regression between the satellite visible channel's recorded intensity and a measuring station at the earth's surface. Today, all operational approaches are based on the use of **semi-empirical models**: they use a simple radiative-transfer approach and some degree of fitting to observations.

Old approaches are typically less elaborated, thus cannot reach the accuracy of the modern models. Even if the models are based on similar principles, differences in implementation may result in different outputs. Already today, the information value of the satellite and atmospheric input data used by these models is very high, and most of it still remains unexploited, thus providing space for future improvements. In this study we applied SolarGIS model, which is operated by GeoModel Solar and applied for routine calculation of high-resolution global database of solar resource and also meteorological parameters.

3.2.1 SolarGIS calculation scheme

In operational data calculations, semi-empirical models are used, in which the algorithms are simplified (in comparison to physical models). However, even semi-empirical models consider most of the physical processes of atmospheric attenuation of solar radiation and use some physical parameters on the input. Therefore, this approach is capable to reproduce real situations. In satellite-based solar radiation models, the data form meteorological satellites are used for identification of *cloud properties*, while the *atmospheric properties* are traditionally derived from meteorological models or measurements.

The simplification of algorithms is also driven by the availability of the input data. For example, the aerosols due to diverse chemical composition and particle size may have different optical properties, but the data describing these properties are in general not available (except for limited number of sites). Thus in the semi-empirical models, the aerosols are represented only by one or two parameters, characterizing their properties in an aggregated way with limited accuracy.

SolarGIS model generates updated solar resource data globally, for the land surface between 60º North and 50º South latitudes. The solar resource annual maps are prepared by aggregation of 15 and 30-minute time series. The maps for Zambia cover a period 1994 to 2013, i.e. they represent longterm average of last 20 years.

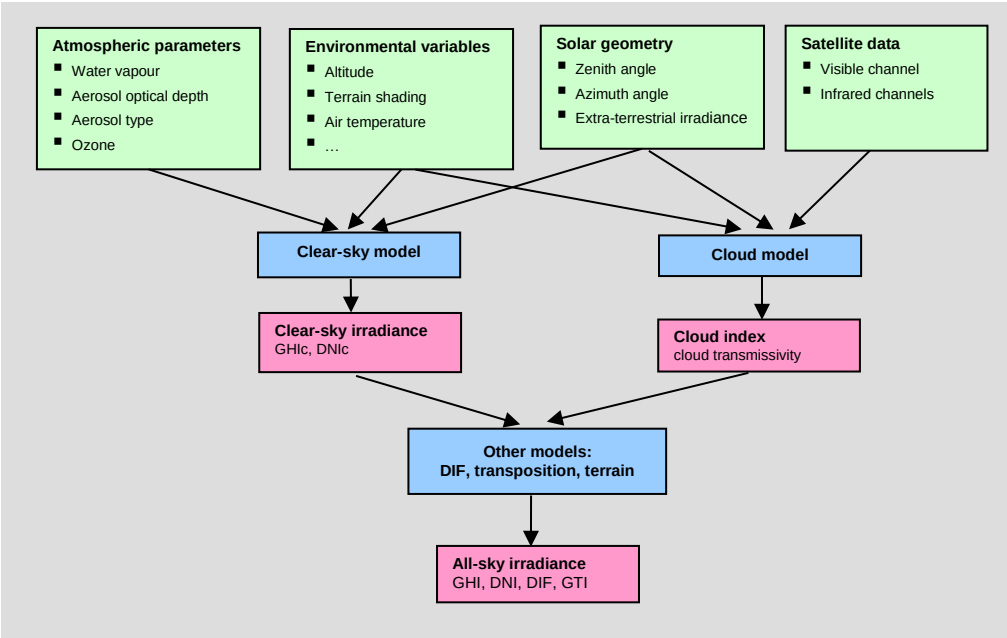

Fig. 3.2: Scheme of the semi-empirical solar radiation model (SolarGIS).

Fig. 3.2 shows a SolarGIS modelling scheme. The solar radiation retrieval is basically split into three steps. First, the clear-sky irradiance (the irradiance reaching ground with assumption of absence of clouds) is calculated using the clear-sky model. Second, the satellite data are used to quantify the attenuation effect of clouds. To retrieve all-sky irradiance the clear-sky irradiance is coupled with cloud index. The outcome of the procedure is direct normal and global horizontal irradiance, which is used for computing diffuse and global tilted irradiance. The data from satellite models are usually further post-processed to get irradiance that fits the needs of specific application (such as irradiance on tilted or tracking surfaces) and/or irradiance corrected for shading effects from surrounding terrain or objects.

3.2.2 Calculation overview

Solar radiation is calculated by models, which use inputs characterizing the cloud transmittance, state of the atmosphere and terrain conditions (Chapter 3.2.1 and Fig. 3.1). A comprehensive overview of the SolarGIS model is available in [1, 2]. The related uncertainty and requirements for bankability are discussed in [3, 4]. SolarGIS model version 1.9 has been used.

The **SolarGIS processing chain** is summarized below. Tab. 3.1 shows parameters of input databases and primary outputs.

Clear-sky model SOLIS [5] calculates clear-sky irradiance from a set of input parameters. Sun position is a deterministic parameter, and it is described by algorithms with good accuracy. Three constituents determine geographical and temporal variability of clear-sky atmospheric conditions:

- **Aerosols** are represented by Atmospheric Optical Depth (AOD), which is derived from the global MACC-II database [6, 7]. The model uses daily variability of aerosols to simulate more precisely the instantaneous estimates of DNI and GHI. Use of daily values reduces uncertainty, especially in regions with variable and high atmospheric load of aerosols [8, 9]. It is to be noted that time coverage of high frequency (daily) aerosol data by MACC-II database is limited to the period from 2003 onwards; the remaining years (from the beginning of the database to 2002) are represented only by monthly longterm averages.
- **Water vapour** is also highly variable, but compared to aerosols, it has lower impact on magnitude of DNI and GHI change. The daily data are derived from CFSR and GFS databases [10, 11] for the whole historical period up to the present time.
- **Ozone** has negligible influence on broadband solar radiation and in the model it is considered as a constant value.

Cloud model estimates cloud attenuation on global irradiance. Data from meteorological geostationary satellites are used to calculate a cloud index that relates radiance of the Earth's surface, recorded by the satellite in several spectral channels with the cloud optical transmittance. For Zambia, Meteosat satellite data are used [12]. Conceptually, the modified Heliosat-2 calculation scheme [13] is used, with a number of improvements introduced to better cope with complex identification of albedo in tropical variable cloudiness, complex terrain, at presence of snow and ice, etc. Other support data are also used in the model, e.g. altitude and air temperature.

To calculate **Global Horizontal Irradiance** (GHI) for all atmospheric and cloud conditions, the clear-sky global horizontal irradiance is coupled with cloud index.

From GHI, other solar irradiance components (direct, diffuse and reflected) are calculated. **Direct Normal Irradiance** (DNI) is calculated by modified Dirindex model [13]. Diffuse horizontal irradiance is derived from GHI and DNI.

Calculation of **Global Tilted Irradiance (GTI)** from GHI deals with direct and disuse components separately. While calculation of direct component is straightforward, estimation of diffuse irradiance for a tilted surface is more complex, and affected by limited information about shading effects and albedo of nearby objects. For converting diffuse horizontal irradiance for a tilted surface, the Perez transposition model is used [14]. Reflected component is also approximated considering that knowledge of local conditions is limited.

Model for simulation of **terrain** effects (elevation and shading) based on high resolution altitude and horizon data. Model by Ruiz Arias is used [15] to achieve enhanced spatial representation – from the resolution of satellite (3 to 4 km) to the resolution of digital terrain model.

Tab. 3.1: Input databases used in the SolarGIS model and related GHI and DNI outputs for Zambia

Inputs to SolarGIS model	Source of input data	Time representation	Original time step	Approx. grid resolution
Atmospheric Optical Depth	MACC-II reanalysis (ECMWF)	1994 to 2002	Monthly longterm calculated from reanalysis	125 km
	MACC-II reanalysis (ECMWF)	2003 to 2012	Daily (calculated from 6-hourly)	125 km
	MACC-II operational (ECMWF)	2013 to date	Daily (calculated from 3-hourly)	85 km

Water vapor	CFSR (NOAA NCEP)	1994 to 2010	1 hour	35 km
	GFS (NOAA NCEP)	2011 to date	3 hours	55 km
Cloud index	Meteosat MFG satellites (EUMETSAT)	1994 to 2004	30 minutes	3 to 4 km
	Meteosat MSG satellites (EUMETSAT)	2005 to date	15 minutes	
Altitude and horizon	SRTM-3 (SRTM)	-	-	90 metres
SolarGIS primary outputs GHI and DNI	-	1994 to 2013	15 minutes	500 m*

** Even though the model operates up to the resolution of 90 metres, target spatial resolution of maps for Zambia is 500 m.*

3.2.3 Sources of uncertainty in the satellite-based model

The conceptual limitations of the models and spatial and temporal resolution of the input atmospheric and satellite data are sources of systematic and random deviation of the DNI and GHI estimates at regional and local levels. Accuracy and characteristics of the model inputs varies geographically, but also over longer period of time and this influences the uncertainty of the resulting DNI and GHI. The main sources of uncertainty come from the cloud and aerosol models. Other factors have smaller contribution [4].

Ground measurements are important for understanding and reducing the model uncertainty. However, only high-quality ground measurements can be used; low-accuracy instruments and measurements with issues in quality do not contribute to reducing the uncertainty of the models.

Clouds

Cloud optical transmissivity is mapped from **geostationary satellite data**, which are available in several spectral bands. In specific regions, e.g. with high reflectivity or changing ground albedo (slat beds, snow. deserts), or with strong variability of clouds, quantification is more challenging. In regions where satellite-viewing angle is low uncertainty of cloud information is also higher. Spectral response of different satellite sensors has to be eliminated by data inter-calibration. Similarly, harmonized geometry of satellite data is important for quality of the model outputs. The way how these issues are addressed by the satellite-based solar models determines their computational accuracy and geographical representativeness.

Aerosols

Atmospheric aerosols have spatial and temporal dynamics, which is quite pronounced in some regions.

For limited number of sites, aerosol data are available from high-accuracy **ground-monitoring network AERONET** [16]. Besides sporadic availability, a limitation is limited time coverage. Therefore ground-measured data cannot be used in operational models. However AERONET data play important role in accuracy analysis of map-based aerosol databases.

Solar models need global (map-based) aerosol data inputs. Modern aerosol databases are used and they are capable delivering high frequency and routinely updated data, which visibly improve DNI and GHI by better capturing the daily and seasonal changes of the state of atmosphere. Data from two approaches: can be used:

- **Satellite-based aerosol models** provide data with higher spatial resolution, but they have lower temporal sampling (several days) and the valid data can be only computed for cloudless weather, which is serious limitation for regions with frequent cloudiness. Another limitation is that their accuracy is affected by high surface albedo in desert conditions, which poses some challenges in desert areas.
- **Chemical-transport models** have higher temporal sampling (3 to 6 hours), but lower spatial resolution (ca. 85 to 125 km). The models are able to characterize different aerosol types, and they are without any data gaps [6, 7]. This type of aerosol databases describe well the temporal variability, but they may have regional bias, which need to be reduced by regional correction [17].

Data from both satellite and chemical-transport models are available only for the last decade or so (satellite aerosols start around year 2000, MACC chemical transport model starts in year 2003), thus averaged aerosol information has to be used for older era.

Recent analysis of aerosol data from chemical transport models shows that due to the complex computing and availability of some input measurements (some measurements are available only with a time delay), differences exist between results from the **operational model** and from **reanalysis model** (which is run typically with one-year delay). Solar resource modelling in regions with high aerosol concentrations and large daily and seasonal variability (e.g. West and Africa and Sahel, Gulf region, North India, some parts of China) may be more challenging compared to regions, where concentrations of aerosols are lower and relatively stable over time (e.g. Atacama, Northwest of the US, South Africa or Australia).

3.3 Solar radiation measurements

Global irradiance for horizontal and tilted plane are most often measured by (i) thermocouple junction based *pyranometers* or (ii) silicon *photodiode cells*. **Diffuse irradiance** is measured with the same sensors as for measurement of global irradiance; just the sun is obscured with a sun-tracking disk or rotating shadow band blocking direct irradiance. **Direct Normal Irradiance** is commonly measured by *pyrheliometers*, where the instrument always aims directly at the sun by continuously sun tracking mechanism.

Global and diffuse components can also be measured by a *Rotating Shadowband Radiometer* (RSR) or by integrated pyranometer such *Sunshine Pyranometer* (e.g. by SPN1). In such a case, DNI is calculated from global and diffuse irradiance.

From the perspective of required accuracy in solar industry and also for the solar model adaptation, it is recommended to measure with the highest-accuracy instruments:

- Secondary standard pyranometers for Global Horizontal Irradiation (GHI) and with shading disc also for Diffuse Horizontal Irradiation (DIF)
- First class pyrheliometer for Direct Normal Irradiation (DNI).

This instrumentation is more expensive, and it is also more susceptible to failures and soiling, thus more demanding on maintenance. However if high-standard cleaning and operation are rigorously followed, the measuring set-up works reliably, delivering data are within the expectation and with the lowest possible uncertainty.

RSR instruments can be installed as an alternative to the above mentioned instruments, if measurements take place in more challenging and remote environment with limited options for frequent cleaning and maintenance. However, if feasible it is proposed to add one redundant measurement for crosschecking consistency of GHI, DNI and DIF components.

Satellite time series should be used as an independent source of information for quality control of ground-measured data (see Chapter 3.4).

3.3.1 Theoretical uncertainty of sensors

Utilization of the state-of-the-art instruments does not alone guarantee good results. Any measurements are subject to uncertainty and the information is only complete, if the measured values are accompanied by information on the associated uncertainty. Sensors and measurement process has inherent features that must be managed by quality control and correction techniques applied to the raw measured data.

Accuracy of Global Horizontal irradiance conventionally measured with a thermopile **pyranometer** is affected by two sources of error - the thermal imbalance problem and the cosine error of the sensor, resulting in a minimum uncertainty (for the most accurate sensor) of daily sums at about ±2%.

Direct Normal Irradiance, if measured by **pyrheliometers**, may be measured at daily uncertainty of about ±1% for a freshly calibrated high-accuracy pyrheliometer under ideal conditions. This uncertainty can more than double in case of rapid fluctuations of radiation, when using older instruments, or after prolonged exposure to challenging weather.

Photodiodes and **RSR** devices are also very affected by cosine error and temperature. Empirical functions are used to correct the raw data, but theoretical daily uncertainty is approx. ±2.5% to ±3.5% for the best possible cases.

Standards for pyrheliometers and pyranometers are defined in [18, 19] and summarized in Tabs 3.2 and 3.3.

Tab. 3.2: Theoretically-achievable daily uncertainty of Direct Normal Irradiation at 95% confidence level

DNI	Pyrheliometers		RSR
	Secondary standard	First class	(After data post-processing)
Hourly	±0.7%	±1.5%	±3.5% to ±4.5%
Daily	±0.5%	±1.0%	±2.5% to ±3.5%

Tab. 3.3: Theoretically-achievable daily uncertainty of Global Horizontal Irradiation at 95% confidence level

GHI	Pyranometers			RSR
	Secondary standard	First class	Second class	(After data post-processing)
Hourly	±3%	±8%	±20%	±3.5% to ±4.5%
Daily	±2%	±5%	±10%	±2.5% to ±3.5%

The lowest possible uncertainties of solar measurements are essential for accurate determination of solar resource. **Uncertainty of measurements in outdoor conditions is always higher than the one declared in the technical specifications of the instrument** (Tab. 3.2 and 3.3). The uncertainty may dramatically increase in extreme operating conditions and in case of limited or insufficient maintenance. Quality of measured data has significant impact on validation and regional adaptation of satellite models.

3.3.2 Operation and maintenance of instruments

Solar radiation measurements are not only subject to errors in determination of instant values. Radiometric response of the instruments also undergoes seasonal variability and longterm drift. Without careful maintenance, periodical check-up and calibration, the measured values can significantly differ from the “true” ones.

Rigorous on-site maintenance is crucial for sustainable quality of the longterm measuring campaign. Not only regular care of instruments is necessary, but also maintaining regular service documentation, changes in instrumentation, calibration, cleaning and variations of the instruments’ behaviour. Quality of solar measurements from data providers using medium-quality instruments or from those not following the best practices is disputable, and use of such data for validation or adaptation of solar models may be limited or even deceptive.

Measuring solar radiation is sensitive to imperfections and errors, which result in visible and hidden anomalies in the output data. The errors may be introduced by measurement equipment, system setup or operation-related problems. Errors in data can severely affect derived data products and subsequent analyses; therefore a thorough quality check is needed prior the data use.

Many problems can be prevented or corrected by a proper and continuous maintenance of the measurement station by qualified personnel. Regular cleaning of radiometers is essential to ensure quality measurements.

3.3.3 Quality control of measured data

The measurement campaign has to be carefully planned and strict quality control must be applied to the measured data. Once the data is collected, procedures have to be employed regularly (ideally every day) to verify the consistency and quality of the dataset and to remove or flag the values not fulfilling defined criteria.

Missing data can be substituted or interpolated and marked by another flag. For solar radiation measurement the following issues are known:

- Time shift of measurements
- Incomplete data
- Outliers – data outside physical limits for a given location
- Patterns revealing systematic or occasional shading
- Inconsistencies between radiation components (direct, diffuse)

Other issues often seen in the improperly managed measurements are:

- Miss-calibrated or soiled sensors
- Data are not quality-controlled
- Wrong metadata (site position, time reference)
- Wrong or missing description of the file format.

Quality control methods relate to all measured components (global, direct, and diffuse) and they are described in several publications, see e.g. SERI QC manual [20], HelioClim quality control [21], BSRN manual [22], ARM [23] and Younes et al [24]. The procedures are typically applied in several steps:

- A first test checks if the measurements fall within the **physical limits** given by the clear sky conditions and heavily overcast conditions calculated for a given location. The tests checking physical limits of solar components are capable to find only gross errors. The small errors due to **miss-calibration** or **sensor soiling** and **dirt** only produce subtle changes (below approx. 5%) and they are difficult to identify. When all three components (GHI, DNI and DIF) are available, a **test of redundancy** between the components can help.
- Common problem are **missing data.** They occur due to instrumentation failures and shutdowns or as a result of reasonable or incorrect rejection of values during the quality assessment. It is difficult to use such data when aggregated statistics is to be derived, such as daily or monthly or yearly sums. If the period of missing data is short, the statistical averaging or interpolation techniques to fill such gaps are be employed (see e.g. [25, 26]). The gap-filled data should be labelled by flags that allow distinguishing measured data from the artificial ones. **Satellite data play important role in gap filling of ground-measured data.**
- In addition to measurement errors, the data quality may be reduced by **missing or erroneous metadata** (descriptive information about the data). Missing information about time reference, time integration (instantaneous vs. averaged data for a given time interval), units, flags, post-processing methods, sensor calibration, etc. may result in wrong application of the data, especially in the case of error in localisation (latitude and longitude).

Examples presented above show that **solar radiation measurements are prone to various errors**. Therefore **quality assessment must be an integral part of the data acquisition and management routines.** The complete quality information must be communicated to users along with the data.

3.3.4 Recommendations on solar measuring stations

Local ground measurements from high-standard instruments are used for better understanding of site-specific weather conditions, and this knowledge is than translated to improved accuracy of solar models. The ultimate objective is to reduce uncertainty of solar resource data and more accurate assessment of energy yield and performance of solar power plants,

The quality control may identify issues, which may reduce reliability and increase uncertainty of ground measurements or may even result in the complete data rejection. To avoid such problems, some recommendations are summarized below:

- **Site selection** – a site should be located in geographically representative areas, which are not affected by excessive dust and pollution. Shaded areas, caused by surrounding buildings, structures and vegetation, should be avoided or eliminated as much as possible. If shading takes place, the affected values should be identified and flagged.
- **Instruments** – to achieve quality measurements with high value for solar energy applications, secondary standard pyranometers and first class pyrheliometers (WMO classification) are to be used. Attention should be given also to installation to avoid levelling problems that have direct effect on quality of measurements. The sensors should be regularly re-calibrated, according to instructions

provided by manufacturers. In remote areas RSR instruments should be preferably deployed. Use of redundant measurements, including satellite-based time series, during the quality control, is a good practice.

- **Rigorous operation practices and regular maintenance** are required to achieve high quality of the measured data. The solar sensors are sensitive to dirt and soiling, having direct effect on data degradation, therefore regular cleaning is therefore very important. Cleaning should take place at least several times a week, in more polluted or dusty areas even daily. In addition a regular check of instrument (levelling, cabling, logging, etc.) is good practice. Cleaning of RSR instrument can be less frequent.
- Regular data **quality control** – provides fast feedback and is a way to prevent longer data losses or persistent issues. Data delivered to customer should be quality controlled, without gaps and with flags indicating various issues.
- **Documentation and maintenance information** – the documentation about meteorological site, instruments and calibration should be provided along with the data. Good practice is also logging of cleaning and maintenance works. Such information may be later used for explanation of specific data patterns found in the data – e.g. sudden increase of values, change of time stamp etc.
- **Database management** – rather than used of spreadsheet formats, data should be preferably managed within the standard SQL databases allowing routine procedures, reporting and back up.

3.4 Ground-measured vs. satellite data – adaptation of solar model

It is important to understand characteristics of ground measurements and satellite-modelled data (Tab. 3.4) for qualified solar resource assessment. In general, top-quality and well-maintained instruments provide data with lower uncertainty than the satellite model. However, such data are rarely available for the required location, and usually the period of measurements is too short to describe longterm weather conditions. On the other hand satellite data can provide long climatic history (20+ years in case of SolarGIS), but may not accurately represent the micro-climatic conditions of a specific site.

Thus, the ground measurements and satellite data complement each other and it is beneficial to correlate both data sources and to adapt the satellite model for the specific site so that long history of time series is computed with lower uncertainty. The model adaptation has two steps:

1. Identification of systematic differences between hourly satellite data and local measurements for the period when both data sets overlap;
2. Development of a correction method that is applied for the whole period represented by the satellite time series.

The improvements of such site-adaptation depend on the quality and accuracy of measured and satellite data. In the most favourable cases, the resulting uncertainty is still slightly higher than uncertainty of ground measurements. In general, site adaptation of satellite data by local measurements will result in lower uncertainty under the following conditions:

- At least one year of ground-measured data is available (preferably two years or more);
- Solar measuring station is equipped by more than one instruments, allowing redundancy checks for GHI, DNI and DIF values;
- Ground measurements are of high quality, which should be traceable in the cleaning, maintenance and calibration logs.
- High quality satellite data are used - with good representation of irradiance variability, extreme situations and with consistent longterm quality.
- Advanced site-adaptation method is used, capable to address specific sources of satellite-ground data differences (e.g. correction of aerosols, cloud identification). Besides reduced uncertainty of longterm estimate (lower bias), the model adaptation method should improve also random deviations (lower RMSD) and should provide more representative sub(hourly) values (lower KSI).

Solar data for Zambia are validated based on the measurements in the wider regions. More information can be consulted in the *Model Validation Report 128-02/2014*.

Tab. 3.4: Comparing solar data from solar measuring stations and from satellite-models

	Data from solar measuring stations	Data from satellite-based models
Availability/ accessibility	Available only for limited number of sites. Most often, data cover only recent years.	Data are available for any location within latitudes 60N and 50S. Data cover long time period, in Zambia more than 20 years.
Original spatial resolution	Local measurements represent the microclimate of a site.	Satellite models represent area with complex spatial resolution: clouds are mapped at approx. 4 km, aerosols at 125 km and water vapour at 34 km. Terrain can be modelled at spatial resolution of up to 90 metres. Methods for enhancement of spatial resolution are often used.
Original time resolution	Seconds to minutes	15 and 30 minutes
Quality	Data need to go through rigorous quality control, gap filling and cross-comparison.	Quality control of the input data is necessary. Outputs are regularly validated. Under normal operation, data has only few gaps, which are filled by intelligent algorithms.
Stability	Instruments need regular cleaning and control. Instruments, measuring practices, maintenance and calibration may change over time. Thus regular calibration is needed. Longterm stability is typically a challenge.	If data are geometrically and radiometrically pre-processed, complete history of data can be calculated with one single set of algorithms. Data computed by an operational satellite model may slightly change over time, as model and its input data evolve. Thus regular reanalysis is needed.
Uncertainty	Uncertainty is related to the accuracy of the instruments, maintenance and operation of the equipment, measurement practices, and quality control.	Uncertainty is given by the characteristics of the model, resolution and accuracy of the input data. Uncertainty of meteorological models is higher than high quality local measurements. The data may not exactly represent the local microclimate, but are usually stable and may show systematic deviation, which can be reduced by good quality local measurements (site-adaptation of the model).

3.5 Typical Meteorological Year

Along with multiyear time series data, Typical Meteorological Year (TMY) data are delivered for 11 meteo sites in Zambia (described in *Site Identification Report 128-03/2014*). TMY contains hourly data derived from the time series covering complete years 1994 to 2013. TMY data is a vital supplement to GIS data and maps, as it can be directly used in energy simulation software, such as SAM, HOMER or PVSYST.

Detailed description of the SolarGIS method is given in [27]. Here we summarize only the key principles. In TMY, the history of 20 years is compressed into one year, following two criteria:

- Minimum difference between statistical characteristics (annual average, monthly averages) of TMY and longterm time series. This criterion is given about 80% weighting.
- Maximum similarity of monthly Cumulative Distribution Functions (CDF) of TMY and full-time series, so that occurrence of typical hourly values is well represented for each month. This criterion is given about 20% weighting.

To derive solar resource parameters with an hourly time step, the original satellite data with time resolution of 15- and 30-minutes were aggregated by time integration. The meteo parameters are derived from original 1-hourly and 3-hourly time step. The TMY datasets were constructed from original–model solar radiation and meteorological data (Chapters 3.2 and 4.2). Time zone was adjusted to UTC + 02:00.

In assembling TMY for Zambia, the weighting of direct (DNI), global (GHI) and diffuse (DIF) irradiance and also Air Temperature at 2 metres (TEMP) is considered. The weights are showing an importance of parameters that are considered for choosing the representative months and they are set as follows: 0.9 is given to DNI, 0.3 to GHI, 0.05 to DIF, and 0.05 to TEMP (divided by the total of 1.3).

For each of eleven sites two TMY data sets are delivered – TMY for P50 and for P90:

- **TMY P50** data set is constructed on the monthly basis. For each month the longterm average monthly value and cumulative distribution for each parameters (DNI, GHI, DIF and TEMP) is calculated. Next, the monthly data for each individual year from the set of 20 years are compared to the longterm parameters. The monthly data from the year, which resembles the longterm parameters more closely, is selected. The procedure is repeated for all 12 months, and the TMY is constructed by concatenating the selected months into one artificial (but representative) year.
- The method for calculation **TMY P90** data set is based on the TMY P50 method. It has been modified in a way in which a candidate month is selected. The search for set of twelve candidates is repeated in iteration until a condition of minimization of difference between annual P90 value and annual average of new TMY is reached (instead of minimization of differences in monthly means and CDFs, as applied in the P50 case). Once the selection converges to the minimum difference, the TMY is created by concatenation of selected months. Note: P90 annual values are calculated from the combined uncertainty of the estimate and inter-annual variability, which can occur in any year.

Tab. 3.5: Annual longterm GHI and DNI averages as represented in time series and TMY data products

ID	Name	DNI [kWh/m^2]			GHI [kWh/m^2]		
		Time series	TMY P50	TMY P90	Time series	TMY P50	TMY P90
1	Copperbelt	1913	1913	1648	2153	2153	2012
2	Chilanga	1998	1998	1702	2113	2114	1964
3	Kabwe	2020	2020	1719	2168	2168	2016
4	Longe	2117	2117	1832	2200	2201	2058
5	Lusaka	2000	2000	1697	2120	2120	1969
6	Mansa	1956	1956	1698	2194	2194	2055
7	Mazabuka	2133	2133	1830	2193	2193	2047
8	Misamfu	1895	1896	1636	2170	2170	2029
9	Mochipapa	2103	2104	1801	2137	2137	1991
10	Msekera	1801	1802	1516	2071	2072	1922
11	Mutanda	1909	1909	1652	2150	2150	2011

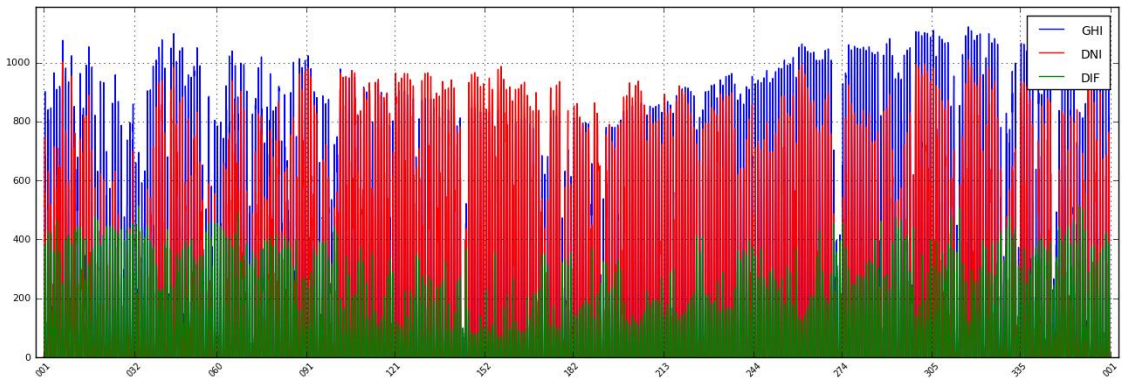

Fig. 3.3: Seasonal profile of GHI, DNI and DIF for P50 Typical Meteorological Year (TMY)
Example of Lusaka: X-axis – day of the year; Y-axis – irradiance W/m^2

As a result of generating TMY and mathematical rounding, longterm monthly and annual averages calculated from TMY data files may not fit accurately to the statistical information calculated from the multiyear time series.

It is important to note that the data reduction in TMY is not possible without loss of information contained in the original multiyear time series. Therefore **time series data are considered as the most accurate reference suitable for the statistical analysis of solar resource and meteorological parameters of the site.** Only time series data can be used for the statistical analysis of solar climate.

4 MEASURING AND MODELLING METEOROLOGICAL DATA

Meteorological parameters are important part of each solar energy project assessment as they determine the operating conditions and effectiveness of operation of solar power plants. Meteorological data can be collected by two approaches: (1) by measuring at meteorological sites and (2) by meteorological models.

Best option is to have **locally-measured data**, for at least 10 recent years. However, meteorological data is available only for sites where longterm meteorological observations are operated; typically by national meteorological service or some other observation network. Even for such sites, the multiyear time series are not always complete, and there may be periods with missing data.

Most typically, the meteorological data are not available for a particular site of interest, and the only option is to derive them from **meteorological models**. Various models are available, a good option is to use CFSR and CSFv2 (source NOAA, NCEP, USA) continuously covering long period of time. Disadvantage of using the modelled data is their lower accuracy (for a specific site) compared to measurements from well-maintained meteorological station with high-standard instruments.

In development of solar energy projects a good practice is to install a meteorological station at a site of interest, as soon as the site is selected. Even a period of one year of operating local meteorological station can provide valuable data for adaptation and validation of meteorological and satellite models. Thus combined use of modelled data and local measurement makes it possible to achieve low uncertainty data, covering climatologically representative period of time.

4.1 Meteorological data measured at meteorological stations

As a standard practice, a meteorological station is deployed at a site of large solar energy project development. The main objective of measuring data at the project site, during the planning phase, is to record accurate local meteo characteristics, to use them in the adaptation of the models and to reduce uncertainty of the longterm time series and aggregated estimates.

Deployment of solar measuring stations in a country has strategic advantage of adapting and validating the model at a country level to provide high-quality data and information for decision-makers and investors.

Parameters, relevant for solar energy projects are identical to the list in Chapter 2.2. Uncertainty of the meteorological instruments (according to the WMO standards) is show in Tab. 4.1.

Tab. 4.1: Uncertainty of meteo sensors by WMO standard (Class A)

Parameter	Instrument	WMO standard
Air Temperature at 2 m	Thermometer	0.2 K
Relative humidity at 2 m	Temperature and relative humidity probe	3%
Atmospheric pressure	Digital barometer	0.3 hPa
Wind speed at 10 m	Ultrasonic sensor	0.5 m s^{-1} for ≤ 5 m s^{-1} 10% for > 5 m s^{-1}
Wind direction at 10 m	Ultrasonic sensor	5°
Rainfall	Weighing type rain gauge	Amount: larger as 5% or 0.1 mm Intensity: under constant flow conditions in the laboratory, 5% above 2 mm/h, 2% above 10 mm/h; in the field, 5 mm/h and 5% above 100 mm/h

4.2 Data derived from meteorological models

Operational models and reanalysis

For Zambia, SolarGIS provides a complete 20-years history of meteorological data for any location. To achieve this objective, numerical meteorological models have to be used and validated by local measurements. SolarGIS reads meteorological data from 3 databases, all operated by NOAA/NCEP:

1. **Historical data dataset 1**: the Climate Forecast System Reanalysis [10]) is a *global numerical weather reanalysis model*. In SolarGIS, a historical period from **1994 to 2010** has been implemented. The CFSR was designed as global, high-resolution, coupled atmosphere-ocean-land surface-sea-ice system to provide the best estimate of the state of these coupled domains over this period.
2. **Historical data dataset 2**: the Climate Forecast System Version 2 [28] is a *global numerical weather reanalysis model*. In SolarGIS, historical period of data from **2011 till the end of last month** has been implemented. The CFS version 2 was developed at the Environmental Modeling Center at NCEP. It is a fully coupled model representing the interaction between the Earth's atmosphere, oceans, land and sea ice.
3. **Operational forecast model**: the Global Forecast System [11] is a *global numerical weather prediction model*. This mathematical model runs four times a day and produces forecasts for every third hour up to 16 days in advance, but with decreasing spatial and temporal resolution over time. The data cover period form **the end of last month up to the 7 days into the future**. GFS is one of the predominant synoptic scale medium-range models in general use.

Original *temporal resolution* of 1 hour (CFSR and CFSv2) and 3 hours (GFS) is interpolated, if necessary, and harmonized to the time step of final data delivery.

Original *spatial angular resolution* of accessible GRIB files containing the primary parameters is 0.3125° for CFSR and 0.2° for CFSv2 and GFS datasets. This translates into spatial resolution of approx. 34 x 35 km for CFSR and approx. 22 x 23 km for CFSv2 for the territory of Zambia. Both data resolutions are post-processed and recalculated to the spatial resolution of 1 km. The SolarGIS algorithms utilize Digital Elevation Model SRTM-3 for post-processing (downscaling) of air temperature. Other data (wind speed and direction; wet bulb temperature, relative humidity and air pressure) are used in the original model resolution. As a result occasional blocky features can be seen on the maps. In general, meteo data from the meteo models represent larger area, they are smoothed and therefore they are not capable to represent accurately the local microclimate, especially in rough mountains.

Time period covered in site-specific meteo data: 01/1994 to 12/2013 (20 years, models CFSR and CFSv2). For preparation of climate GIS data layers (Air Temperature only) only CFSR model was used (20 years, from 01/1991 to 12/2010) to avoid additional resampling of spatial data. GFS data are used only in the delivery of site-specific hourly time series and TMY for 11 sites.

The accuracy of meteorological models depends on the input data. Being a mathematical representation of dynamic processes, the models are based on a set of partial differential equations, solution of which strongly depends on initial and boundary conditions. The initialization parameters come from meteo measurements at different locations. The accuracy in the lowest layer of the atmosphere (2 m for air temperature, and relative humidity, and 10 m for wind speed and wind direction) depends on spatial distribution and quality of measurements from the meteo observation networks.

Tab. 4.2: Availability of CFSR and CFSv2 data from meteorological models for Zambia through SolarGIS

	Climate Forecast System Reanalysis (CFSR)	Climate Forecast System version 2 (CFSv2)
Data available	1994 to 2010	2011 to last month of 2014
Original spatial resolution	Approx. 34 x 35 km	Approx. 22 x 23 km
Original time resolution	1 hour	1 hour

Numerical meteorological models have lower spatial and temporal resolution, compared to solar resource modelled data. Thus local values from the models may deviate from the local measurements.

The data from global meteorological models have to be post-processed in order to provide parameters with local representation. Two approaches are available:

1. Running mesoscale weather prediction models, such as WRF [29]
2. Post processing using simpler methods.

First approach can provide more localized data. Second approach is simpler and may include higher uncertainty. The best practice is to combine modelled data with short-term local measurements to reduce data uncertainty.

SolarGIS meteorological parameters, delivered as **spatial data products** (GIS data layers and maps):

- Air Temperature at 2 metres, TEMP [°C]

SolarGIS meteorological parameters, delivered in the **site-specific data products** (time series and TMY):

- Air Temperature at 2 metres, TEMP [°C]
- Wet Bulb Temperature, WBT [°C]
- Relative Humidity, RH [%]
- Wind Speed at 10 metres, WS [m/s2]
- Wind Direction at 10 metres, WD [°]
- Air Pressure, AP [hPa].

For time series and TMY data, original temporal resolution of 1-hour is used. In map products only aggregated Air Temperature data is supplied. Meteorological data is validated in the *Model Validation Report 128-02/2014*.

4.3 Measured vs. modelled data – features and uncertainty

Data from both sources have their advantages and disadvantages (Tab. 4.3). Meteo parameters retrieved from the meteorological models have lower spatial and temporal resolution compared to on-site meteorological measurements, and they have lower accuracy. Thus modelled parameters may characterize only regional climate patterns rather than local microclimate; especially extreme values may be smoothed and not well represented.

Tab. 4.3: Comparing data from meteo stations and weather models

	Meteo station data	Data from meteorological models
Availability/ accessibility	Available only for selected sites. Data may cover various periods of time	Data are available for any location Data cover long period of time (decades)
Original spatial resolution	Local measurement representing microclimate with all local weather occurrences	Regional simulation, representing regional weather patterns with relatively coarse grid resolution. Therefore the local values may be smoothed, especially extreme values.
Original time resolution	Sub-hourly, 1 hour	1 hour
Quality	Data need to go through rigorous quality control, gap filling and cross-comparison.	No need of special quality control. No gaps Relatively stable outputs if data processing systematically controlled.
Stability	Sensors, measuring practices, maintenance and calibration may change over time. Thus longterm stability is often a challenge.	In case of reanalysis, long history of data is calculated with one single stable model. Data for operational forecast model may slightly change over time, as model development evolves
Uncertainty	Uncertainty is related to the quality and maintenance of sensors and measurement practices, usually sufficient for solar energy applications.	Uncertainty is given by the resolution and accuracy of the model. Uncertainty of meteorological models is higher than high quality local measurements. The data may not exactly represent the local microclimate, but are usually sufficient for solar energy applications.

5 SOLAR TECHNOLOGIES AND SOLAR RESOURCE DATA

This project delivers two principal solar resource data sets that are exploited by different solar power generation technologies:

- Global Horizontal Irradiance (GHI) and Global Tilted Irradiance (GTI) used by photovoltaic (PV) flat plate technologies
- Direct Normal Irradiance (DNI) used by Concentrating Photovoltaic (CPV) and by Solar Thermal Power Plants, often denoted as Concentrating Solar Power (CSP) plants.

5.1 Photovoltaic technology

Photovoltaic technology (PV) exploits global horizontal or tilted irradiation, which is sum of direct and diffuse components. To simulate power production by a PV system, global irradiance received by a flat surface of PV modules must be correctly calculated. Due to clouds, PV power generation reacts to changes of solar radiation in the matter of seconds or minutes (depending on the size of a module field), thus intermittency (short-term variability) of the PV power production is to be considered. Effect of seasonal variability is also to be considered.

PV will most likely dominate in solar energy applications in Zambia. Therefore, in addition to solar and meteorological data, theoretical photovoltaic (PV) production potential has been calculated for the region. A number of technical options are available for Zambia, and they are briefly described below.

For Zambia two PV system types are relevant:

- Grid-connected PV power plants:
  - Build in open space, where PV modules can be mounted in a fixed position or on sun-trackers
  - Mounted on roofs or facades of buildings
- Off-grid and mini-grids systems, which operate in a standalone regime.

5.1.1 Open space systems

The majority of utility scale PV power plants have **PV modules mounted at fixed position** with optimum inclination (tilt). Fixed mounting structures are basic, simplest and lowest-cost choice for implementing the PV power plants. A well-designed structure is robust and ensures long-life performance even during harsh weather conditions with low maintenance costs.

Sun-tracking systems are the other alternative. Solar trackers adjust the orientation of the PV modules during a day to a more favourable position in relation to the sun, so the PV modules collect more solar radiation for during the day:

- One of the most common types of tracking system is **1-axis horizontal tracker with North-South orientation of rotating axis**. The positive feature - in comparison to fixed mounted systems - is elongated power generation profile stretching from early morning till late afternoon. The downside of this tracker is its limited power output at the peak of the day in season with lower sun angle due to horizontal position of the PV modules.
- Another option is **2-axis tracker**, where modules are positioned in both azimuth and zenith axes to direct the modules towards the sun. 2 axis trackers can gain vs. 1-axis horizontal tracker about 10% or more energy (depending on geographical location). Drawback of such systems is a more complex mounting structure (and higher price). Also, in case of failure of 2-axis system, the modules may remain stuck in a suboptimal position.

In this study, the PV power potential is studied for the mainstream technology – for a system with fixed-mounted PV modules.

Key characteristics of large utility scale PV power plants are centralised inverters, optimized to high performance and efficiency. Large power plants – in contrast to a network of small size distributed PV systems – may have significant impact on the medium voltage distribution grid in the point of connection caused by intermittent supply of electricity in a cloudy weather.

Installed capacity of a PV power planned is usually determined by the grid operator to ensure the stability of the power grid.

5.1.2 Roof (façade) mounted space systems

Considering installed power, roof-mounted PV systems are typically small to medium size, i.e. ranging from hundreds of watts to hundreds of kilowatts. Modules can be mounted on roofs (flat or tilted), façades or can be directly integrated as a part of a building structure.

The main characteristic of these systems is their geographic dispersion and connection into low voltage distribution grid. Direct connection into grid also means that the inverter must provide all protections required by regulations (voltage, frequency, isolation check, etc.). For comparison, a utility scale power plant has its own protection equipment, separated from the inverter and assembled typically on the high-voltage side. It is also required that inverters have anti-islanding protection, which means that they work only if grid voltage is present (due to safety reasons). Other connection options, combined with batteries, are more often used. Since these are low-power systems (compared to open space utility-scale projects), inverters have lower efficiencies, especially those with internal isolation transformer.

PV modules are often installed in suboptimal position (deviating from the optimum angle), and this results in lower performance ratio. Air circulation between modules in a roof or a façade system is worse, compared to free-standing systems, and thus PV power output is further reduced by higher temperature of modules. PV modules, which are mounted at low tilt, are affected by higher surface pollution due to less effective natural cleaning. Another reduction of PV power output is often determined by nearby shading structures. Especially trees, masts, neighbouring buildings, roof structures or self-shading of crystalline silicon modules has some influence on reduced PV system performance.

5.1.3 Off-grid and mini-grid systems

Off-grid PV systems are not connected to a centralized grid and they are equipped in vast majority of cases with energy storage (classic lead acid or modern-type batteries). Off-grid PV system can be a stand-alone systems or a mini-grid typically to provide a smaller community with electricity. Off-grid electrification is the only approach to access electricity in areas with no direct access to electricity, due to scattered population or distant energy supply infrastructure.

5.1.4 Principles of PV energy simulation

PV energy simulation results, presented in Chapter 8, are based on software developed by GeoModel Solar. This Chapter summarizes key elements of the simulation chain.

Tab. 5.1: Specification of SolarGIS database used in the PV calculation in this study

Data inputs for PV simulation	Global Tilted Irradiation (GTI) for optimum angle (range of 14° to 22°) towards North derived from GHI and DNI; Air Temperature at 2 meters (TEMP) is also used
Spatial grid resolution (approximate)	Primary data (GHI and DNI) are available at 3.5 km (2.5 arc-minute); meteo parameters and atmospheric data are resampled to the resolution of supplied data
Time resolution	15-minute
Geographical extent (this study)	Republic of Zambia
Period covered by data (this study)	01/1994 to 12/2013

The PV software has implemented the scientifically proven methods [30 to 37] and it uses 15-minute time series of solar radiation and air temperature data on the input (Tab. 5.1). Data and model quality is checked using field tests and ground measurements. The software makes it possible to use historical, near-real time and also forecast data. The interactive version is implemented in online SolarGIS tools.

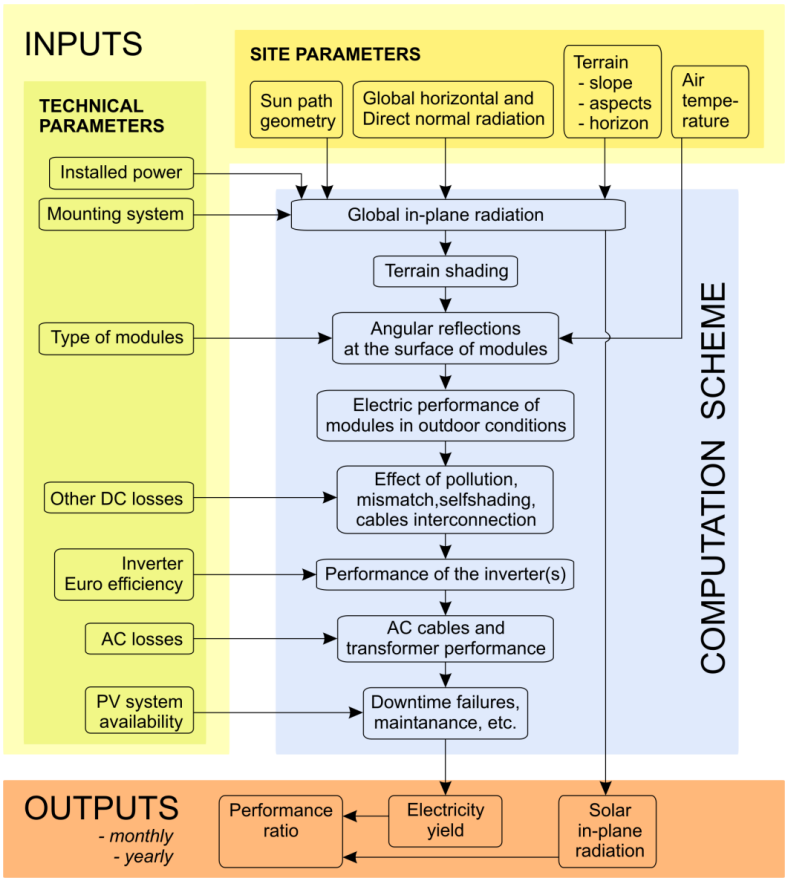

Fig. 5.1: SolarGIS PV simulation chain

In PV energy simulation procedure there are several energy losses occurring in the individual steps of energy conversion (Fig. 5.1):

- **Losses due to terrain shading.** Shading of local features such as from nearby building, structures or vegetation is not considered in the map calculation. For open space systems the uncertainty of this estimate is very low due to use of high-resolution data and accurate model [15]. For urban areas, an additional analysis should be undertaken to consider the detailed terrain surface model.
- **Losses due to angular reflectivity** depend on relative position of the sun and plane of the module. For the calculation the model by Martin and Ruiz is used in SolarGIS approach [35]. The losses at this stage depend on the module surface type and cleanness.
- **Losses due to dirt and soiling.** Losses of solar radiation at the level of surface of PV modules depend mainly on the environmental factors and cleaning of the PV modules surface.
- **Losses due to performance of PV modules outside of STC conditions.** Relative change of produced energy at this stage of conversion depends on the module technology and mounting type. Typically, for crystalline silicon modules, these losses are higher when modules mounted on a tracker than at a fixed position [30 to 33].
- **Losses by inter-row shading.** Row spacing leads to electricity losses due short-distance shading. These losses can be avoided by optimising distances between rows of module tables. For Zambia these losses will be negligible because sun in very high and tilt of the modules is small.

- **Power tolerance of modules.** Modules are connected in strings, and power tolerance of modules determines mismatch losses for these connections. If modules with higher power tolerance are connected in series, the losses are higher. The higher power tolerance of modules increases uncertainty of the power output estimation.
- **Mismatch and DC cabling losses.** These are given by slight differences between nominal power of each module and small losses on cable connections.
- **Inverter losses from conversion of DC to AC.** Although power efficiency of inverter is high, each type of inverter has its own efficiency function. Losses due to performance of inverters can be estimated using inverter power curve or using the less accurate pre-calculated value given by the manufacturer.
- **AC and transformer losses.** These losses apply only for large–scale open space systems. The inverter output is connected to the grid through the transformer. The additional AC losses reduce the final system output by a combination of cabling and transformer losses.
- **Availability.** This empirical parameter quantifies electricity losses incurred by shutdown of a PV power plant due to maintenance or failures, including issues in the power grid. Availability of well operated PV system is approx. 99%.
- **Longterm degradation.** Many years of operation of PV power plants is the ultimate test for all components. Currently produced modules represent a mature technology, and low degradation can be assumed. However, it has been observed that performance degradation rate of PV modules is higher at the beginning of the exposure, and then stabilizes at a lower level, Initial degradation may be close to value of 0.8% for the first year and 0.5% or less for the next years [34].

Results of calculation of PV power potential for Zambia are shown in Chapter 8.

5.2 Concentrating technologies

Concentrating technologies can only exploit DNI (as diffuse irradiance cannot be concentrated). Instant (short-term) variability of DNI is very high and this is especially relevant for Concentrating PV (CPV) systems. On contrary, solar thermal power plants, often denoted as Concentrating Solar Power (CSP) technology, has lot of means to control short term and also daily variability. This is given by the inertia of the whole system (solar field, heat transfer and storage), which can be in addition supported by fossil fuels.

Solar resource seasonal variability in Zambia is determined by rainy and dry seasons.

5.2.1 Concentrating Solar Power

A distinctive characteristic of Concentrated Solar Power technology (CSP) is that, when deployed with thermal energy storage, it can produce electricity on demand providing a dispatchable source of renewable energy. Therefore, it can provide electricity whenever needed to meet demand, performing like a traditional base-load power plant. There are several groups of a solar thermal power plants:

- **Parabolic troughs**: solar fields using trough systems capture solar energy using large mirrors that track the sun's movement throughout the day. The curved shape reflects most of that heat onto a receiver pipe that is filled with a heat transfer fluid. The thermal energy from the heated fluid generates steam and electricity in a conventional steam turbine. Heated fluid in the trough systems can also provide heat to thermal storage systems, which can be used to generate electricity at times when the sun is not shining;
- **Power towers**: they use flat mirrors (heliostats) to reflect sunlight onto a solar receiver at the top of a central tower. Water is pumped up the tower to the receiver, where concentrated thermal energy heats it up. The hot steam then powers a conventional steam turbine. Some power towers use molten salt in place of the water and steam. That hot molten salt can be used immediately to generate steam and electricity, or it can be stored and used at a later time.
- **Fresnel reflectors**: they are made of many thin, flat mirror strips to concentrate sunlight onto tubes through which working fluid is pumped. The rest of the energy cycle works similarly as in the above mentioned systems.
- **Stirling dish**: consists of a stand-alone parabolic reflector that concentrates light onto a receiver positioned at the reflector's focal point. The reflector tracks the Sun along two axes. The working fluid in the receiver is heated and then used by a Stirling engine to generate power.

One of the advantages of technology is thermal storage, very often in the form of molten salt. CSP can also be integrated with fossil-based generation sources in a hybrid configuration.

5.2.2 Concentrating photovoltaics

Different type of conversion of DNI into to electricity is Concentrated Photovoltaic (CPV). This technology is based on the use of lenses or curved mirrors to concentrate sunlight onto a small area of high-efficiency PV cells. High concentration CPV has to use very precise solar trackers. The advantage of CPV over flat plate PV is a potential for cost reduction due to smaller area of photovoltaic material. The necessity of sun tracking partially balances out the smaller price of semiconductor material used. CPV technology requires also more maintenance during the lifetime of power plant. Power production from CPV may be more sensitive to changing weather conditions. The advantage of CPV over CSP is full scalability, similar to flat plate PV modules.

6 GEOGRAPHY AND AIR TEMPERATURE IN ZAMBIA

6.1 Representative sites

Zambia is located in Africa, between **latitudes 8° and 18° South** and **longitudes 22° and 33° East**.

For demonstration of climate variability of solar climate and PV power potential, six representative sites in Zambia are selected. Position of these sites coincides with meteorological stations locates at Zambia Agriculture Research Institute (ZARI). Position of these sites is summarised in Tab. 6.1 and shown in Fig. 6.1.

All the data in tables and graphs, shown in Chapters 7 and 8, relate to these six sites.

Tab. 6.1 Position of six representative sites in Zambia

ID	Site name	Closest town	Province	Latitude [°]	Longitude [°]	Altitude [metres a.s.l.]
1	Longe	Kaoma	Western	-14.8397	24.9319	1167
2	Lusaka	Lusaka	Lusaka	-15.3950	28.3371	1262
3	Mochipapa	Choma	Southern	-16.8382	27.0703	1282
4	Msekera	Chipata	Eastern	-13.6461	32.5631	1027
5	Misamfu	Kasama	Northern	-10.1726	31.2231	1382
6	Mutanda	Solwezi	North-west	-12.4236	26.2153	1317

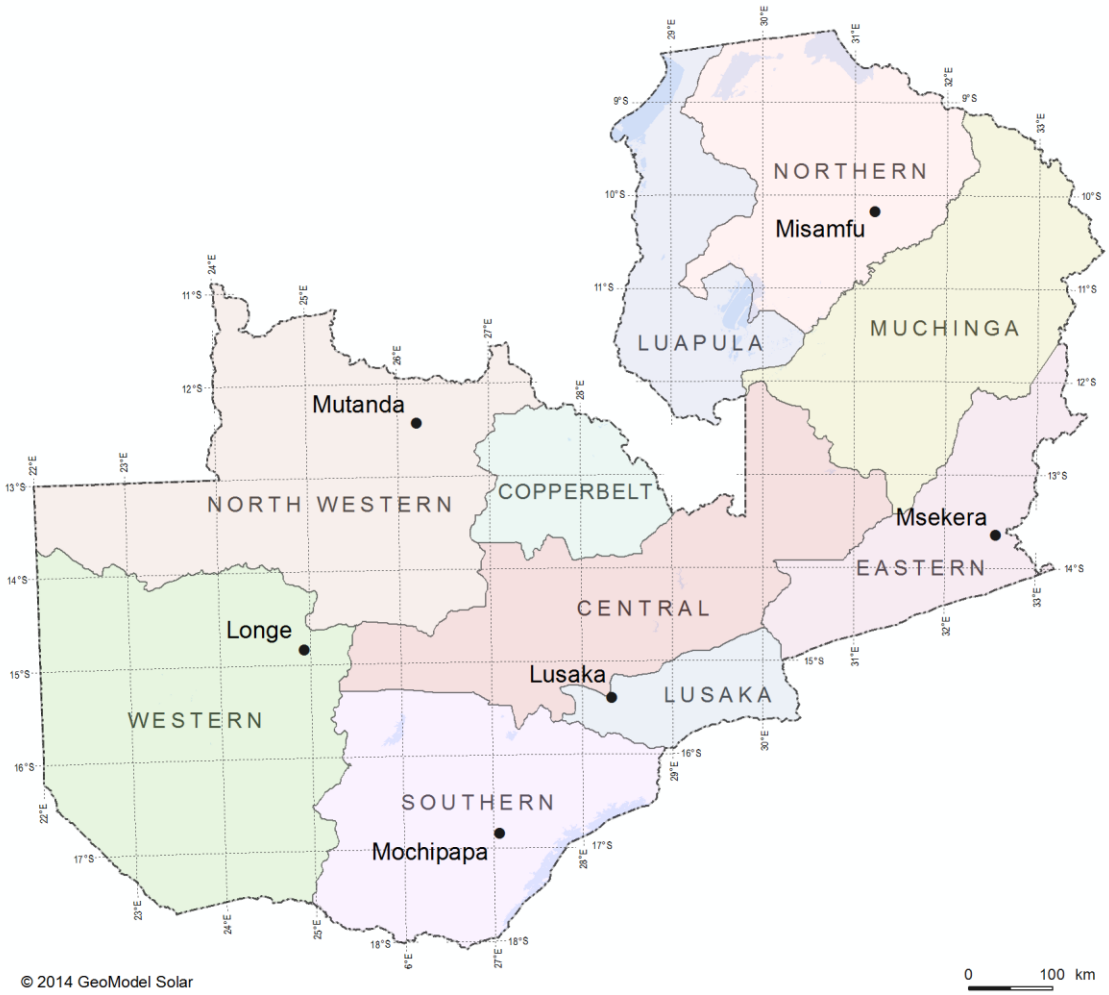

Fig. 6.1: Position of six sites within the provinces in Zambia.
Source: VMAP0 and GeoModel Solar

6.2 Geographic data

Geographic information and maps bring additional value to the solar data. Geographical characteristics of the country from regional to local scale may represent technical and environmental prerequisites, but also constraints for solar energy development.

In this Solar Modelling Report we collected the following data:

- Terrain (physical limitation for development)
- Population centres (centres of power consumption)
- Sites with mining a related activities (centres of large industrial needs for power)
- Main road and railroad network (defining accessibility of sites for location of power plants).

Urbanisation centres, similar to mining areas are the centres of energy consumption and at the same time centres of air pollution. Areas of more complex orographic conditions (terrain) are generally less populated and most often not suitable for large-scale solar energy development.

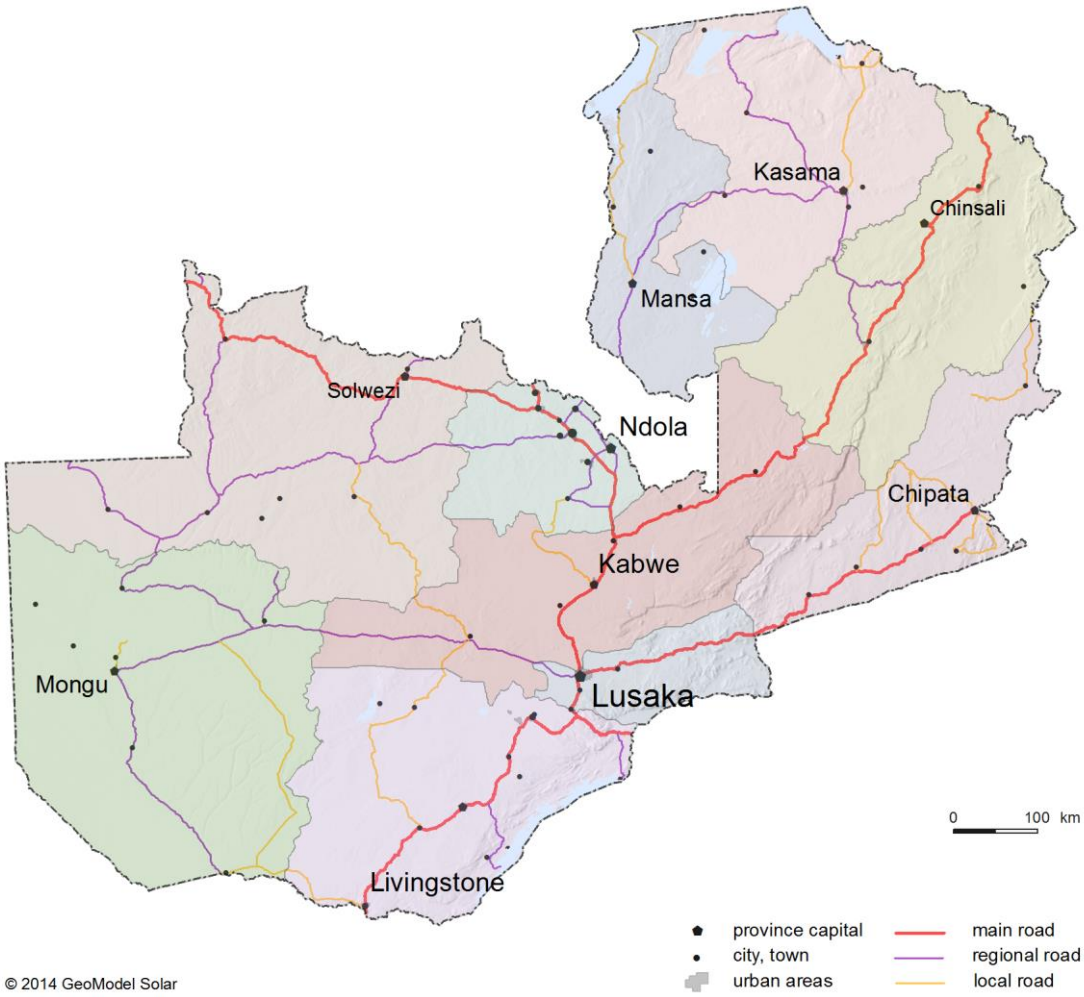

Fig. 6.2: Towns and cities, main mines and sites with related activities, main roads and railways.
Source: VMAP0, GeoModel Solar

Terrain is mostly flat with some less pronounced mountains. Steep slopes are identified prevailingly in the Rift Valley zone.

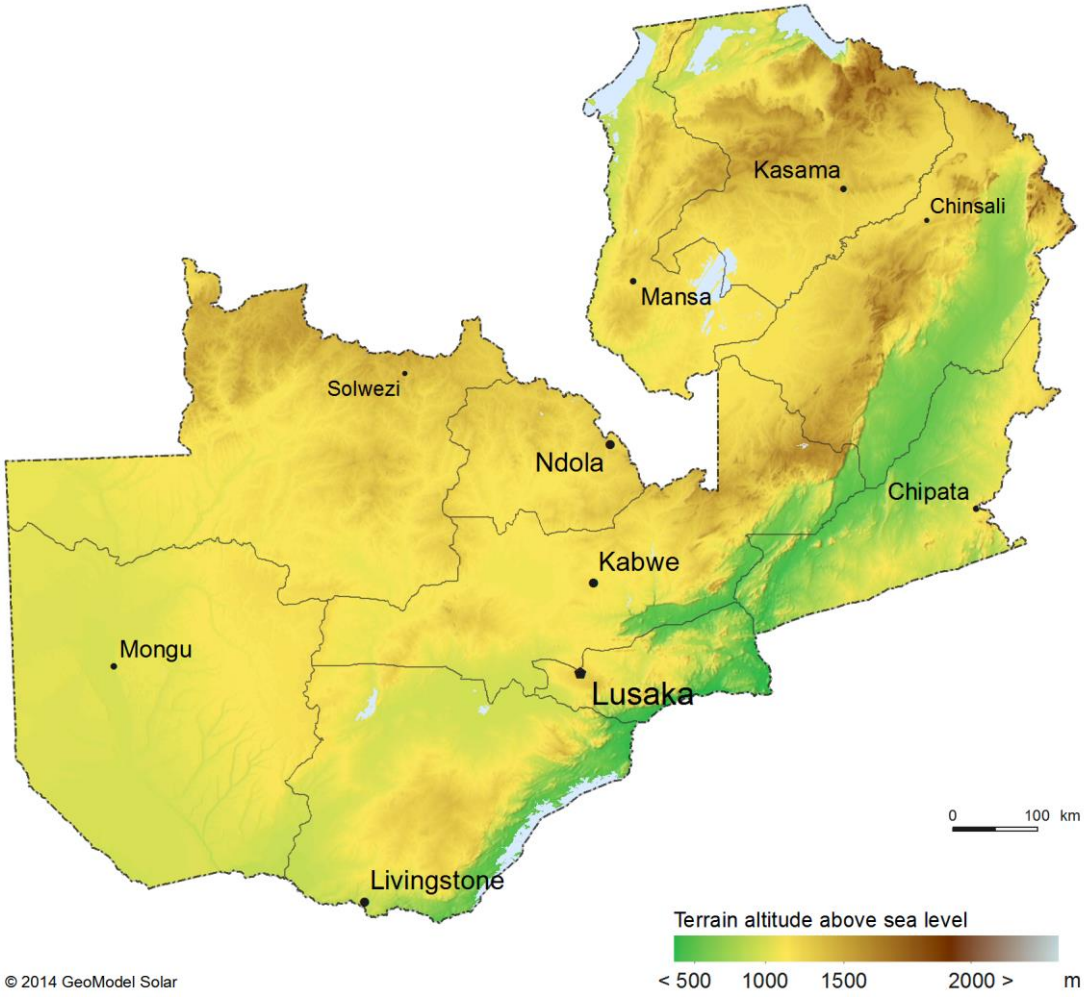

Fig. 6.3: Terrain altitude. Source: SRTM-3.

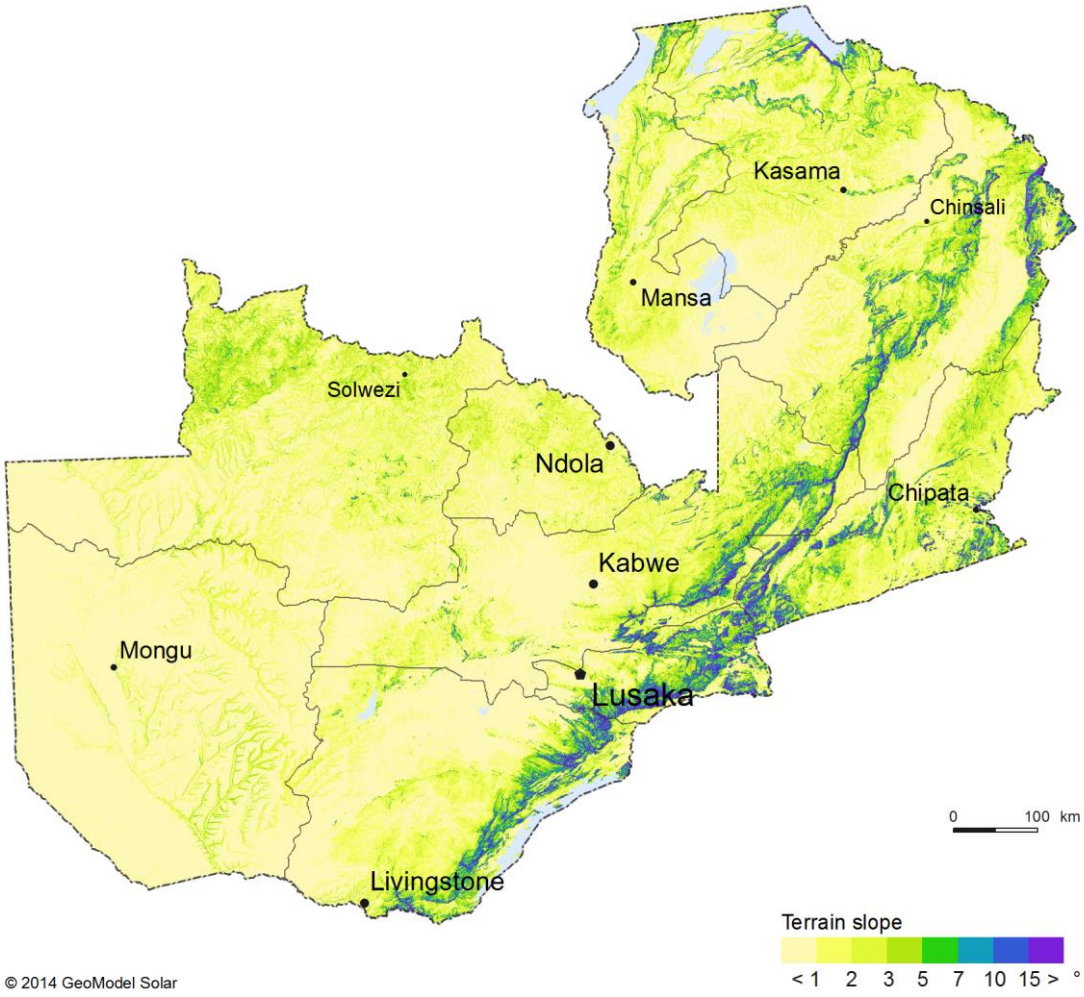

Fig. 6.4: Terrain slope. Source: SRTM-3 and SolarGIS.

6.3 Air temperature

Knowledge of **air temperature** is important, as it determines the operating environment and performance efficiency of solar power systems. Air temperature is used as one of inputs in energy simulation models. In this report yearly and monthly average maps are presented.

In case of PV power plants, air temperature determines energy conversion efficiency in the PV modules, and it also influences other components (inverters, transformers, etc.). Increasing air temperature has negative influence on performance of PV systems.

The temperature data in time series are derived from CFSR and CFSv2 meteorological models (see Chapter 4.2) by SolarGIS post-processing, and they represent regional climate patterns rather than local microclimate. This means that extreme values may be partially smoothed and they not always well represent the local microclimate. The temperature maps are developed only using the CFSR model data (Figs. 6.5 and 6.6).

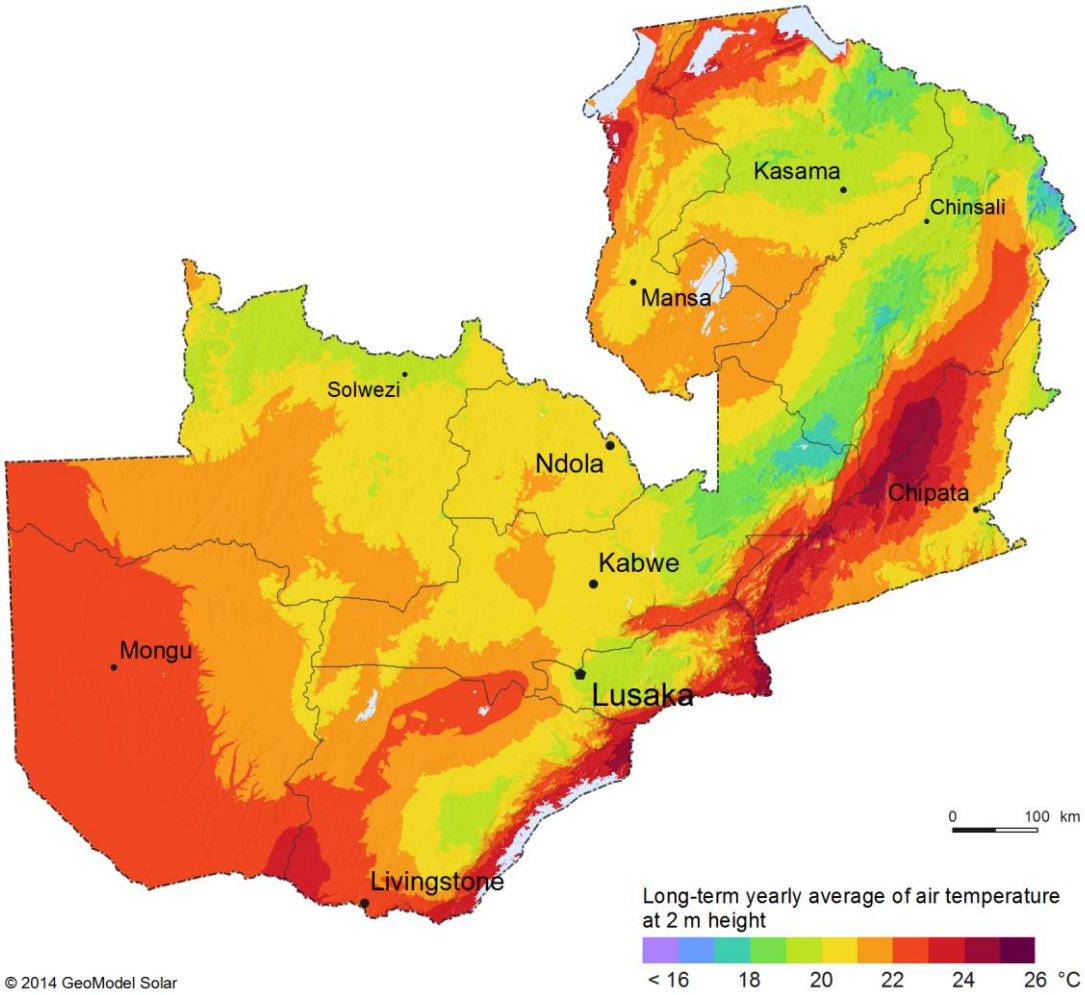

Fig. 6.5: Longterm yearly average of air temperature at 2 metres.
Source: CFSR

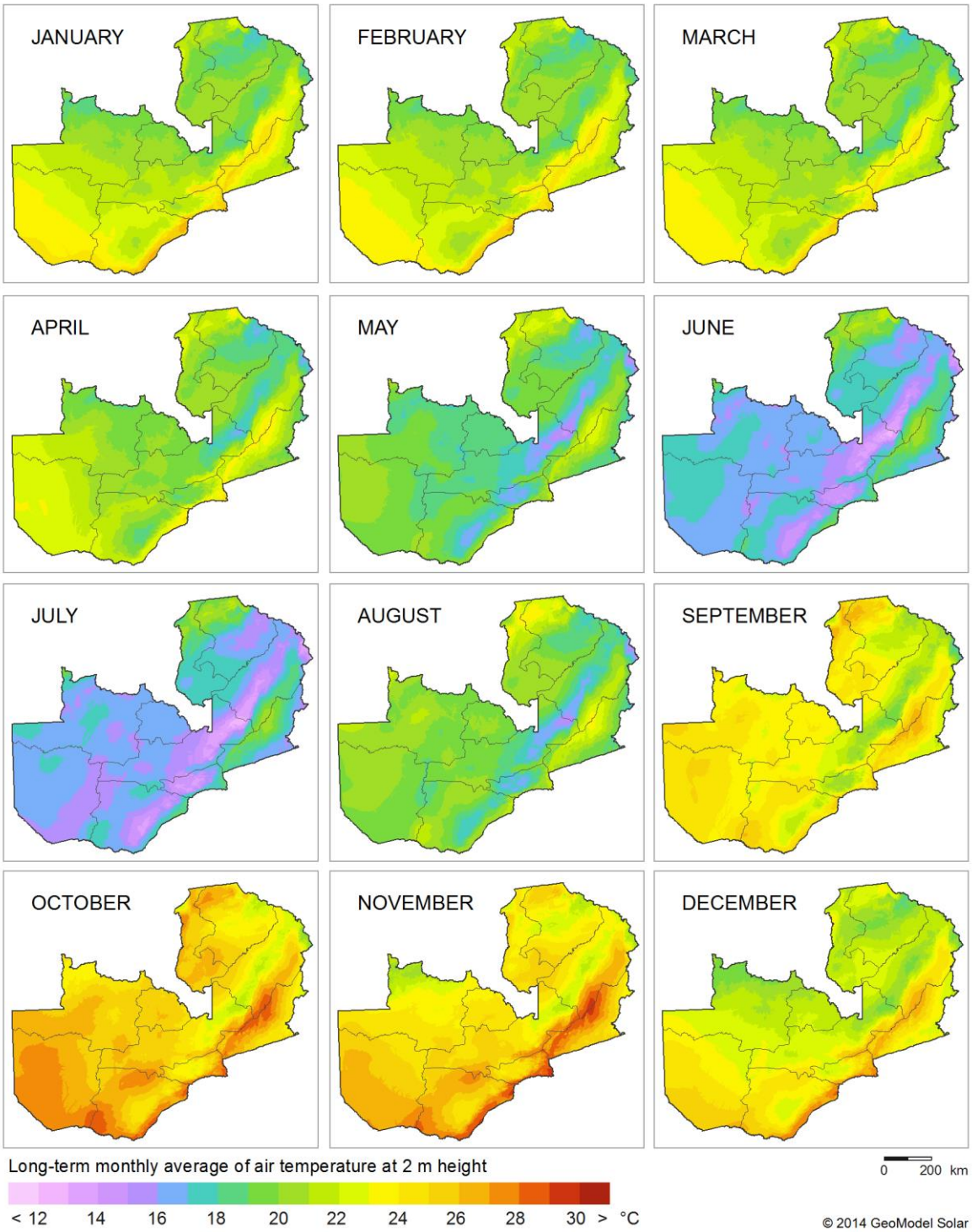

Fig. 6.6: Longterm monthly average of air temperature. Source CFSR.
Source: CFSR

Tab. 6.2 shows monthly characteristics of air temperature at six selected sites; they represent statistics calculated over 24-hour diurnal cycle. Minimum and maximum air temperature are calculated as average of minimum and maximum values of temperature during each day (assuming full diurnal cycle - 24 hours) of the given month.

Tab. 6.2: Monthly averages and average minima and maxima of air-temperature at 2 m at 6 sites

Month	Temperature [°C]											
	Longe		Lusaka		Misamfu		Mochipapa		Msekera		Mutanda	
	Average	Min Max	Average	Min Max	Average	Min Max	Average	Min Max	Average	Min Max	Average	Min Max
January	**22.0**	20.5 23.9	**20.9**	19.4 22.8	**19.6**	18.5 21.0	**21.4**	19.1 23.9	**21.5**	20.7 22.6	**20.1**	19.4 21.4
February	**21.9**	20.8 23.8	**20.4**	19.1 21.9	**19.6**	18.6 20.7	**20.7**	19.0 23.0	**21.1**	19.8 22.4	**20.1**	19.3 21.5
March	**21.8**	20.6 24.4	**20.1**	18.5 22.3	**19.4**	18.4 20.8	**20.3**	18.5 23.0	**20.9**	19.5 22.8	**20.0**	18.6 21.4
April	**21.1**	19.4 23.0	**18.9**	17.4 20.6	**18.6**	17.4 19.9	**18.7**	16.8 20.5	**19.9**	17.8 21.6	**19.7**	17.8 21.8
May	**19.1**	17.7 20.4	**16.8**	15.3 17.9	**17.6**	16.1 18.8	**16.6**	14.8 18.4	**18.8**	17.0 20.0	**18.5**	16.7 20.1
June	**16.8**	15.0 18.0	**14.9**	13.4 16.0	**16.0**	14.2 17.1	**14.5**	13.0 15.4	**17.2**	15.5 18.3	**16.8**	14.5 18.2
July	**16.4**	15.3 19.3	**14.5**	13.4 17.2	**15.7**	14.2 17.8	**14.2**	13.0 17.1	**17.0**	15.8 20.2	**16.8**	15.5 19.3
August	**20.0**	18.5 21.0	**17.7**	16.1 19.3	**18.6**	17.1 19.8	**17.7**	15.8 19.2	**19.8**	18.6 21.5	**20.4**	19.0 21.6
September	**24.0**	22.9 25.1	**21.6**	19.9 23.5	**21.9**	20.9 23.4	**21.9**	19.8 23.8	**23.2**	21.7 24.8	**23.8**	23.1 25.0
October	**25.9**	24.8 26.9	**23.9**	22.3 25.3	**23.6**	22.5 24.7	**24.4**	22.8 26.1	**24.8**	23.2 26.1	**25.2**	23.8 26.2
November	**24.8**	22.9 26.2	**24.4**	22.7 25.8	**23.3**	21.9 24.8	**24.5**	22.6 25.7	**25.2**	23.9 26.5	**23.0**	21.2 24.5
December	**22.7**	21.1 25.5	**22.2**	20.8 24.2	**20.9**	19.3 23.1	**22.4**	20.4 24.7	**22.9**	21.2 24.6	**20.7**	19.6 23.3
YEAR	**21.4**		**19.7**		**19.6**		**19.8**		**21.0**		**20.4**	

Monthly averages of minimum and maximum daily values show their typical daily amplitude in each month (Fig. 6.7). See Chapter 9 discussing the uncertainty of the air temperature model estimates.

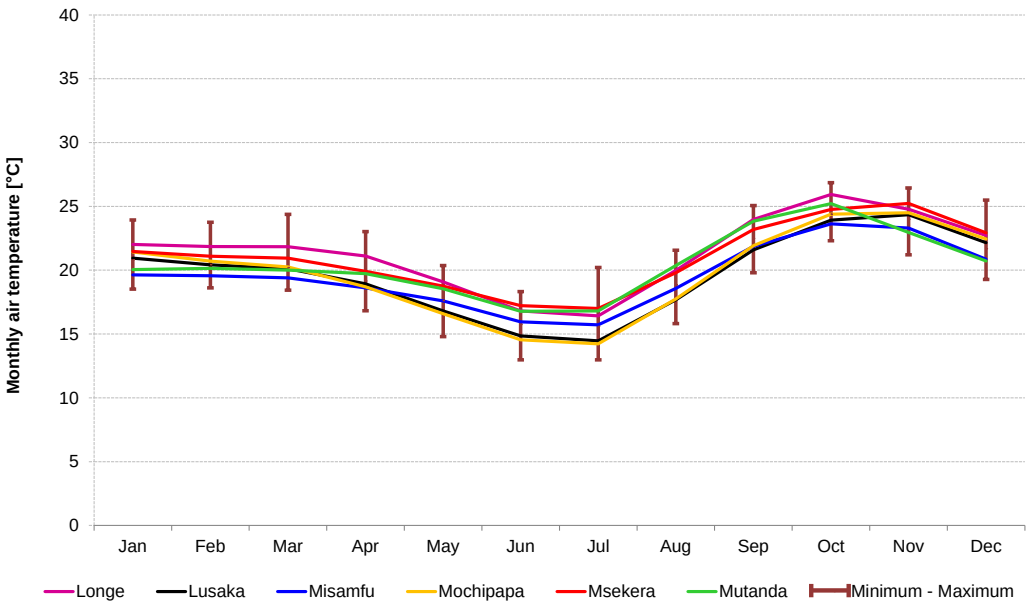

Fig. 6.7: Monthly averages, minima and maxima of air-temperature at 2 m for selected sites.

7 SOLAR RESOURCE IN ZAMBIA

- In this chapter the regional differences of basic solar parameters are shown. **Global Horizontal Irradiation** (GHI) is often considered as a climate reference as it enables to compare individual sites or regions.
- The most important parameter for photovoltaic (PV) power potential evaluation is **Global Tilted Irradiation** (GTI), i.e. sum of direct and diffuse solar radiation falling at the tilted surface of PV modules. It is the combination of diffuse and direct components of GTI (or GHI) that determine performance characteristics of the PV technology (Chapter 5.1).
- **Direct Normal Irradiation** (DNI) is relevant for solar thermal power plants (CSP) and photovoltaic concentrating technologies (CPV; see Chapter 5.2).

The data and maps in Chapters 7 and 8 are based on the data representing a history of 20 continuous years: from 1994 to 2013. This report may not reflect a possible man-induced climate change or occurrence of extreme events such as large volcano eruptions [38, 39].

7.1 Global Horizontal Irradiation

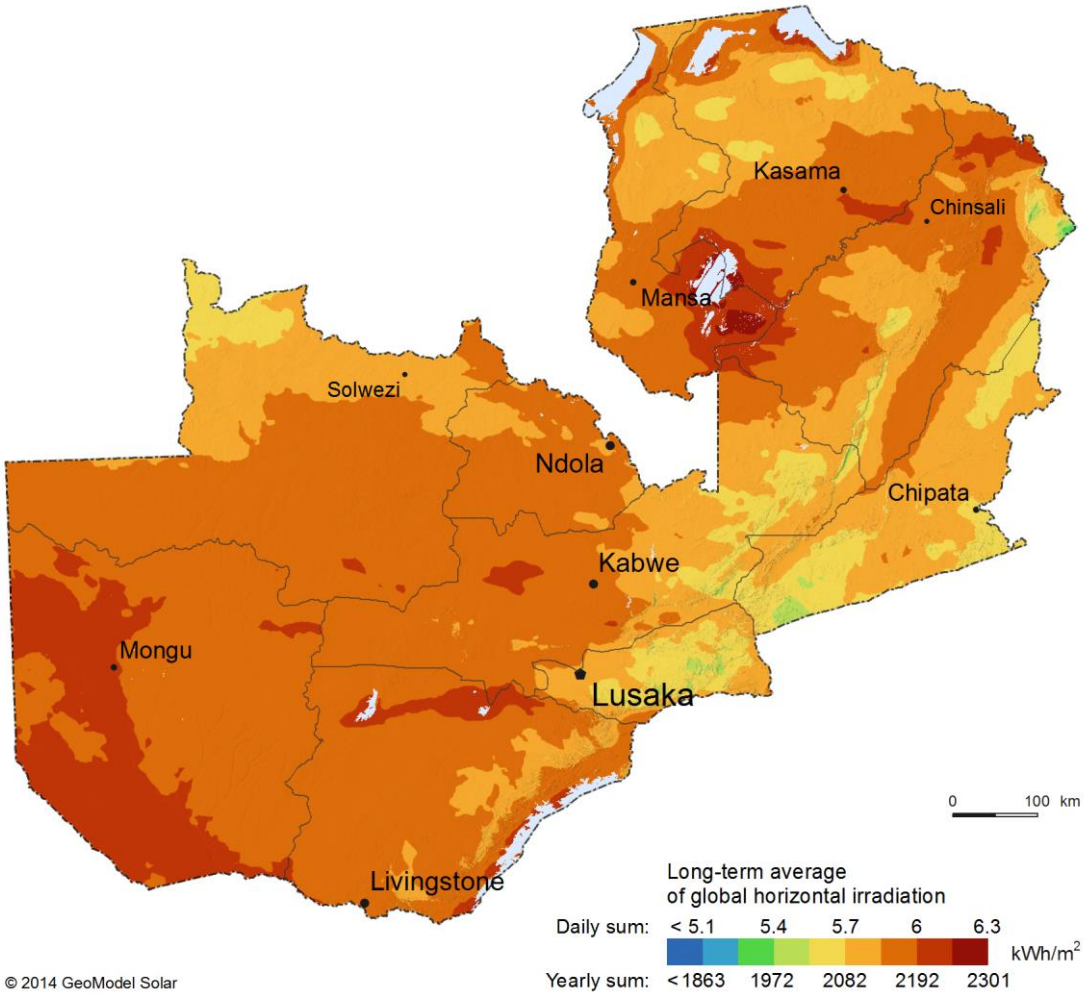

Fig. 7.1: Global Horizontal Irradiation - longterm averages of daily/yearly sum.

Global Horizontal Irradiation (GHI) is used as a reference value for comparing geographical conditions related to PV electricity systems, ignoring possible modifications, given by choice of PV system components and the configuration of a module field.

The highest GHI is identified in the South-west part of the Western province and in South-east part of Luapula province, where average daily sums reach 6.3 kWh/km^2 (yearly sum about 2300 kWh/km^2) and more (Fig. 7.1). Season of highest irradiation lasts four months (from August to November, Fig. 7.2).

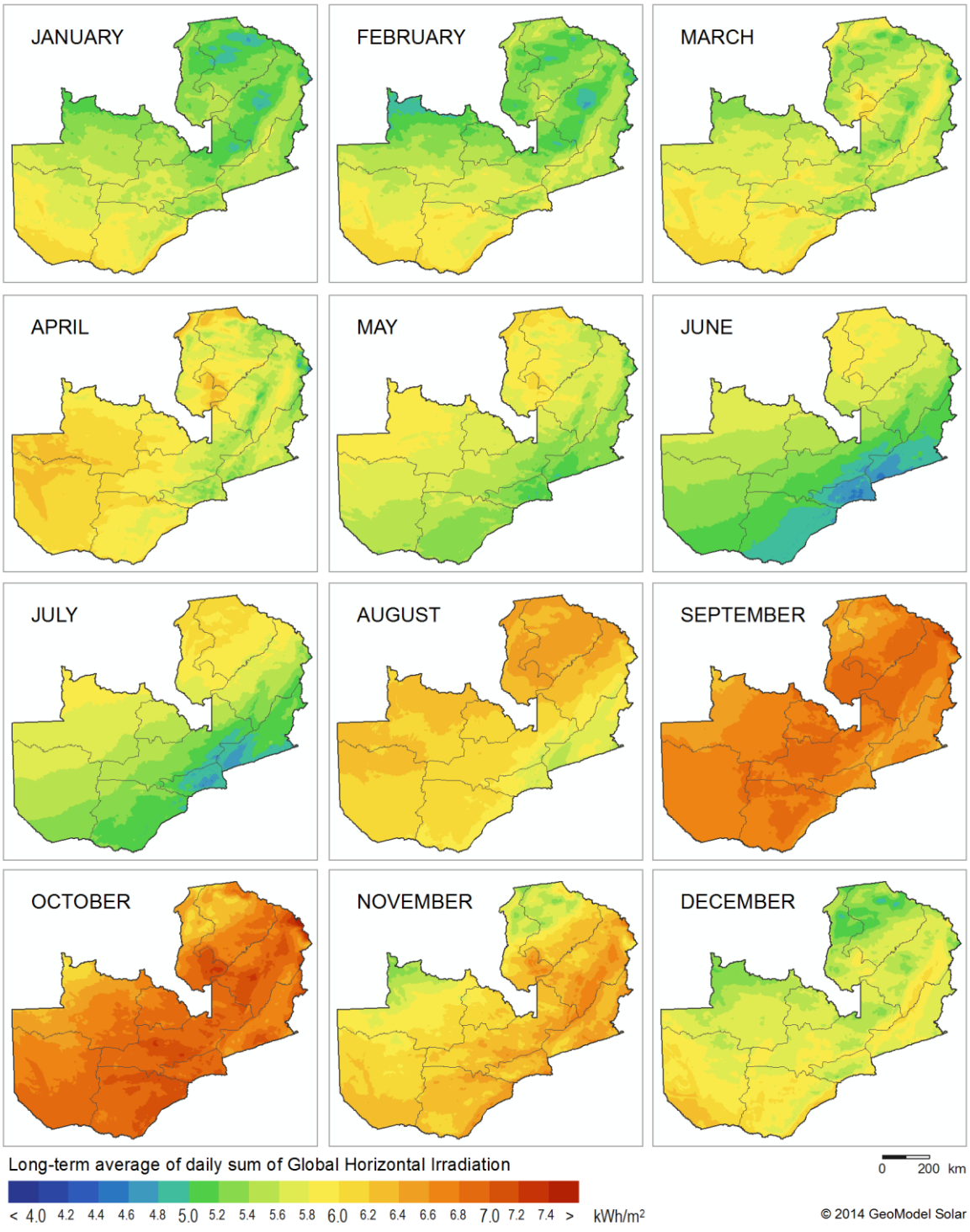

Fig. 7.2: Global Horizontal Irradiation - longterm monthly averages.

Tab. 7.1 shows longterm average, and average minima and maxima of daily summaries of Global Horizontal Irradiation (GHI) for a period 1994 to 2013 for six selected sites.

Tab. 7.1: Daily averages and average minima and maxima of Global Horizontal Irradiation at 6 sites

Month	Global Horizontal Irradiation [kWh/m^2]											
	Longe		Lusaka		Misamfu		Mochipapa		Msekera		Mutanda	
	Average	Min Max	Average	Min Max	Average	Min Max	Average	Min Max	Average	Min Max	Average	Min Max
January	**5.73**	5.06 6.74	**5.51**	4.43 6.30	**5.26**	4.54 5.82	**5.65**	4.61 6.69	**5.33**	4.48 5.98	**5.31**	4.94 5.84
February	**5.87**	4.90 6.74	**5.52**	4.04 6.57	**5.38**	4.60 6.29	**5.74**	4.47 7.02	**5.51**	4.52 6.42	**5.32**	4.69 6.36
March	**5.86**	4.97 7.22	**5.57**	4.84 6.58	**5.57**	5.12 6.11	**5.69**	4.89 7.00	**5.52**	4.76 6.64	**5.60**	4.85 6.95
April	**6.22**	5.66 6.56	**5.69**	5.04 6.32	**5.69**	4.96 6.07	**5.77**	5.02 6.26	**5.56**	4.80 6.16	**5.98**	5.44 6.33
May	**5.74**	5.28 6.12	**5.41**	4.46 5.95	**5.68**	4.56 6.18	**5.34**	4.25 5.89	**5.32**	4.04 5.86	**5.84**	4.79 6.25
June	**5.40**	4.93 5.62	**4.93**	4.22 5.48	**5.73**	5.38 6.07	**4.92**	4.15 5.35	**4.93**	4.33 5.51	**5.68**	5.40 5.90
July	**5.60**	5.08 5.77	**5.12**	4.43 5.58	**5.90**	5.42 6.15	**5.13**	4.29 5.58	**5.03**	4.24 5.62	**5.80**	5.36 5.98
August	**6.22**	5.98 6.50	**5.95**	5.50 6.25	**6.47**	5.73 6.87	**6.07**	5.70 6.30	**5.66**	4.51 6.28	**6.27**	5.85 6.57
September	**6.79**	6.32 7.17	**6.77**	5.99 7.06	**6.86**	5.97 7.29	**6.86**	6.17 7.15	**6.52**	6.09 7.06	**6.71**	5.86 7.10
October	**6.86**	6.21 7.50	**7.01**	6.18 7.63	**6.80**	6.07 7.45	**7.01**	6.41 7.97	**6.65**	5.85 7.29	**6.67**	6.14 7.39
November	**6.18**	5.67 6.75	**6.40**	5.68 6.90	**6.25**	5.17 6.91	**6.22**	5.42 7.31	**6.36**	5.43 6.93	**5.89**	5.19 6.48
December	**5.82**	5.29 6.48	**5.75**	4.63 6.65	**5.67**	4.91 6.37	**5.80**	4.58 6.53	**5.68**	4.71 6.54	**5.54**	5.12 6.46
YEAR	**6.02**	**5.45** **6.60**	**5.80**	**4.96** **6.44**	**5.94**	**5.20** **6.46**	**5.85**	**5.00** **6.58**	**5.67**	**4.81** **6.36**	**5.89**	**5.31** **6.47**

Fig. 7.3 compares daily values of Global horizontal irradiation (GHI). When comparing the sites, GHI monthly values have similar pattern. Most stable weather with highest GHI values is from September to December, the highest variability of GHI is observed in a period from April to August. Relatively small variability between the sites is caused by their similar geographical characteristics, and this indicates that all sites will experience similar performance of PV power systems.

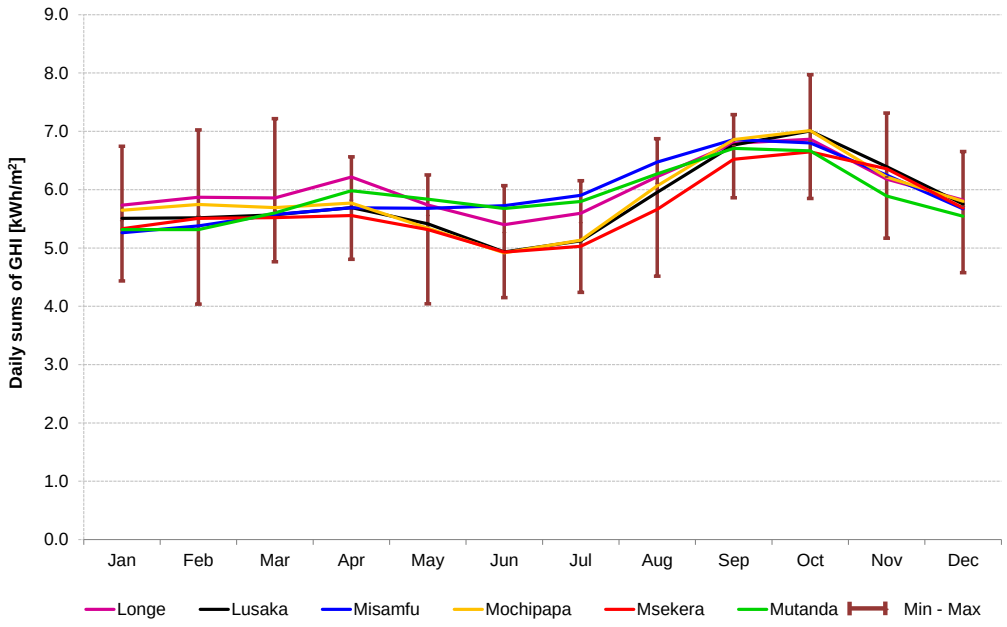

Fig. 7.3: Longterm monthly averages, minima and maxima of Global Horizontal Irradiation.

Weather changes in cycles and has also stochastic nature. Therefore annual solar radiation in each year can deviate from the longterm average in the range of few percent. Fig 7.4 shows interannual variability, i.e. the magnitude of the year-by-year GHI change.

The interannual variability of GHI for the selected sites is calculated from the unbiased standard deviation of GHI over 20 years, considering a simplified assumption of normal distribution of the annual sums. All sites show similar patterns of varying GHI over the recorded period. Extremes for all sites (minimum and maximum) or values close to the extremes are reached almost in the same years. The most stable GHI values (the smallest interannual variability) are observed in Mutanda. Longe and Misamfu have almost the same GHI interannual variability. The most variable site is Msekera; this site has also the lowest irradiation.

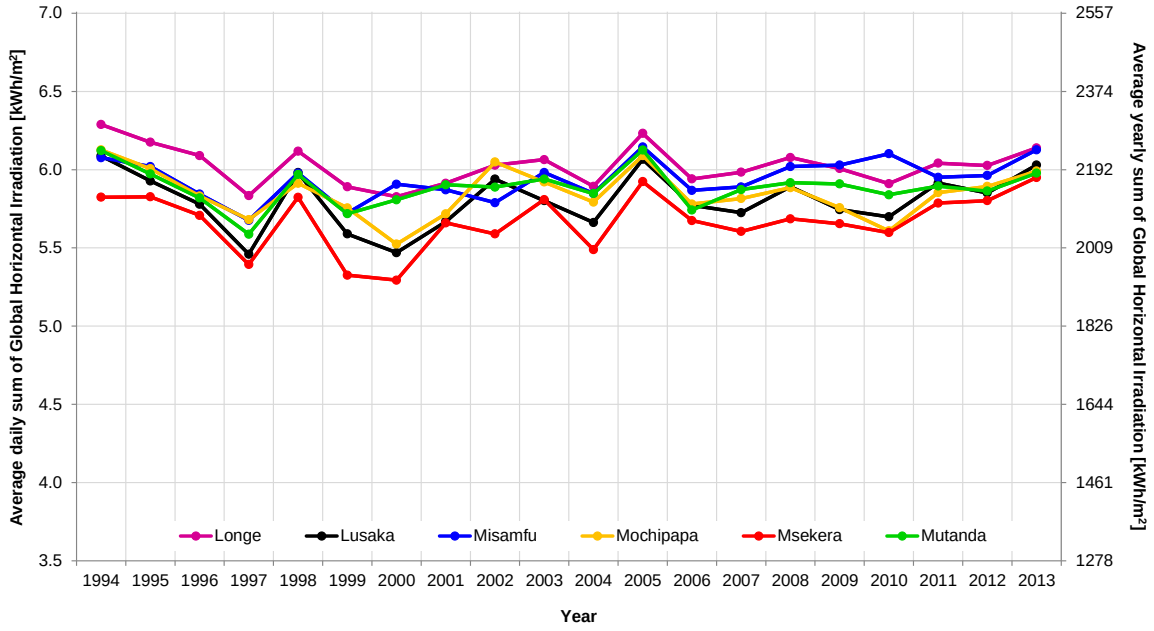

Fig. 7.4: Interannual variability of GHI for selected sites.

7.2 Ratio of diffuse and global irradiation

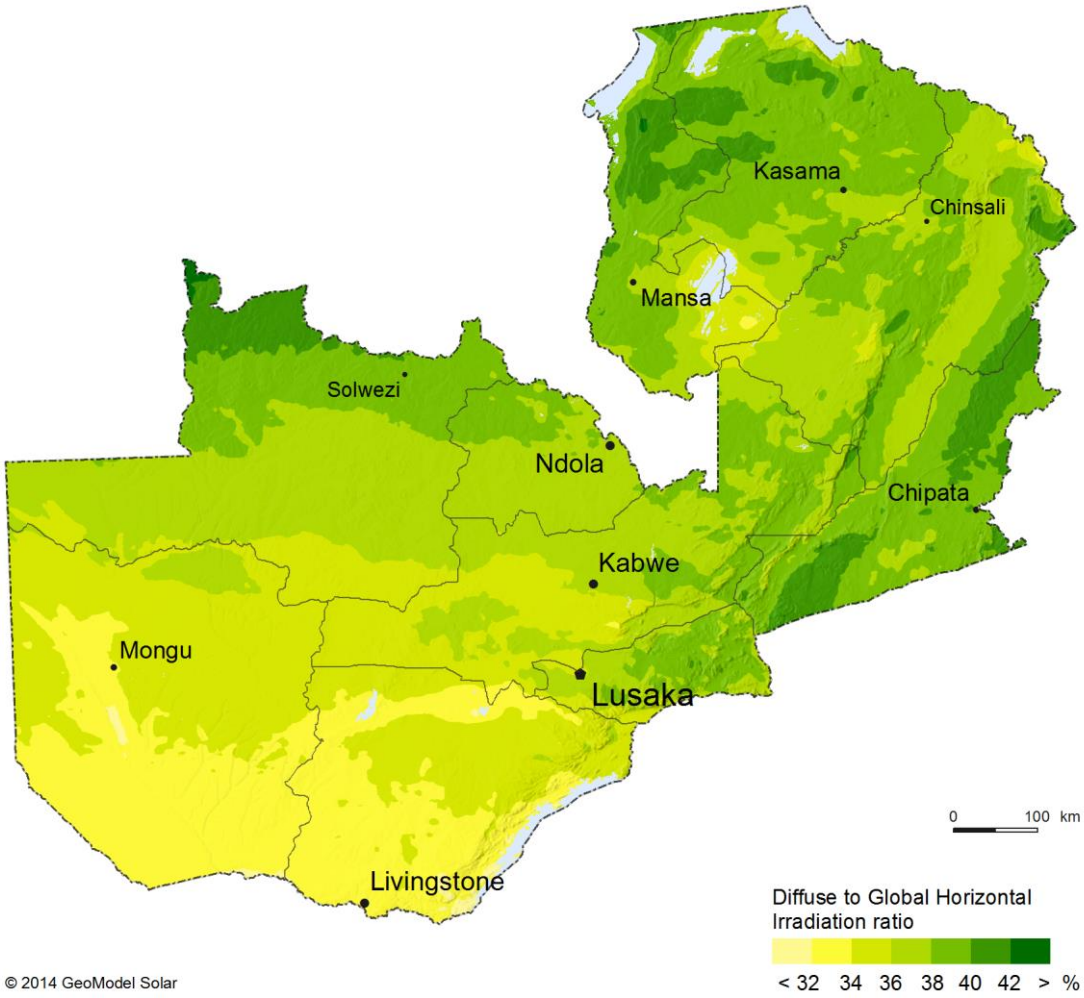

Fig. 7.5: Ratio of Diffuse to Global Horizontal Irradiation (DIF/GHI) - longterm yearly average

Higher values of DIF/GHI ratio represent: less stable weather, higher occurrence of clouds, higher atmospheric pollution or higher water vapour. The lowest DIF/GHI values are identified in the Western and Southern provinces, where the yearly average ratio falls below 34% (Fig 7.5).

Season with the most stable weather is May and June in Zambia (Fig 7.6). During humid season, from October to March all sites show stable, but relatively high DIF/GHI ratio. The best conditions with clear sky and low aerosols typically occur from April to August, when DIF/GHI ratio is reduced approximately to half.

The period of low DIF/GHI ratio is shorter and not constant, which indicates a potential for concentrator technologies (see Chapter 7.4).

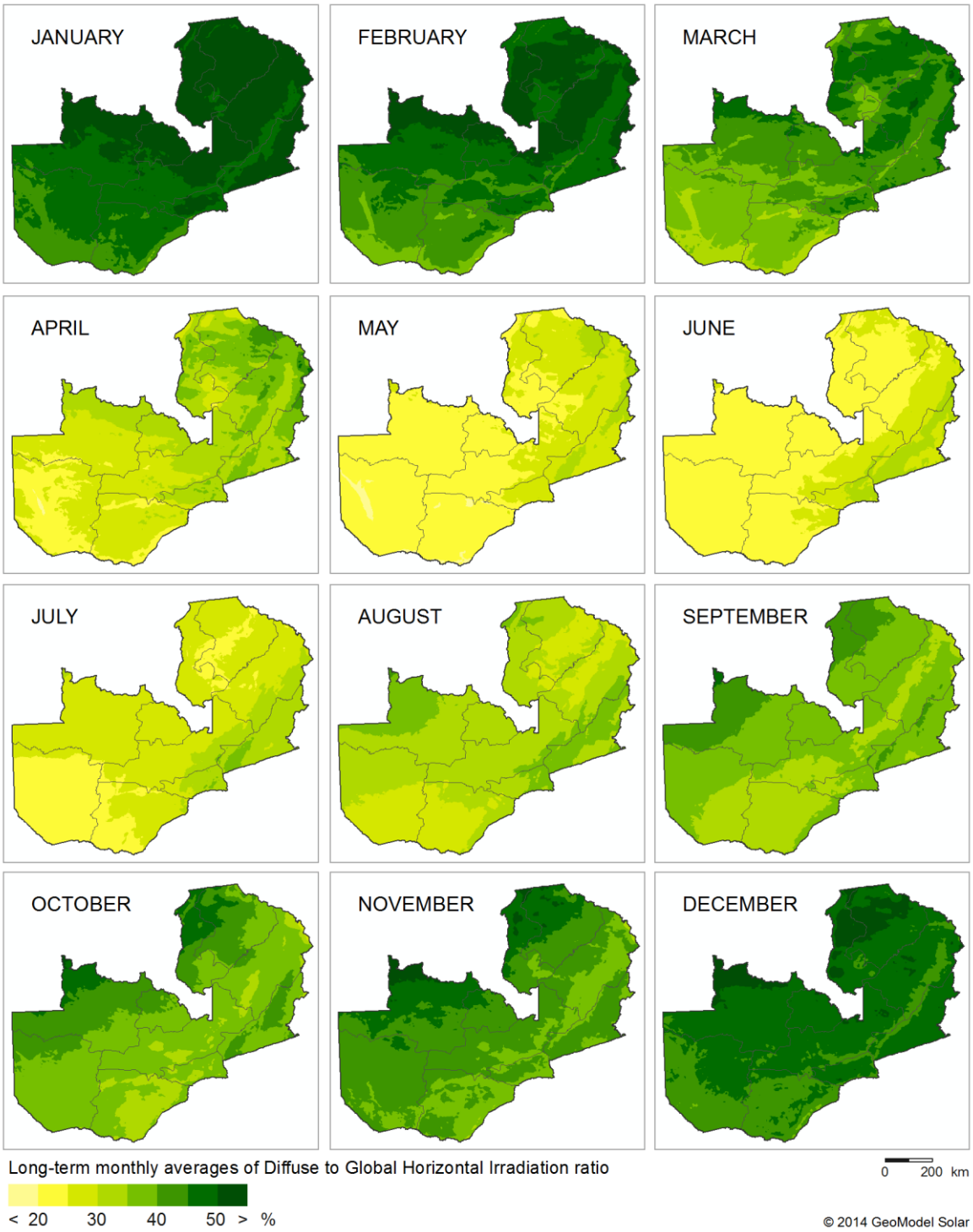

Fig. 7.6: Ratio of Diffuse to Global Horizontal Irradiation - longterm monthly averages

Tab. 7.2 and Fig. 7.7 show ratio of longterm averages of Diffuse Horizontal Irradiation to Global Horizontal Irradiation (noted also as DIF/GHI) for each of selected sites in every month.

Tab. 7.2: Monthly averages of Ratio of Diffuse to Global Horizontal Irradiation (DIF/GHI)

Month	Average Diffuse to Global Horizontal Irradiation Ratio [%]					
	Longe	Lusaka	Misamfu	Mochipapa	Msekera	Mutanda
January	46.9	49.3	54.5	48.4	53.9	52.3
February	43.7	47.4	52.3	45.3	50.6	51.1
March	37.9	43.1	48.2	40.1	45.4	43.3
April	24.6	31.3	39.3	29.1	35.7	31.7
May	20.8	23.9	28.8	23.2	29.3	23.1
June	21.9	26.1	23.6	23.9	29.8	21.8
July	24.0	27.7	25.5	25.7	32.1	26.7
August	30.6	30.7	29.2	27.6	35.4	34.5
September	36.0	33.2	36.9	31.5	38.5	40.0
October	37.7	34.0	39.9	33.3	41.1	42.7
November	41.6	38.6	42.6	40.5	42.7	46.7
December	46.2	45.8	48.2	45.8	49.2	49.0
YEAR	**34.4**	**36.0**	**38.7**	**34.7**	**40.4**	**38.3**

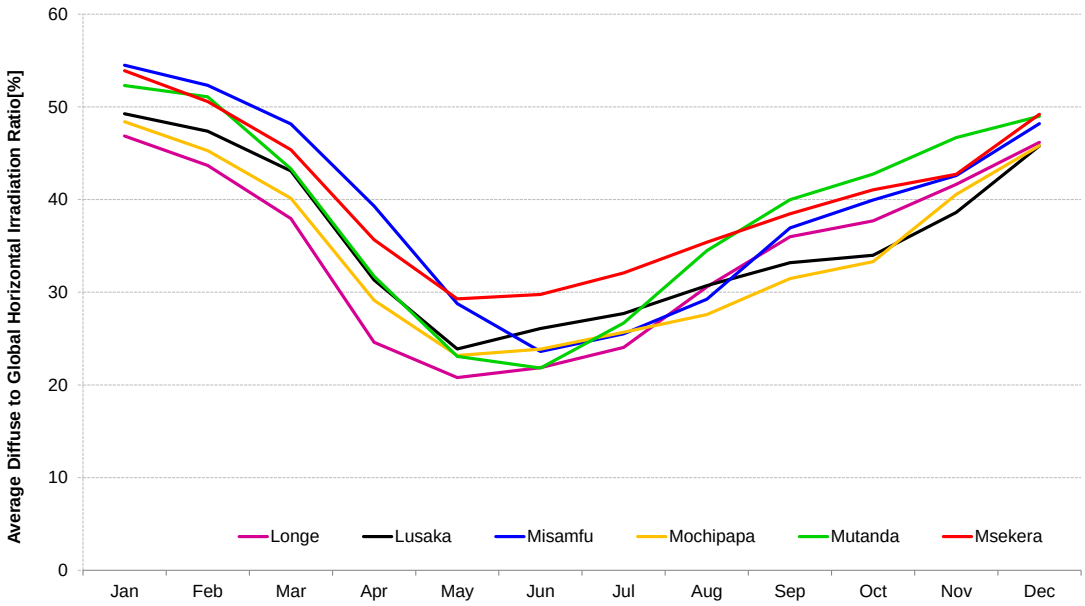

Fig. 7.7: Monthly averages of Ratio of Diffuse to Global Horizontal Irradiation.

The lowest DIF/GHI ratio is found in Longe and Mochipapa sites, which are located in the South-west of the country. The highest DIF/GHI ratio is recorded in Msekera.

7.3 Global Tilted Irradiation

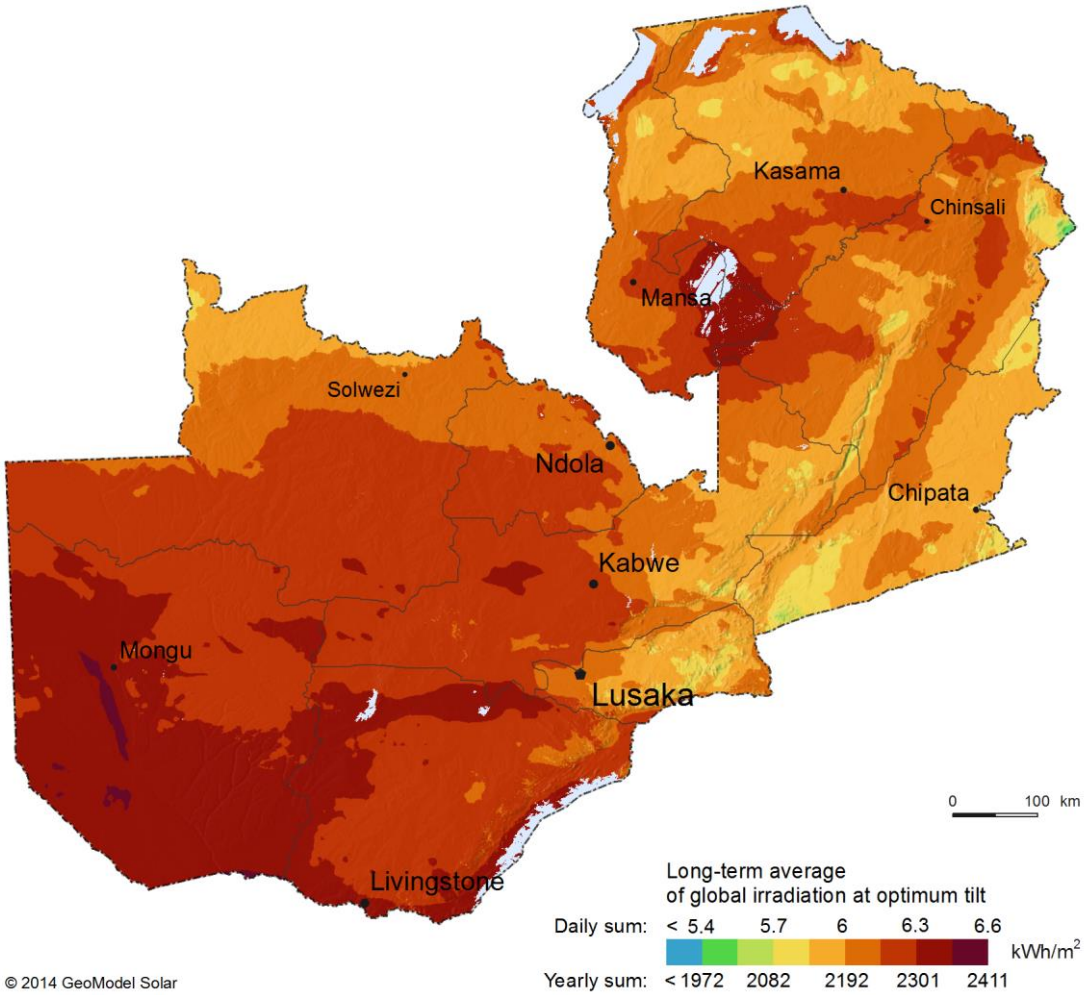

Fig. 7.8: Global Tilted Irradiation at optimum angle – longterm averages of daily/yearly sum.

Global Tilted Irradiation (GTI) is harvested by flat-plate photovoltaic (PV) technologies (Chapter 5.1).

The regional trend of Global Tilted Irradiation received by PV modules tilted at optimum angle (GTI) is similar to GHI (Fig. 7.8). Moving PV modules to optimum tilt (module inclination; Fig. 7.9) results in increased average daily sum of GTI up to 6.6 kWh/km^2 (yearly sum about 2410 kWh/km^2) and more, especially in Western, Southern and Luapula provinces.

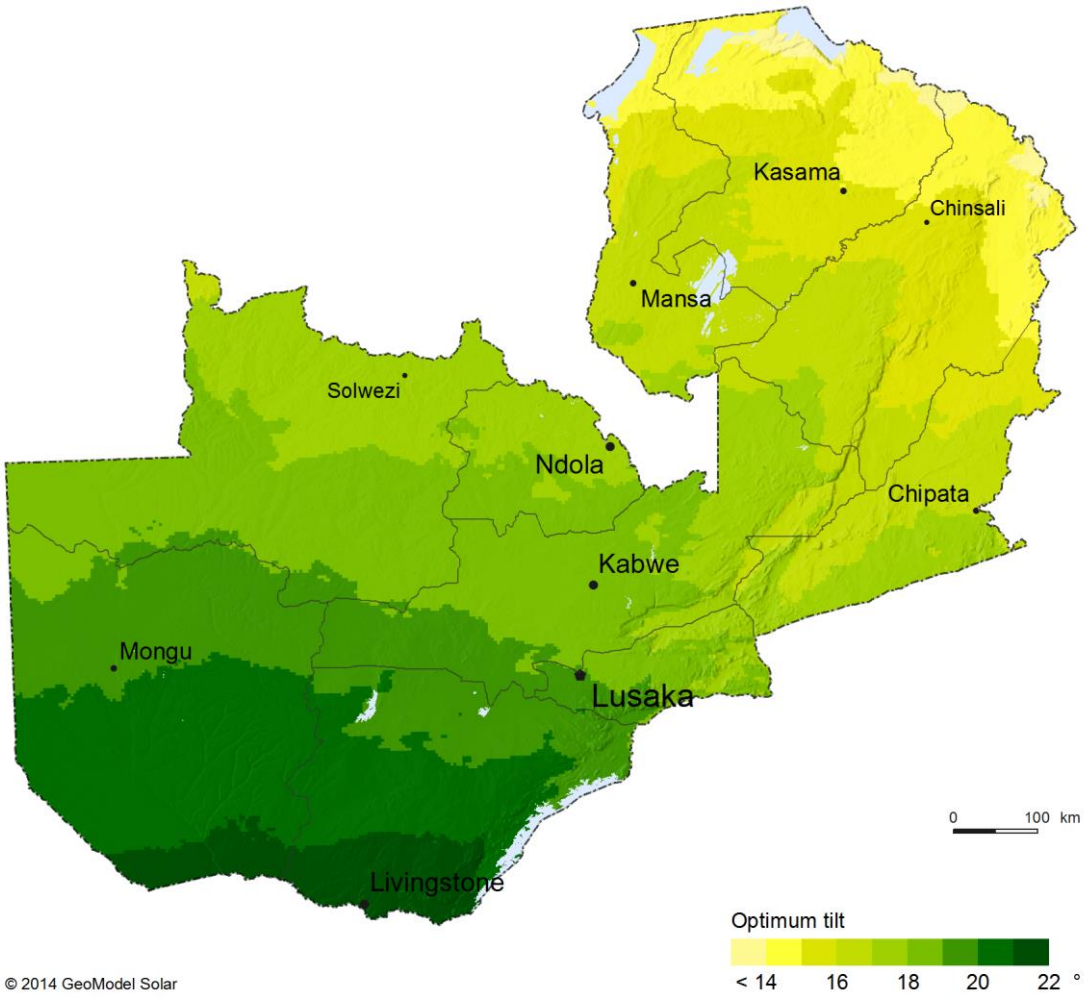

Fig. 7.9: Optimum tilt of PV modules towards North to maximize yearly energy yield.

The main parameter influencing optimum tilt in Zambia is latitude, which spans between 8° and 18° South. For this region, optimum tilt is North between 14° and 22° (increasing from North to South; Fig. 7.9). As can be observed, the optimum tilt is determined by latitude but also by ratio between diffuse and global horizontal irradiation which reduces the effect of latitude in the humid North and augments it in more arid South (Fig. 7.5).

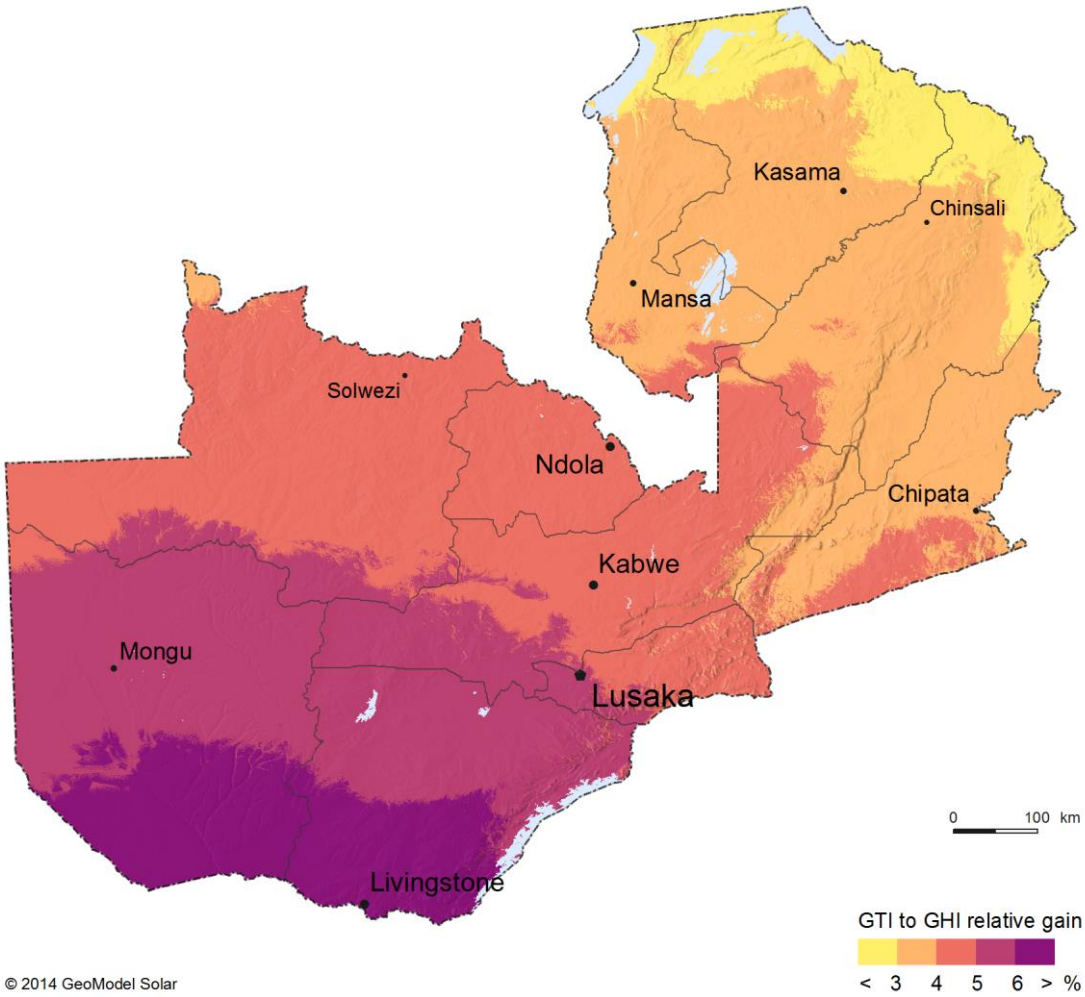

Fig. 7.10: Gain of yearly Global Tilted Irradiation relative to Global Horizontal Irradiation. GTI is calculated for North-oriented PV modules tilted at optimum tilt.

Fig 7.10 shows regional comparison of GTI and GHI solar radiation. GTI represents the global irradiation that is received by surface of PV modules optimally tilted to maximize yearly energy yield. Unlike horizontal surface, the tilted surface also receives small amount of ground-reflected radiation. Highest GTI gains are recorded in Western and Southern provinces, which are further from the equator and where the DIF/GHI ratio is lower.

Tab. 7.3 show longterm averages of average daily sums of Global Tilted Irradiation (GTI) for selected sites. It is assumed that solar radiation is received by plane tilted at optimum tilt.

Tab. 7.3: Daily averages and average minima and maxima of Global Tilted Irradiation at 6 sites

Month	Global Tilted Irradiation [kWh/m^2]											
	Longe		Lusaka		Misamfu		Mochipapa		Msekera		Mutanda	
	Average	Min Max	Average	Min Max	Average	Min Max	Average	Min Max	Average	Min Max	Average	Min Max
January	**5.20**	4.63 6.05	**5.02**	4.09 5.70	**4.86**	4.23 5.35	**5.12**	4.23 6.02	**4.95**	4.18 5.54	**4.87**	4.55 5.31
February	**5.59**	4.68 6.38	**5.27**	3.87 6.27	**5.15**	4.41 6.00	**5.48**	4.29 6.70	**5.30**	4.37 6.18	**5.07**	4.49 6.04
March	**5.99**	5.09 7.41	**5.70**	4.94 6.77	**5.61**	5.13 6.14	**5.86**	5.01 7.27	**5.62**	4.83 6.78	**5.68**	4.89 7.06
April	**6.97**	6.29 7.38	**6.36**	5.56 7.11	**6.10**	5.26 6.51	**6.54**	5.58 7.14	**6.08**	5.20 6.77	**6.55**	5.91 6.95
May	**6.93**	6.34 7.45	**6.53**	5.27 7.27	**6.47**	5.08 7.09	**6.57**	5.13 7.33	**6.19**	4.57 6.90	**6.85**	5.51 7.39
June	**6.76**	6.06 7.12	**6.15**	5.13 6.93	**6.74**	6.26 7.22	**6.28**	5.12 6.92	**5.91**	5.11 6.70	**6.89**	6.50 7.21
July	**6.86**	6.13 7.15	**6.26**	5.32 6.92	**6.84**	6.23 7.17	**6.41**	5.19 7.03	**5.92**	4.90 6.69	**6.88**	6.30 7.18
August	**7.11**	6.80 7.52	**6.82**	6.25 7.22	**7.12**	6.25 7.60	**7.07**	6.63 7.40	**6.31**	4.94 7.06	**6.99**	6.49 7.35
September	**7.17**	6.64 7.57	**7.17**	6.32 7.48	**7.08**	6.12 7.54	**7.34**	6.56 7.64	**6.83**	6.34 7.41	**6.98**	6.07 7.39
October	**6.71**	6.06 7.33	**6.86**	6.04 7.44	**6.61**	5.91 7.23	**6.89**	6.29 7.81	**6.52**	5.74 7.15	**6.50**	5.98 7.20
November	**5.67**	5.21 6.18	**5.88**	5.24 6.33	**5.78**	4.82 6.35	**5.71**	4.99 6.66	**5.92**	5.09 6.43	**5.45**	4.81 5.96
December	**5.20**	4.75 5.75	**5.15**	4.20 5.90	**5.15**	4.52 5.74	**5.18**	4.13 5.80	**5.20**	4.36 5.93	**5.01**	4.64 5.78
YEAR	**6.35**	**5.73** **6.94**	**6.10**	**5.19** **6.78**	**6.13**	**5.36** **6.66**	**6.21**	**5.27** **6.98**	**5.90**	**4.97** **6.63**	**6.15**	**5.52** **6.74**

Fig. 7.11 compares longterm daily averages for sites. Less stable weather, but with high GTI is seen from April to October. Variability of GTI between sites is largest in a period between April and September. Daily averages in a period from October to February are similar for all sites, and this relates to rainy season.

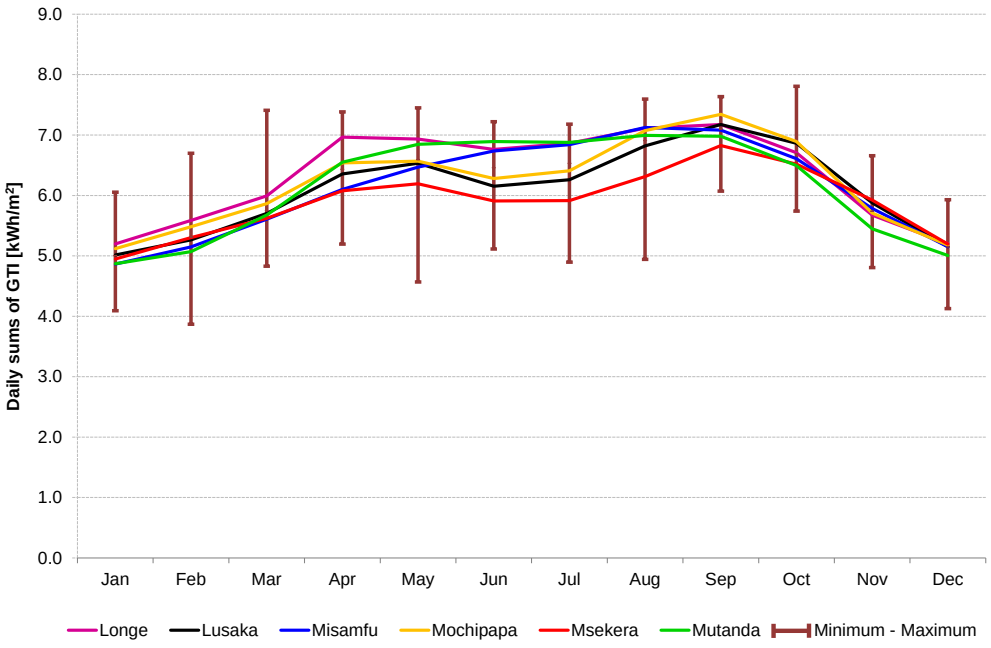

Fig. 7.11: Global Tilted Irradiation - longterm daily averages, minima and maxima.

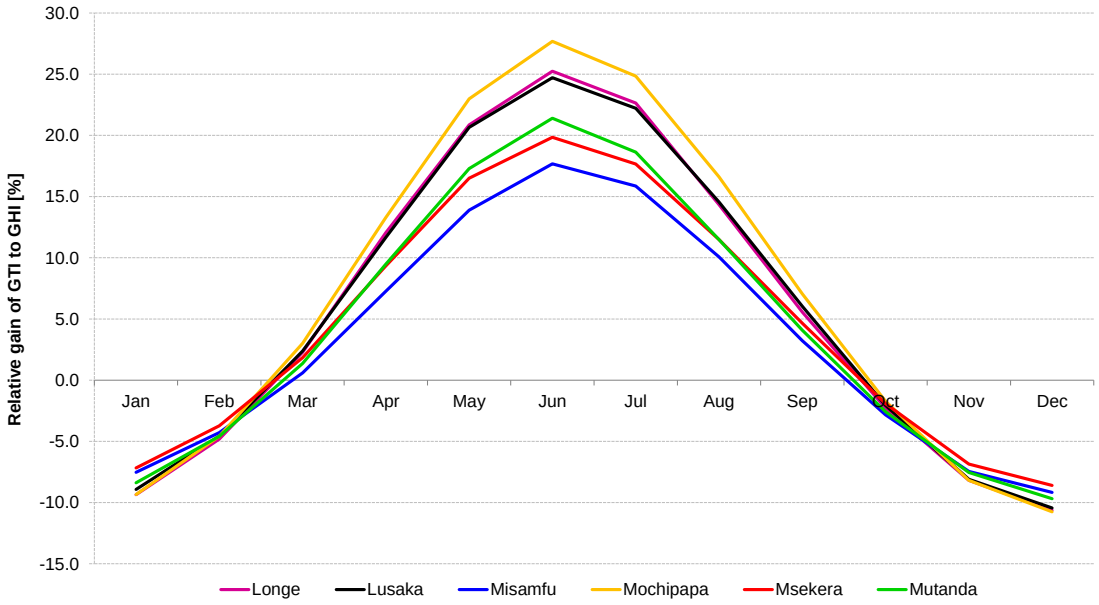

Fig. 7.12: Monthly relative gain of Global Tilted Irradiation to Global Horizontal Irradiation at 6 sites.

Surface inclined at optimum tilt gains more yearly irradiation than horizontal surface (Fig. 7.12). Gains are site-dependent and pronounced in dry season. The gain in June is about 17% for Misamfu site and up to 27% for the Mochipapa site. On the other side, in humid season, with highest sun position, the horizontal surface can receive more global irradiation (about 9% to 10%) than optimally tilted surface. This occurs during shorter period of year (from October to February), thus overall the yearly gains of irradiation for optimally tilted surface remain higher than for horizontal surface.

Detailed comparison of daily GTI and GHI values for Lusaka is shown in Fig. 7.13 and Tab. 7.4.

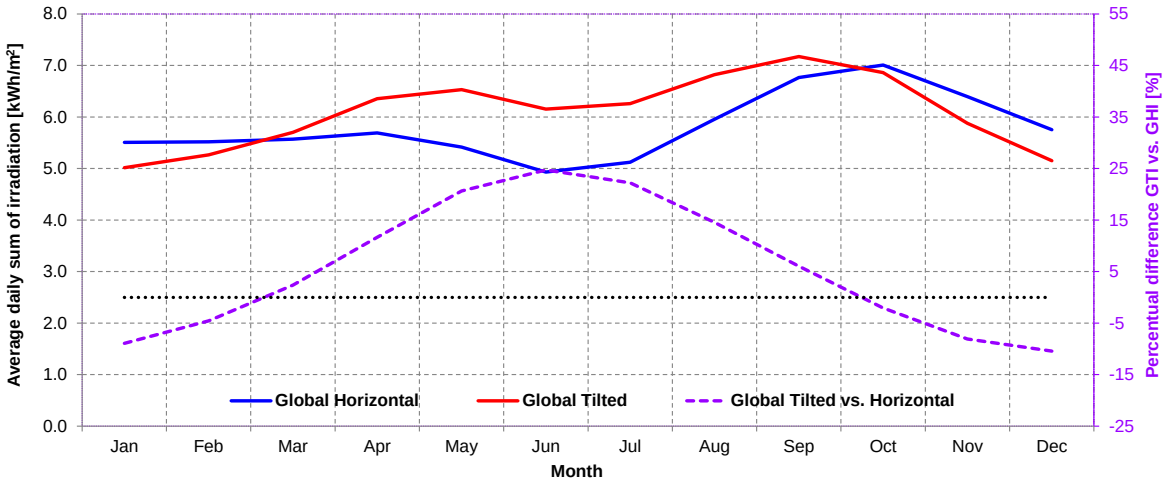

Fig. 7.13: Daily GHI (blue), GTI (red) and relative gain of monthly Global Tilted Irradiation relative to Global Horizontal Irradiation (violet) in Lusaka

Tab. 7.4: Relative gain of daily GTI to GHI in Lusaka

Site	Average daily sum of irradiation [kWh/m^2]												Year
	Jan	Feb	Mar	Apr	May	Jun	Jul	Aug	Sep	Oct	Nov	Dec	
Global Horizontal	5.51	5.52	5.57	5.69	5.41	4.93	5.12	5.95	6.77	7.01	6.40	5.75	5.80
Global Tilted	5.02	5.27	5.70	6.36	6.53	6.15	6.26	6.82	7.17	6.86	5.88	5.15	6.10
Global Tilted vs. Horizontal [%]	**-9**	**-5**	**2**	**12**	**21**	**25**	**22**	**15**	**6**	**-2**	**-8**	**-10**	**5**

Daily sums for each particular year are shown for better visual presentation of gain for tilted surfaces in comparison to horizontal ones. Fig. 7.14 shows daily sums for year 2013 in Lusaka. Blue pattern, representing GHI sums is transparent in order to make visible lower values of red, GTI pattern, during humid season.

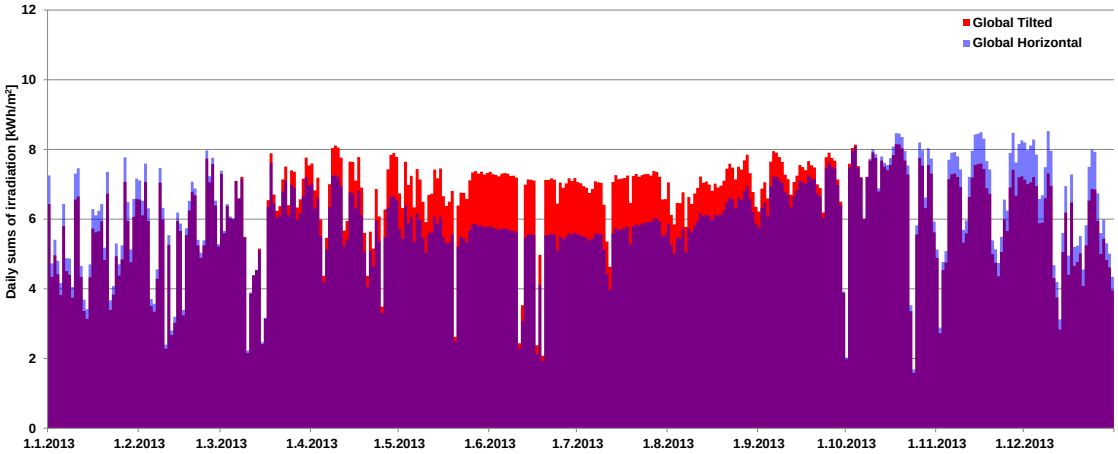

Fig. 7.14: Daily values of GHI and GTI for Lusaka, year 2013

7.4 Direct Normal Irradiation

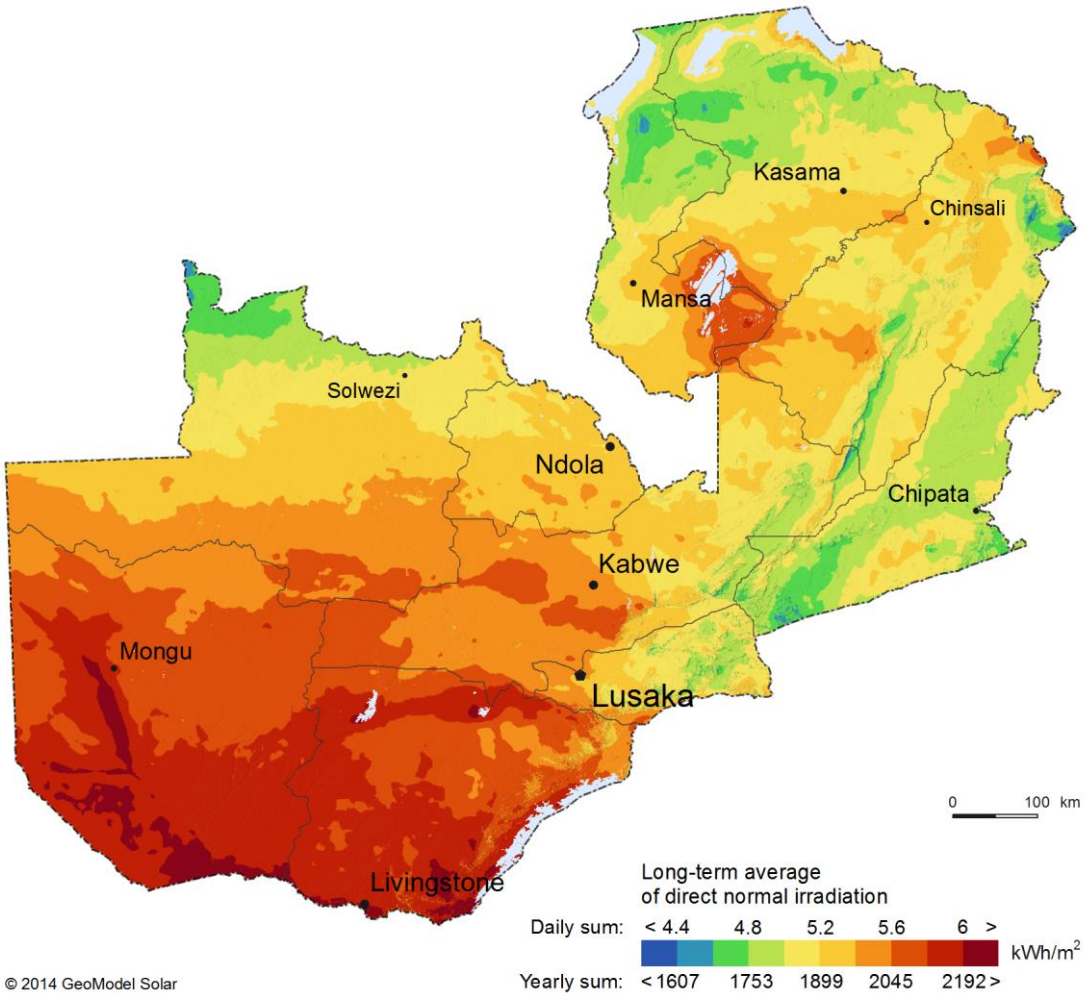

Fig. 7.15: Direct Normal Irradiation (DNI) - longterm averages of daily/yearly sum.

DNI parameter is decisive for solar thermal power plants and for concentrated PV technologies (Chapter 5.2).

The highest values are found in South of Zambia; lower values in the North are influenced by higher presence of aerosols and clouds in the atmosphere (Fig. 7.15).

When comparing monthly values of DNI with GHI it is apparent, that season of highest DNI yields is longer, and it lasts from April to August (Fig. 7.16).

South of the country indicates a promising DNI potential for installing CSP or CPV power plants. This potential has to be further explored by analysis also other factors important for developing concentrating technology.

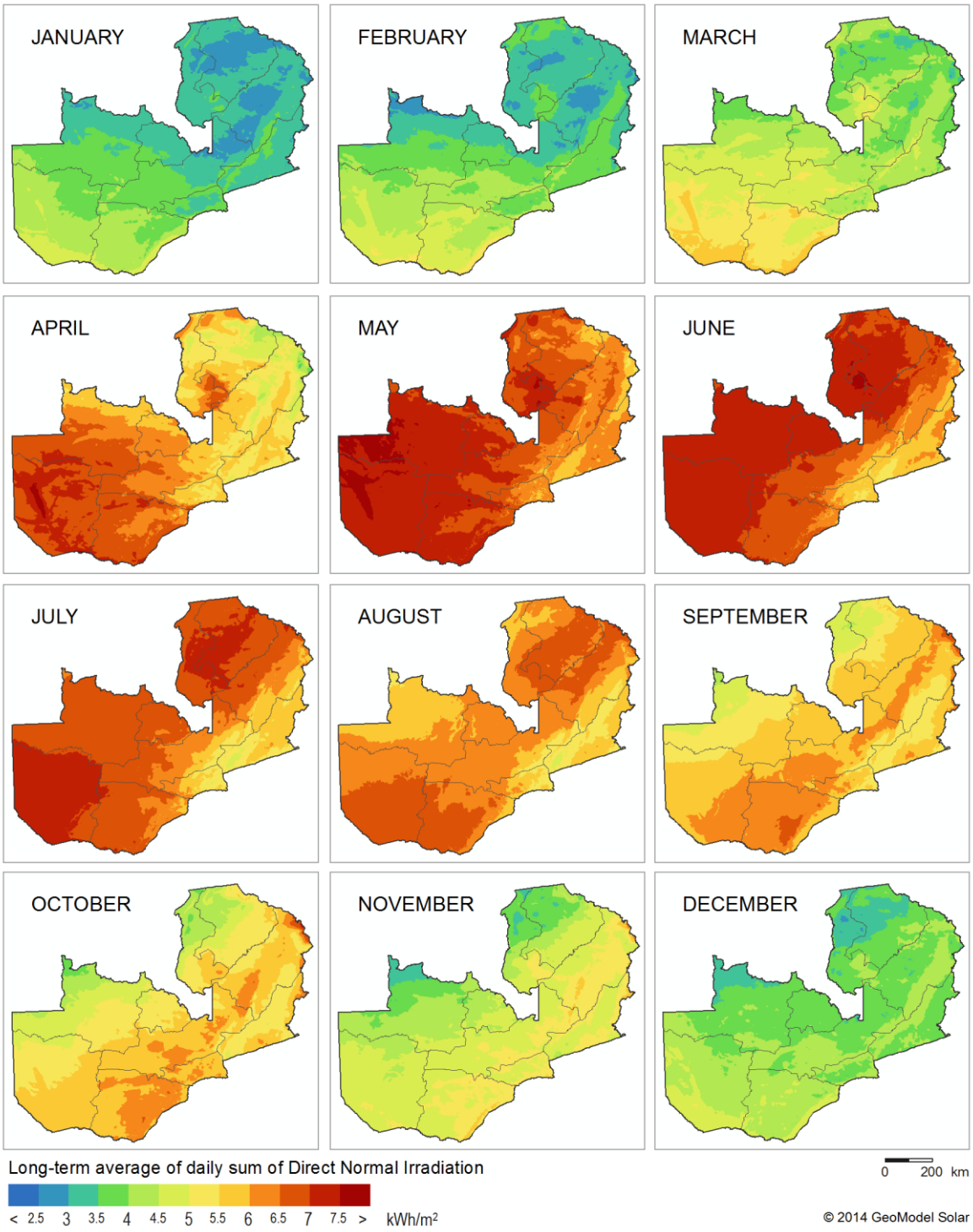

Fig. 7.16: Direct Normal Irradiation (DNI) - longterm monthly averages.

Tab. 7.5 and Fig. 7.17 show longterm average daily sums and average daily minimum and maximum of Direct Normal Irradiation (DNI) for six sites, assuming a period 1994 to 2013. Highest DNI is found in the Longe and Mochipapa sites, the lowest in the Msekera site.

Tab. 7.5: Daily averages and average minima and maxima of Direct Normal Irradiation at 6 sites

Month	Direct Normal Irradiation [kWh/m^2]											
	Longe		Lusaka		Misamfu		Mochipapa		Msekera		Mutanda	
	Average	Min Max	Average	Min Max	Average	Min Max	Average	Min Max	Average	Min Max	Average	Min Max
January	**4.07**	2.89 5.75	**3.73**	2.16 5.03	**3.07**	2.01 4.16	**3.98**	2.25 5.72	**3.20**	2.22 4.13	**3.32**	2.77 4.35
February	**4.42**	2.93 6.08	**3.91**	1.85 5.79	**3.28**	2.24 4.82	**4.33**	2.21 6.55	**3.60**	2.12 5.24	**3.40**	2.25 5.17
March	**5.08**	3.35 7.79	**4.46**	2.94 6.36	**3.84**	3.03 4.77	**4.91**	3.52 7.33	**4.17**	2.97 6.53	**4.31**	3.01 6.69
April	**7.13**	5.74 7.99	**6.01**	4.37 7.47	**5.12**	3.75 5.90	**6.42**	4.64 7.48	**5.43**	3.87 6.85	**6.11**	4.93 6.90
May	**7.48**	6.35 8.52	**6.85**	4.83 8.27	**6.41**	4.21 7.43	**7.02**	4.79 8.50	**6.17**	3.48 7.50	**7.21**	5.07 8.44
June	**7.25**	5.81 8.18	**6.39**	4.54 7.74	**7.10**	6.05 8.46	**6.72**	4.57 8.16	**5.93**	4.55 7.42	**7.41**	6.56 8.28
July	**7.07**	5.65 7.94	**6.27**	4.73 7.71	**6.96**	5.99 7.89	**6.63**	4.52 7.68	**5.65**	4.09 6.97	**6.80**	5.71 7.88
August	**6.48**	5.92 7.81	**6.25**	5.19 7.16	**6.65**	5.00 7.43	**6.82**	6.07 7.78	**5.50**	3.40 6.82	**5.96**	5.08 6.95
September	**5.92**	5.07 6.80	**6.22**	5.08 6.88	**5.75**	4.37 6.94	**6.59**	5.46 7.46	**5.50**	4.78 6.62	**5.35**	4.07 6.09
October	**5.64**	4.71 7.25	**6.15**	5.08 7.53	**5.32**	4.26 6.35	**6.31**	5.46 8.48	**5.26**	3.97 6.27	**4.94**	3.95 6.10
November	**4.77**	3.70 5.96	**5.21**	4.22 6.41	**4.75**	3.10 6.01	**5.02**	3.82 6.91	**4.89**	3.25 5.77	**4.09**	3.15 5.27
December	**4.19**	3.21 5.33	**4.19**	2.59 5.82	**3.91**	2.64 4.98	**4.28**	2.58 5.26	**3.83**	2.23 5.01	**3.72**	3.20 5.17
YEAR	**5.80**	**4.62** **7.12**	**5.48**	**3.97** **6.85**	**5.19**	**3.90** **6.27**	**5.76**	**4.17** **7.28**	**4.93**	**3.41** **6.26**	**5.23**	**4.15** **6.45**

DNI in all sites shows similar pattern of variability, given by minimum and maximum range of values. The highest DNI but also seasonally variable is reached in a period from April to June. This is in a contrast with season from December to February, where DNI reduced to about a half.

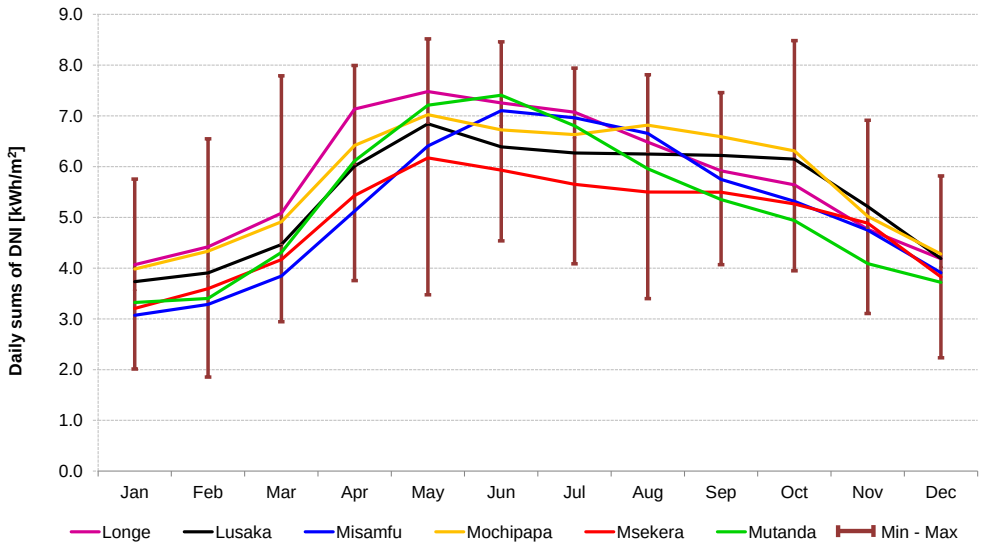

Fig. 7.17: Daily averages of Direct Normal Irradiation at selected sites.

Interannual variability of DNI for selected sites is calculated from the unbiased standard deviation of yearly DNI over 20 years and it is based on a simplified assumption of normal distribution of the yearly sums. All sites show similar patterns of DNI changes over the recorded time (Fig 7.18), The extremes (minimum and maximum) or values close to extremes are reached almost in the same years. The most stable DNI (the smallest interannual variability) is observed in Mutanda, Longe and Misamfu.

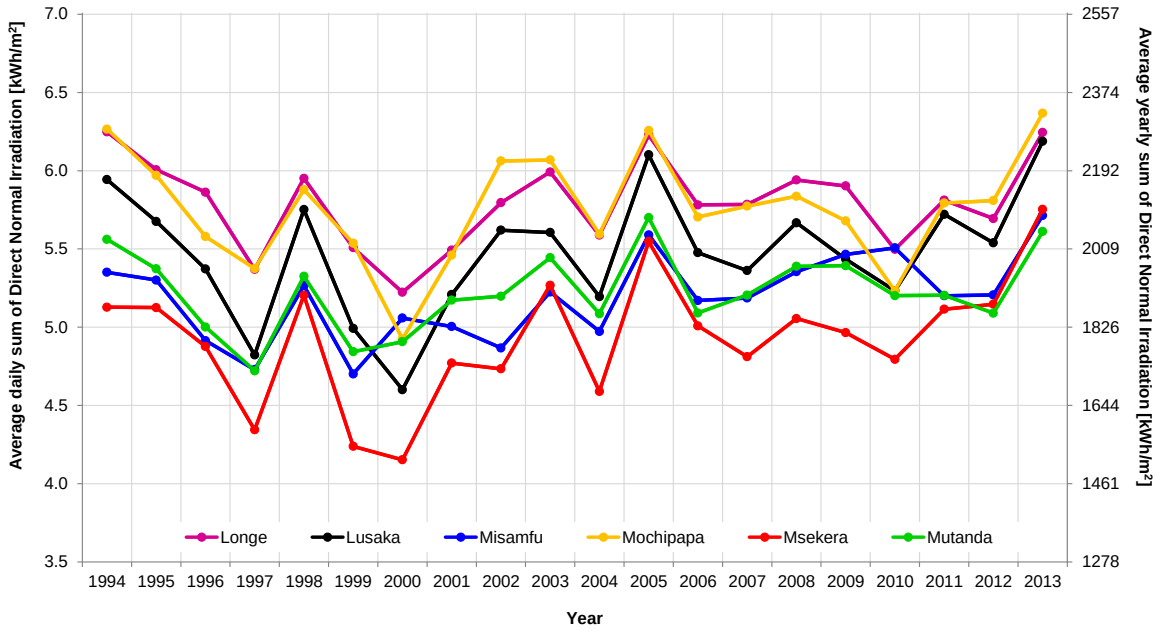

Fig. 7.18: Interannual variability of DNI for representative sites

Daily sums in a particular year can be displayed for better visual presentation of DNI in relation to GHI. Fig. 7.19 shows daily sums for year 2013 in Lusaka. Blue pattern, representing GHI sums is transparent in order to make visible lower values of DNI pattern (yellow).

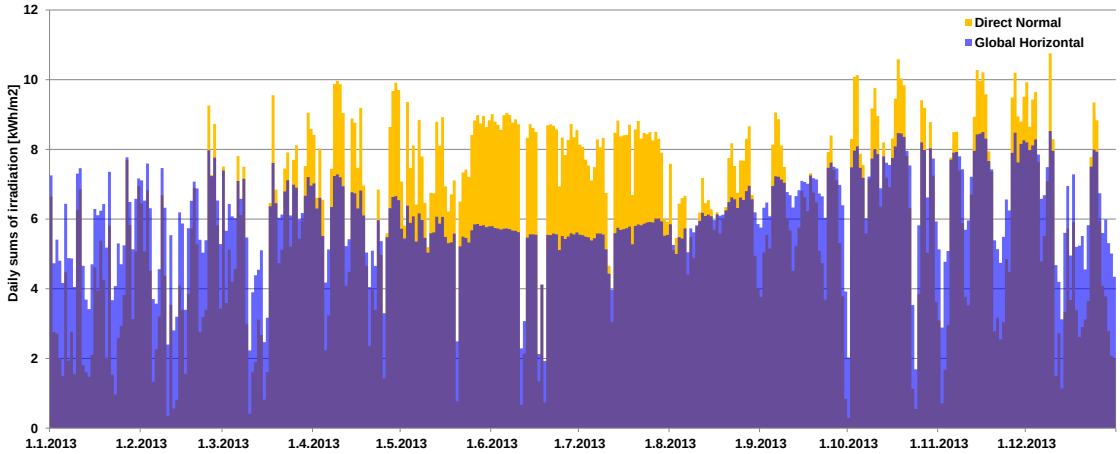

Fig. 7.19: Daily values of GHI and DNI for Lusaka, year 2013

8 PHOTOVOLTAIC POWER POTENTIAL

8.1 Reference configuration

Amount of Global Tilted Irradiation (GTI), as shown in Fig 7.8, depends on the mounting of photovoltaic (PV) modules. Map of potential PV power output presents theoretical potential power production of a PV system installed with mainstream technology configuration, which is described in Tab. 8.1.

Tab. 8.1: Reference configuration - photovoltaic power plant with fixed-mounted PV modules

Feature	Description
Nominal capacity	Configuration represents a typical PV power plant of 1 MW-peak or higher. All calculations are scaled to 1 kWp, so that they can be easily multiplied for any installed capacity.
Modules	Crystalline silicon modules with positive power tolerance. NOCT 45ºC and temperature coefficient of the Pmax -0.44 %/K
Inverters	Central inverter with Euro efficiency 98.0%
Mounting of PV modules	Fixed mounting structures facing North with optimum tilt in the range of 13º to 22º. Relative row spacing 2.5 (ratio of absolute spacing and table width)
Transformer	Standard transformer

Photovoltaic power production has been calculated using numerical models developed and implemented in-house by GeoModel Solar. As introduced in Chapter 5.1.4, 15-minute **time series of solar radiation and air temperature**, representing last 20 years, are used as an input to the simulation. The models are developed and tested based on the most advanced algorithms, expert knowledge, monitoring results and recommendations given in [24]. Tab. 8.2 summarizes losses and related uncertainty throughout the PV computing chain.

The reference configuration for PV potential calculation is a PV system with crystalline-silicon (c-Si) modules mounted in a fixed position on a table facing North and inclined at an angle close to optimum, i.e. at the angle at which the yearly sum of global tilted irradiation received by PV modules is maximized (range between 13º and 22º is geographically dependent). This type of mounting is very common and provides a robust solution with a minimum maintenance effort. Geographic differences in potential PV production are demonstrated at six selected sites.

The results presented in the Chapter do not consider performance degradation of PV modules due to aging. They also lack a necessary detail, thus these results cannot be used for financial assumptions of any particular project. Detailed assessment of energy yield of a specific power plant is within a scope of site-specific bankable expert studies.

Tab. 8.2: Summary of yearly energy losses and related uncertainty in each step of PV power simulation

Simulation step	Losses	Uncertainty	Notes
	[%]	[± %]	
Global Tilted Irradiation (model estimate)	N/A	7.0	Annual Global Irradiation falling on a surface of PV modules
Polluted surface of modules (empirical estimate)	-3.0	2.0	Losses due dirt, dust, soiling, and bird droppings
Module surface angular reflectivity (numerical model)	-2.5 to -2.9	1.0	Clean to medium polluted surface is considered
Module inter-row shading (model estimate)	-0.5	0.5	Partial shading of strings by modules from the preceding rows
Conversion in modules relative to STC (numerical model)	-9.5 to -13.0	3.5	Depends on the temperature and irradiance. NOCT of 45ºC is considered
Mismatch between modules (empirical estimate)	-0.5	0.5	Well-sorted modules and lower mismatch are considered.
Power tolerance (value from the data sheet)	0.0	0.0	Value given in the module technical data sheet (modules with positive power tolerance)
DC cables (empirical estimate)	-2.0	1.5	This value can be calculated from the electrical design
Conversion in the inverter (value from the technical data sheet)	-2.0	0.5	Given by the Euro efficiency of the inverter, which is considered at 98.0%
Transformer and AC losses (empirical estimate)	-1.5	0.5	Standard transformer and AC connection is assumed
Availability	0.0	0.0	A theoretical value of 100% technical availability is considered
Range of cumulative losses and indicative uncertainty	-21.5 to -25.4	8.3	These values are indicative and do not consider a number of project specific features and performance degradation of a PV system over its lifetime

PV electricity potential is calculated based on a set of assumptions shown in Tab. 8.1 and Tab. 8.2. These assumptions are indicative, as they will differ in real projects.

8.2 PV power potential of Zambia

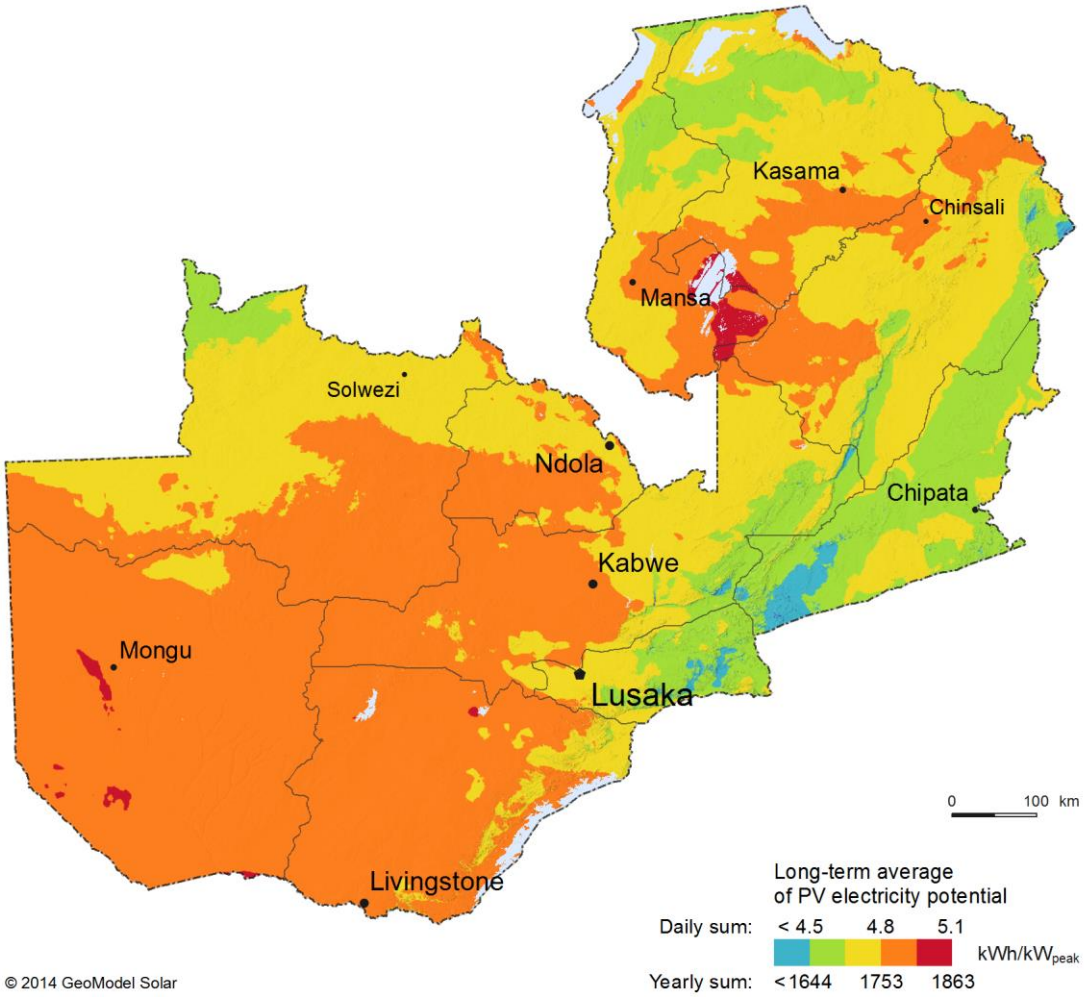

Fig. 8.1: PV electricity output from a free-standing fixed-mounted PV system with a nominal peak power of 1 kWp - longterm averages of daily/yearly sum

Fig. 8.1 shows the average daily sum of specific PV electricity output from a typical open-space PV system with a nominal peak power of 1 kWp system, i.e. the values are in kWh/kWp. Calculating PV output for 1 kWp of installed power makes it simple to scale the PV power production estimate depending on the size of a power plant. Besides the technology choice, the electricity production depends on geographical position of the power plant.

In Zambia, the average daily sums of specific PV power production from a reference system vary between 4.5 kWh/kWp (equals to yearly sum of about 1640 kWh/kWp) and 5.1 kWh/kWp (about 1860 kWh/kWp yearly) with extreme values in Western province and South-east of Luapula province, where the values are higher than 5.1 kWh/kWp. This positions Zambia to regions with very high potential for PV power generation.

Fig. 8.2 shows monthly production from a PV power system, and Fig. 8.3 breaks down the values for six sites.

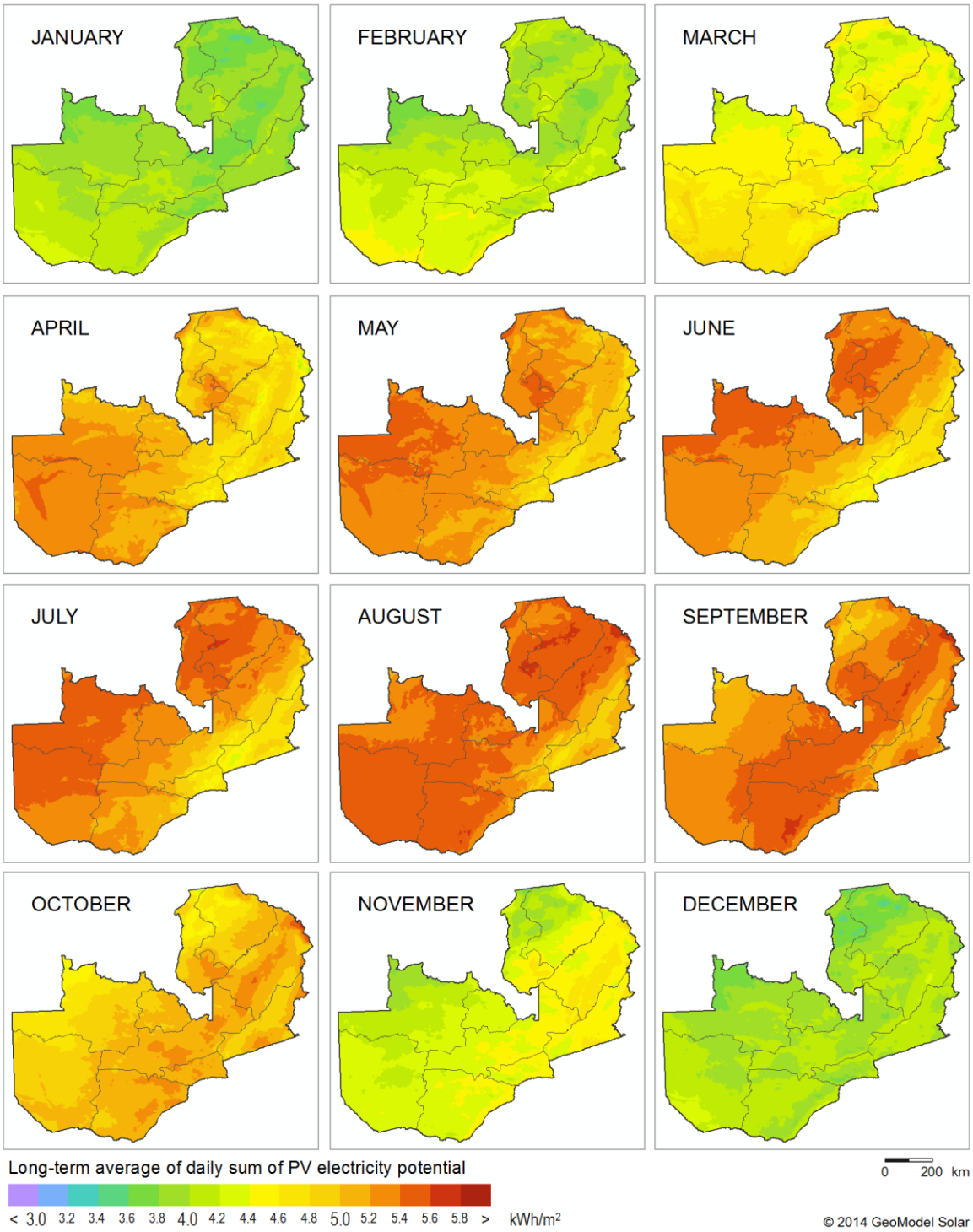

Fig. 8.2: PV electricity potential for open-space fixed PV system - longterm monthly averages

Tab. 8.3: Annual performance parameters of a PV system with modules fixed at optimum angle

	Longe	Lusaka	Misamfu	Mochipapa	Msekera	Mutanda
Average daily sum of PV electricity yield for fixed-mounted modules at optimum angle	4.89 kWh/kWp	4.86 kWh/kWp	4.80 kWh/kWp	4.83 kWh/kWp	4.59 kWh/kWp	4.78 kWh/kWp
Yearly sum of PV electricity yield for fixed-mounted modules at optimum angle	1789 kWh/kWp	1741 kWh/kWp	1753 kWh/kWp	1766 kWh/kWp	1677 kWh/kWp	1747 kWh/kWp
Optimum angle	20º	20º	16º	21º	17º	18º
Annual ratio of diffuse/global horizontal irradiation	34.4%	36.0%	38.7%	34.7%	40.4%	38.3%
System performance ratio (PR) for fixed-mounted PV	77.1%	78.1%	78.3%	77.9%	77.9%	77.8%

Season of relatively high PV yield is long enough for effective operation of a PV installation. As it was presented in Chapter 7.3, it is recommended to install modules in optimum tilt rather than on horizontal surface. Besides higher yield, a benefit of tilted modules is improved self-cleaning of the surface pollution by rain.

Electricity production in a potential PV power plant is similar for all sites (except Msekera site) and follows a combined pattern of global tilted irradiation and air temperature. Difference between production from the best site (Longe, 4.89 kWh/kWp) and the site with lowest production in Zambia (Msekera, 4.59 kWh/kWp) is about 6.6%. Msekera site is specific due to higher DIF/GHI ratio in comparison with other sites, especially during the summer season, and this results in slightly reduced PV power output.

Also monthly power production profiles are very similar for all sites. High and stable production can be reached during dry season from April to September.

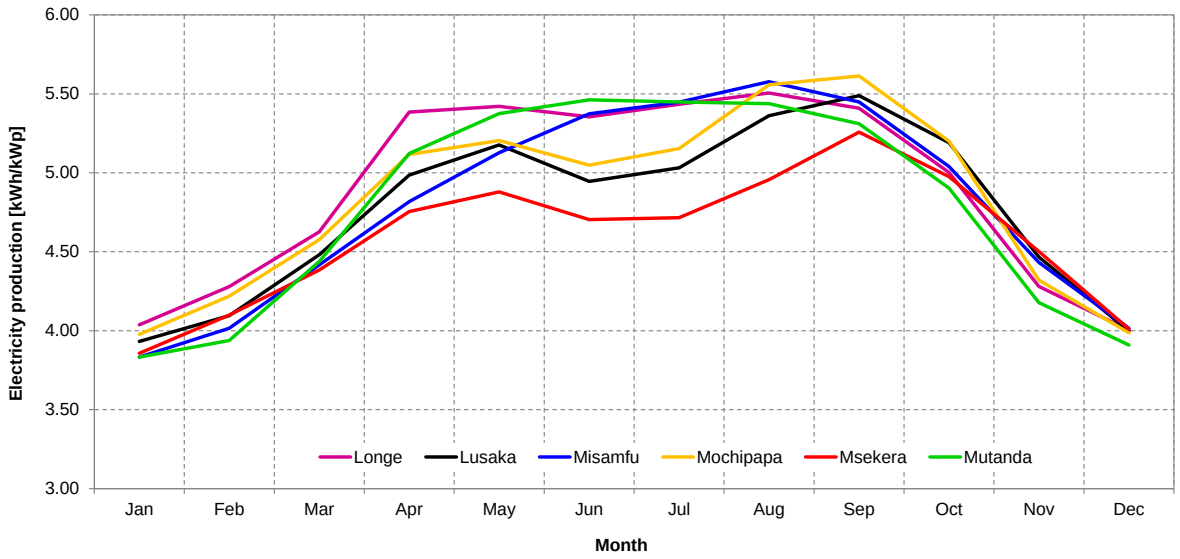

Fig. 8.3: Daily sum of power production from the fixed tilted PV systems at six sites with a nominal peak power of 1 kW [kWh/kWp]

Monthly and yearly performance ratio (PR) of reference installation for the selected sites is shown in Tab. 8.5 and Fig. 8.4. Yearly PR of the reference installation is found in range between 77.1% (Longe) and 78.3% (Misamfu). Monthly changes in PR may fluctuate in the range ±5%, depending on specific climatic conditions of a site, especially air temperature.

Performance ratio is higher in a season from April to July, when PV output of modules is not influenced by high air temperature. In Longe, the PV performance is reduced by higher air temperature.

Tab. 8.4: Average daily sums of PV electricity output from an open-space fixed PV system with a nominal peak power of 1 kW [kWh/kWp]

Site	Average daily sum of electricity production [kWh/kWp]												Year
	Jan	Feb	Mar	Apr	May	Jun	Jul	Aug	Sep	Oct	Nov	Dec	
Longe	4.04	4.28	4.63	5.39	5.42	5.35	5.43	5.50	5.41	5.00	4.28	4.00	4.89
Lusaka	3.93	4.10	4.48	4.99	5.18	4.95	5.03	5.36	5.49	5.19	4.47	4.00	4.76
Misamfu	3.83	4.02	4.42	4.82	5.13	5.37	5.45	5.58	5.45	5.04	4.43	4.02	4.80
Mochipapa	3.98	4.22	4.58	5.12	5.20	5.05	5.15	5.56	5.61	5.20	4.32	3.99	4.83
Msekera	3.86	4.10	4.39	4.75	4.88	4.70	4.72	4.96	5.26	4.98	4.50	4.01	4.59
Mutanda	3.83	3.94	4.44	5.12	5.38	5.46	5.45	5.44	5.31	4.90	4.18	3.91	4.78

Impact of air temperature to performance of power plants is clearly visible when comparing monthly temperature profiles in Fig. 6.7 with monthly PR profiles in Fig. 8.4. The lowest PR values between September and November are corresponding to hot and dry season, where PV output is visibly reduced by higher air temperature, despite the highest GTI (Fig. 7.8).

Tab. 8.5: Monthly and annual Performance Ratio of a free standing PV system with fixed modules

Site	Monthly Performance Ratio [%]												Year
	Jan	Feb	Mar	Apr	May	Jun	Jul	Aug	Sep	Oct	Nov	Dec	
Longe	77.7	76.6	77.2	77.3	78.2	79.2	79.2	77.4	75.4	74.6	75.5	76.9	77.1
Lusaka	78.4	77.8	78.6	78.4	79.2	80.4	80.4	78.6	76.5	75.6	76.0	77.6	78.1
Misamfu	78.8	78.0	78.8	79.0	79.3	79.8	79.6	78.3	77.0	76.3	76.7	77.9	78.3
Mochipapa	77.7	77.0	78.1	78.3	79.2	80.4	80.4	78.6	76.5	75.4	75.7	77.0	77.9
Msekera	78.0	77.3	78.0	78.2	78.8	79.6	79.7	78.5	77.0	76.3	76.0	77.2	77.9
Mutanda	78.7	77.6	78.2	78.2	78.5	79.2	79.2	77.8	76.1	75.5	76.7	78.1	77.8

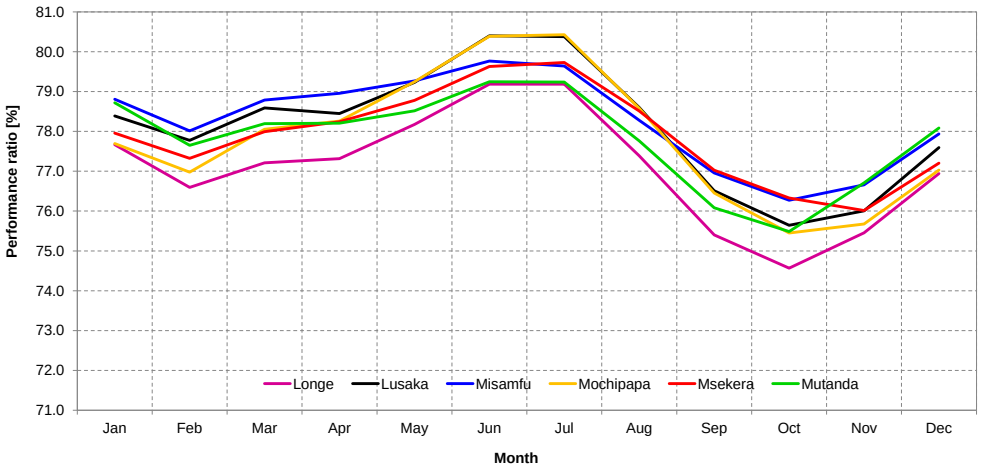

Fig. 8.4: Monthly performance ratio of the fixed tilted PV systems at six sites with a nominal peak power of 1 kW [kWh/kWp]

9 SOLAR AND METEO DATA UNCERTAINTY

The expected data uncertainty is based on the validation exercise and it is summarized in Tabs. 9.1 and 9.2. For more details, please refer to Chapter 6 of the *Model Validation Report 128-02/2014*.

Tab. 9.1: Uncertainty of longterm estimate for GHI, GTI and DNI values in Zambia

	Acronym	Yearly uncertainty	Monthly uncertainty
Global Horizontal Irradiation	GHI	±6.0%	±8%
Global Tilted Irradiation	GTI	±7.0%	±9%
Direct Normal Irradiation	DNI	±12.0%	±15%

Tab. 9.2: Uncertainty of the longterm modelled meteorological parameters in Zambia

	Acronym	Unit	Yearly	Monthly	Hourly
Air temperature at 2 m	TEMP	°C	<1.5	<2.0	<3.0 (night time) <2.0 (day time)
Relative humidity at 2 m	RH	%	<10	<15	<25 (night time) <15 (day time)
Average wind speed at 10 m	WS	m/s	<1.0	<1.5	<2.0

10 APPLICATION OF SOLAR AND METEO DATA

Good quality solar resource data are critical for economic and technical assessment of solar electricity infrastructure in the country. Bankability is about understanding uncertainty and managing risk. Technically, good bankable solar resource data should:

- Be based on proven methods, systematically validated and traceable
- Represent at minimum 10 years of history, optimally 20 or more
- Follow standards, especially in quality-control
- Include information about solar resource uncertainty
- Include metadata and be supported by a technical report
- Be supported by dedicated professional service provider.

Important part of bankable data is uncertainty assessment, which includes two aspects:

- Uncertainty of the estimate
- Uncertainty given by longterm weather variability

The uncertainty has probabilistic nature and it can be expressed in different levels of confidence.

The need for a specific type of data depends on a stage of solar power project development. The data products are described in Chapter 2 and also here, in Fig. 10.1.

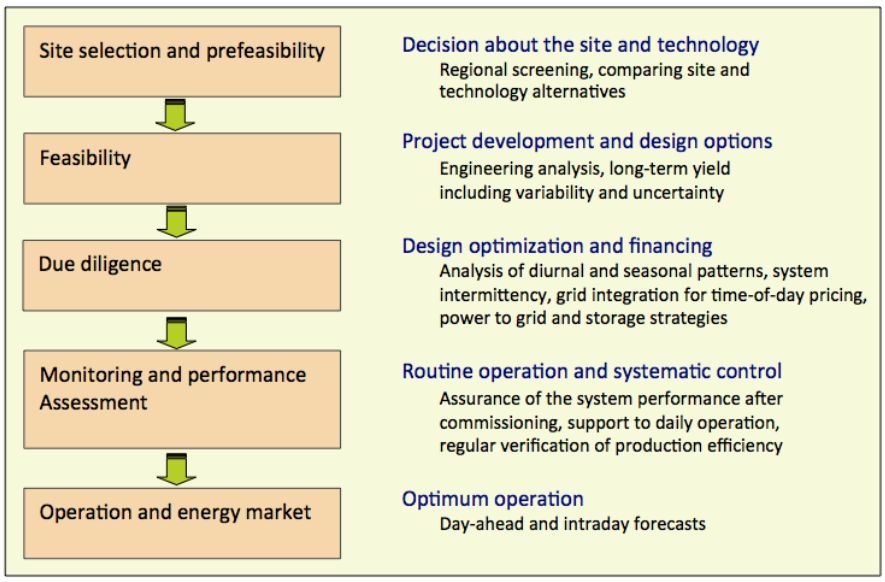

Fig. 10.1: Stages of development and operation of a solar power plant

10.1 Site selection and prefeasibility

Candidate sites are evaluated to determine which are the most suitable for a project development. *Annual longterm averages or aggregated statistics* are required at this stage. *Monthly longterm averages* are also useful, optimally in the form of maps. Additionally, map information on terrain, population, landscape, grid power lines, etc. is used.

The comparison of candidate sites and considered technologies requires considering a number of options and discussing them within a group of partners. This task can be effectively performed when using web-based tools with an option for generating PDF reports and downloading data in a format that can be further used in desktop applications or simulation programs. This stage can be documented with reports providing a first estimate of solar resource and local climate.

A thorough GIS analysis capability, involving spatial data and support information can be used to rank the territory and help with preselecting the candidate sites.

10.2 Feasibility and project development

Once a decision about the prospective site(s) is made for a larger project, a meteorological station should be installed to produce short-term measurements of local solar and meteorological variables. This is particularly important for CPV and CSP projects, and for medium size and large PV projects.

For the selected site(s), the next important step is an assessment of possible design and operational variants to optimize energy performance. At this stage, a more comprehensive knowledge of the annual solar resource, as well as an understanding of seasonal and interannual variability and related uncertainties is required. Hourly (or sub-hourly) times series of GTI or DNI and are needed. Also other meteo parameters are relevant, such as air temperature, wind speed and direction and (for CSP projects) also humidity. The data are used in the TMY format (typically applied in engineering simulation software) or preferably as multiyear time series.

It is generally accepted that a minimum length of data needed for obtaining a representative picture of solar microclimate is 10 years. In Zambia, 20 or more years of data is possible and preferred.

The ground measurement campaign is required for quality enhancement of satellite-derived solar data. Prior to be used, the local measurements have to pass quality control procedures. When a representative data set of local measurements is available (at least one year), the next step is to conduct site adaptation of satellite-based time series. The resulting site-adapted time series should have a minimum bias, minimum RMSD and balanced probability distribution function.

10.3 Due diligence

Due diligence includes detailed performance analysis of a solar power plant over its projected economic lifetime and includes elaboration on the following information:

- Uncertainty of longterm solar resource estimate and meteorological data;
- Seasonal and diurnal variability, including probability distribution and uncertainty of production within a day and for each month/season;
- Uncertainty due to variability of solar resource considering the established confidence limits, most typically P90. Confidence limits are used to describe probability of exceedance values - for any single year (e.g. to assess financial reserve funds for low production years) and also for the lifetime of the energy installation (to asses longterm possible weather fluctuation). Understanding the impact of weather extremes, including risk of large-scale volcano eruptions, is important;

These analyses are to assess performance of the solar project from the point of view of technology but also cash flow and the related risk.

A typical consultancy reports prepared in this stage for a specific development site are Site-specific Solar Resource Assessment Studies. In addition, Energy Yield Assessment Studies is prepared for PV projects, and these provide in-depth characteristics of the site, analyse the performance of considered technology options, optimise planned design and calculate variability and uncertainty of power production.

10.4 Performance assessment and monitoring

Once a project is commissioned, the monitoring of a solar power plant involves measuring of technological parameters at the level of the components, and this includes measuring solar resource and meteo data. This data are cross-analysed to better characterise a relationship of the power plant performance to the environmental conditions, and to identify potential improvements.

For CPV and CSP projects, installing a meteo station with high-quality radiometers and other meteo instruments is obligatory. For larger PV projects, to obtain high-quality solar resource data, deploying a local meteo station is a justifiable expense. In case of medium size and small PV projects, data from satellite-based and meteorological models are a satisfactory compromise between required accuracy and costs of monitoring.

Time series of continuously measured on-site or satellite-based data are used for performance monitoring and reporting. The longterm solar resource monitoring includes systematic collection of measurements, their quality control to enable: (i) monitoring, support to operation and failure assessment during daily routines, (ii) regular technology appraisal and reporting, e.g., on an quarterly or annual basis.

High frequency (minute up to sub-hourly) time series of solar irradiance data are used at this stage to systematically check the actual performance characteristics. The requirement is that the data from the most recent period are needed with minimum bias and lowest possible RMSD. The uncertainty of either the installed ground instruments or satellite-derived has to be estimated. Cross-comparison of irradiance data sources (from several radiometers and with satellite-based tie series) is used for minimizing errors.

Performance of the power plant degrades in a longterm, due to technology ageing, and it also varies depending on the seasonal cycles and short-term weather changes. In technology performance assessment, real weather and production data are compared with solar radiation and expected (calculated) production to analyse trends and fluctuation of performance in PV projects and detect any possible shortcomings or needs for operational improvements. The objective of the performance assessment report is to (i) confirm the longterm production hypothesis, and to (ii) identify starting conditions for longterm monitoring. Data from the real-time observations for the most recent period are needed with minimum bias, lowest possible RMSD and quantified uncertainty.

Even though day-by-day monitoring can be performed by on-site personnel, it is a good practise to involve an independent service provider. Regular reporting keeps a track of the production history and makes management routines more efficient. Regular monitoring provides important information about the events affecting production and performance efficiency and their possible deviation from the expected behaviour and trends. Before any analysis, the input measured data have to be validated, cleaned and qualified, otherwise the interpretation of results may be biased or misleading.

10.5 Operation and energy market

An important aspect of solar power plant operation is forecasting − for optimisation of power generation and for participation in the energy markets. For grid-integrated solar power plants, forecasts for a time horizon of up to two days ahead are important for transactions on the day-ahead electricity markets. Intraday trading is based on forecasts for a time horizon of few hours. Also for standalone applications and small grids, stability and efficient use of backup solutions depend on solar forecasting. Solar irradiance data products include forecasted time series of GHI, GTI or DNI at hourly time step, and the requirement is zero bias and low RMSD and information availability ahead one day or up to few hours.

11 SOLARGIS DATA DELIVERY FOR ZAMBIA

The key features of the delivered data and maps for Zambia are:

- Harmonized solar, meteorological and geographical data, based on the best available methods and input data sources.
- Historical longterm averages representing 20 years at high spatial and temporal resolution, available for any location.
- SolarGIS database and energy simulation software is extensively validated by GeoModel Solar, and also by independent organizations. They are also verified within monitoring of commercial PV power plants and solar measuring stations worldwide.
- Additional data can be accessed online at http://solargis.info.

The delivered data and maps offer a good basis for knowledge-based decision-making and project development. This data is updated in real time can be further used in solar monitoring, performance assessment and forecasting.

11.1 Spatial data products

High-resolution SolarGIS data have been delivered in the format suitable for the Geographical Information Systems (GIS). The *Primary data* represent solar radiation, meteorological data, PV potential production and terrain characteristics. The *Support data* includes various vector data, such administrative division, road network, etc.

11.1.1 Primary data

Tab. 11.1 and 11.2 show information about the data layers. Technical specification is summarized in Tab. 11.3, and Tab 11.4. File name convention, used for the individual data sets, is described in Tab. 11.5.

Tab. 11.1: General information about GIS data layers

Geographical extent	Republic of Zambia with buffer 10 km along the borders
Map projection	Geographic (Latitude/Longitude), datum WGS84 (also known as *GCS_WGS84*; *EPSG: 4326*)
Data format	ESRI ASCII raster data format

Tab. 11.2: Description of primary GIS data layers

Acronym	Full name	Unit	Type of use	Type of data layers
GHI	Global Horizontal Irradiation	kWh/m^2	Reference information for the assessment of flat-plate PV (photovoltaic) and solar heating technologies (e.g. hot water)	Longterm average of daily sums
DNI	Direct Normal Irradiation	kWh/m^2	Assessment of Concentrated PV (CPV) and Concentrated Solar Power (CSP) technologies	Longterm average of daily sums
DIF	Diffuse Horizontal Irradiation	kWh/m^2	Complementary parameter to GHI and DNI	Longterm average of daily sums
GTI	Global Irradiation at optimum tilt	kWh/m^2	Assessment of solar resource for PV technologies	Longterm average of daily sums
OPTA	Optimum angle	°	Optimum tilt to maximize yearly PV production	-
PVOUT	Photovoltaic electricity output of free-standing fixed-mounted c-Si modules, optimally tilted Northwards	kWh/kWp	Assessment of PV power production potential for a free standing PV power plant with modules mounted at optimum tilt to maximize yearly PV production	Longterm average daily sums
TEMP	Air Temperature at 2 m above ground level	°C	Defines operating environment of solar power plants	Longterm (diurnal) annual and monthly averages
GHISTD	Interannual variability of Global Horizontal Irradiation	%	Relative standard deviation of yearly values indicates year-by-year variability of GHI	-
DNISTD	Interannual variability of Direct Normal Irradiation	%	Relative standard deviation of yearly values indicates year-by-year variability of DNI	-
GTISTD	Interannual variability of Global Irradiation at optimum tilt	%	Relative standard deviation of yearly values indicates year-by-year variability of GTI	-
ELE	Terrain elevation	m	Defines limiting conditions for location of solar power plants	-
SLO	Terrain slope	°	Defines limiting conditions for location of solar power plants	-
AZIM	Terrain azimuth	°	Defines limiting conditions for location of solar power plants	-

Tab. 11.3: Technical specification of primary GIS data layers

Acronym	Full name	Data format	Spatial resolution	Time representation	No. of data layers
GHI	Global Horizontal Irradiation	Raster	15 arc-sec. (approx. 450x460 m)	1994 - 2013	12+1
DNI	Direct Normal Irradiation	Raster	15 arc-sec. (approx. 450x460 m)	1994 - 2013	12+1
DIF	Diffuse Horizontal Irradiation	Raster	15 arc-sec. (approx. 450x460 m)	1994 - 2013	12+1
GTI	Global Irradiation at optimum tilt	Raster	15 arc-sec. (approx. 450x460 m)	1994 - 2013	12+1
OPTA	Optimum angle	Raster	2 arc-min (approx. 3600x3700 m)	-	1
PVOUT	Photovoltaic electricity output for fixed-mounted modules at optimum tilt	Raster	15 arc-sec. (approx. 235x275 m)	1994 - 2013	12+1
TEMP	Air Temperature at 2 m above ground level	Raster	30 arc-sec. (approx. 900x920 m)	1994 - 2009	12+1
GHISTD	Interannual variability of Global Horizontal Irradiation	Raster	30 arc-sec. (approx. 900x920 m)	1994 - 2013	1
DNISTD	Interannual variability of Direct Normal Irradiation	Raster	30 arc-sec. (approx. 900x920 m)	1994 - 2013	1
GTISTD	Interannual variability of Global Irradiation at optimum tilt	Raster	30 arc-sec. (approx. 900x920 m)	1994 - 2013	1
ELE	Terrain elevation	Raster	9 arc-sec. (approx. 270x275 m)	-	1
SLO	Terrain slope	Raster	9 arc-sec. (approx. 270x275 m)	-	1
AZIM	Terrain azimuth	Raster	9 arc-sec. (approx. 270x275m)	-	1

Tab. 11.4: Characteristics of the raster output data files

Characteristics	Range of values
West − East	21:00:00E − 34:00:00E
North − South	07:00:00S − 19:00:00S
Resolution (GHI, DNI, GTI, DIF, PVOUT)	00:00:15 (3120 columns x 2880 rows)
Resolution (TEMP)	00:00:30 (1560 columns x 1440 rows)
Resolution (ELE, SLO, AZIM)	00:00:09 (5200 columns x 4800 rows)
Resolution (OPTA)	00:02 (390 columns x 360 rows)
Data type	Float or integer
No data value	-9999

* http://help.arcgis.com/en/arcgisdesktop/10.0/help/index.html#/ESRI_ASCII_raster_format/009t0000000z000000/

Tab. 11.5: File name convention for GIS data

Acronym	Full name	Filename pattern	Number of files	Size (approx.)
GHI	Global Horizontal Irradiation, longterm monthly (or yearly) sum	GHI_MM	13	695 MB
DNI	Direct Normal Irradiation, longterm monthly (or yearly) sum	DNI_MM	13	695 MB
DIF	Diffuse Horizontal Irradiation, longterm monthly (or yearly) sum	DIF_MM	13	695 MB
GTI	Global Irradiation at optimum tilt (27°), longterm monthly (or yearly) sum	GTI_MM	13	695 MB
OPTA	Optimum angle	OPTA	1	0.5 MB
PVOUT	Photovoltaic electricity output for fixed-mounted modules at optimum tilt	PVOUT_MM	13	695 MB
TEMP	Air Temperature at 2 m above ground	TEMP_MM	13	160 MB
GHISTD	Interannual variability of Global Horizontal Irradiation	GHI_STD	1	12 MB
DNISTD	Interannual variability of Direct Normal Irradiation	DNI_STD	1	12 MB
GTISTD	Interannual variability of Global Irradiation at optimum tilt	GTI_STD	1	12 MB
ELE	Terrain elevation	ELE	1	160 MB
SLO	Terrain slope	SLO	1	130 MB
AZI	Terrain azimuth	AZI	1	130 MB

Explanation:

- MM: month of data – from 01 to 12 (13 means yearly average)

11.1.2 Support GIS data

Delivered support GIS datasets are useful for creating cartographic outputs or performing spatial analysis using the *primary data* (such distance, density, summary analysis, etc.). Support GIS data are provided in a vector format (ESRI shapefile, Tab. 11.6).

Tab. 11.6: Support GIS data

Data type	Source	Data format
City location	World gazetteer © 2006 Stefan Helders, http://world-gazetteer.com	Point shapefile
Administrative boundaries	Vector dataset VMAP0 2006, adapted by GeoModel Solar	Polygon shapefile
Roads	Map data © 2013 OpenStreetMap.org contributors	Polyline Shapefile
Water bodies	Shuttle Radar Topography Mission version 2 © 2000-2006 SRTM Mission team	Polygon shapefile

11.1.3 Project in QGIS and ARCGIS format

Selected vector and raster data files are integrated into the QGIS project with colour schemes and annotation (see Fig. 11.1). The data are also delivered in the ArcGIS project format.

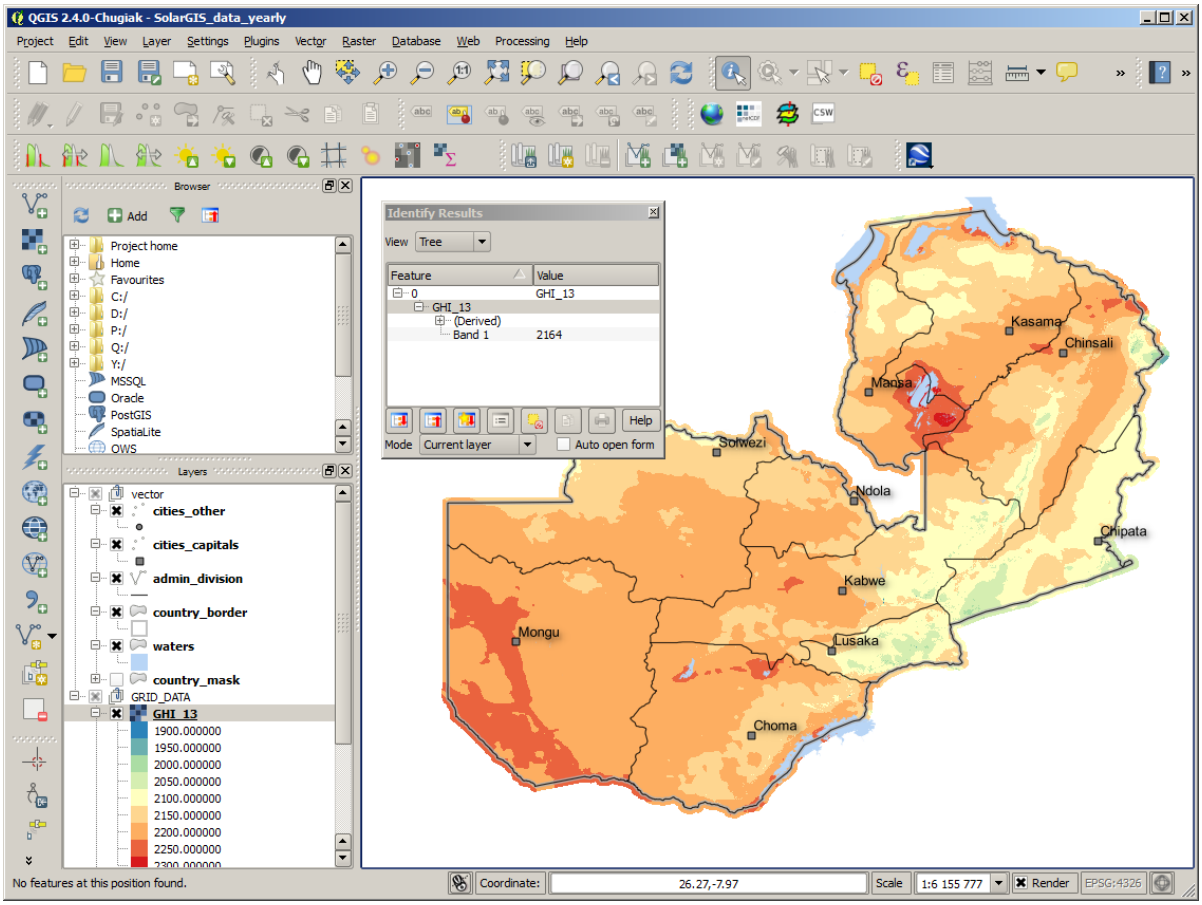

Fig. 11.1: Screenshot of the map and data in the QGIS environment

11.2 Digital maps

Besides GIS data layers, the digital maps are delivered for selected data layers for presentational purposes. Digital maps are prepared in three types; each suits different purpose:

- High-resolution poster maps
- Medium-resolution maps for presentations
- Image maps for Google Earth.

11.2.1 High-resolution poster maps

Digital images for high-resolution poster printing (size 114x114 cm). The colour-coded maps are prepared in a TIFF format at 300 dpi density and lossless compression.

Following five map files are delivered for high-resolution poster printing:

- Global Horizontal Irradiation – longterm average yearly sum
- Direct Normal Irradiation – longterm average yearly sum
- Air temperature at 2 metres – longterm yearly average
- Photovoltaic electricity production from a free-standing power plant with optimally tilted c-Si modules – longterm average yearly sum
- Terrain

Besides the main parameter, the poster maps include visualization of the following data layers:

- Additional map with an important support parameter
- Longitude and latitude lines
- City location and names
- Urban areas
- Administrative borders
- Road network
- Water bodies

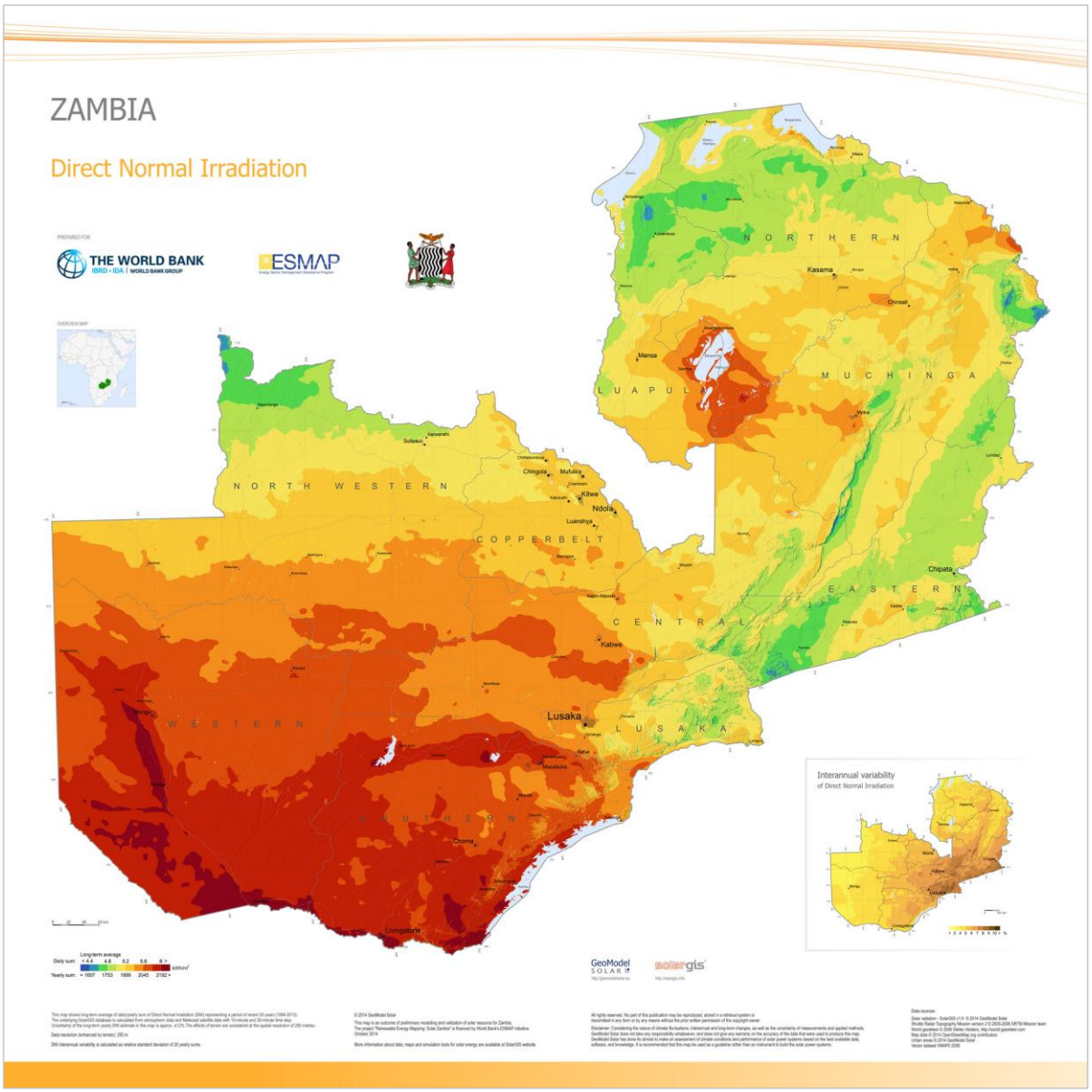

Fig. 11.2: Example of high-resolution DNI poster map
prepared in a resolution suitable for large format printing (original size 114x114 cm)

11.2.2 Medium-resolution maps for presentations

Digital images prepared in a resolution suitable for A4 printing or on-screen presentation. The colour-coded maps are prepared in PNG format at 300 dpi density and lossless compression.

Following map files are delivered:

- Annual and monthly longterm averages of Global Horizontal Irradiation
- Annual and monthly longterm averages of ratio Diffuse/Global Horizontal Irradiation
- Annual and monthly longterm averages of Global Tilted Irradiation (for optimum tilt)
- Annual and monthly longterm averages of Direct Normal Irradiation
- Annual and monthly longterm averages of Air Temperature
- Annual and monthly longterm averages of Photovoltaic (PV) Electricity Potential
- High resolution Terrain Elevation
- Zambia in the world context of Global Horizontal Irradiation map

The maps also include visualization of the following layers:

- Main cities, location and names
- Administrative borders
- Water bodies

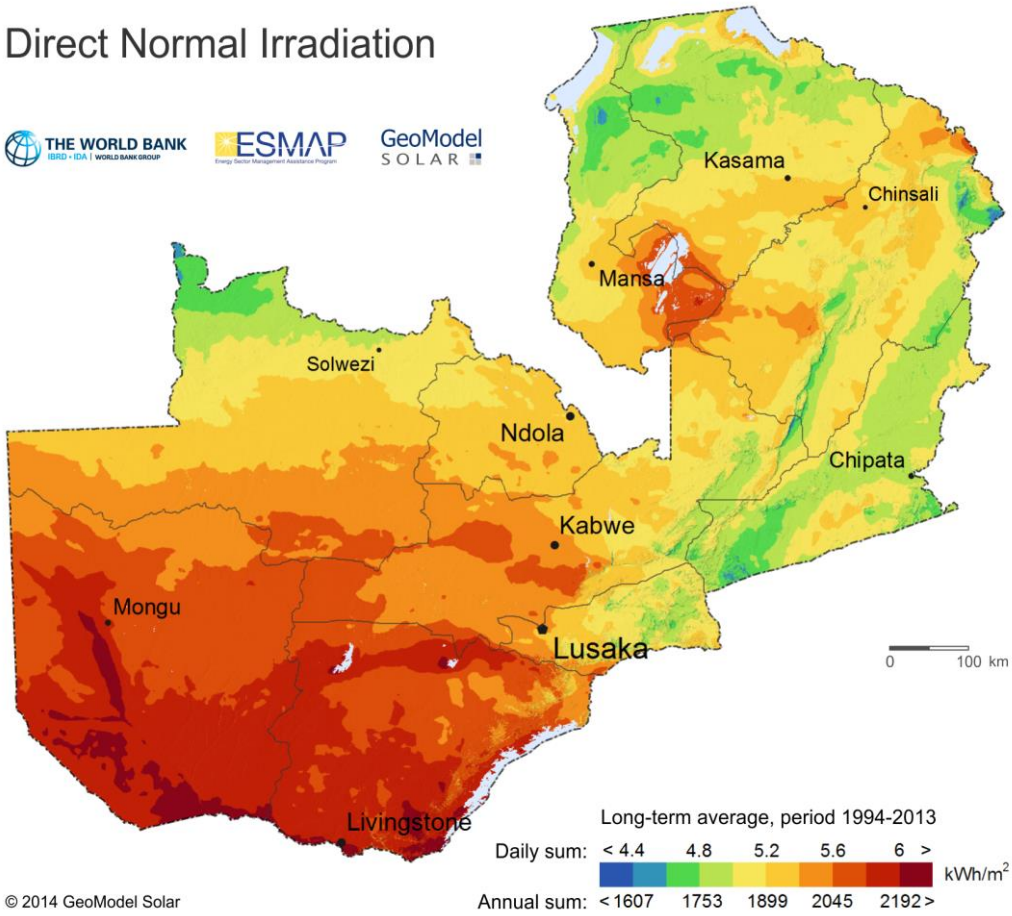

Fig. 11.3: Example of medium resolution DNI map
prepared in a resolution suitable for A4 printing or on-screen presentation

11.2.3 Image maps for Google Earth

Spatially referenced digital image maps with corresponding KML file can be displayed in Google Earth application or any other GIS software.

Map layers representing the following datasets are delivered:

- Annual longterm average of Global Horizontal Irradiation
- Annual longterm average of Direct Normal Irradiation
- Annual longterm average of Photovoltaic (PV) Electricity Potential
- Annual longterm average of Air Temperature at 2 metres
- High resolution Terrain Elevation map

Note: Image maps for Google Earth are delivered in two versions (high and medium resolution). Displaying high resolution image map requires higher computer and application performance, thus for some devices high resolution files might not display.

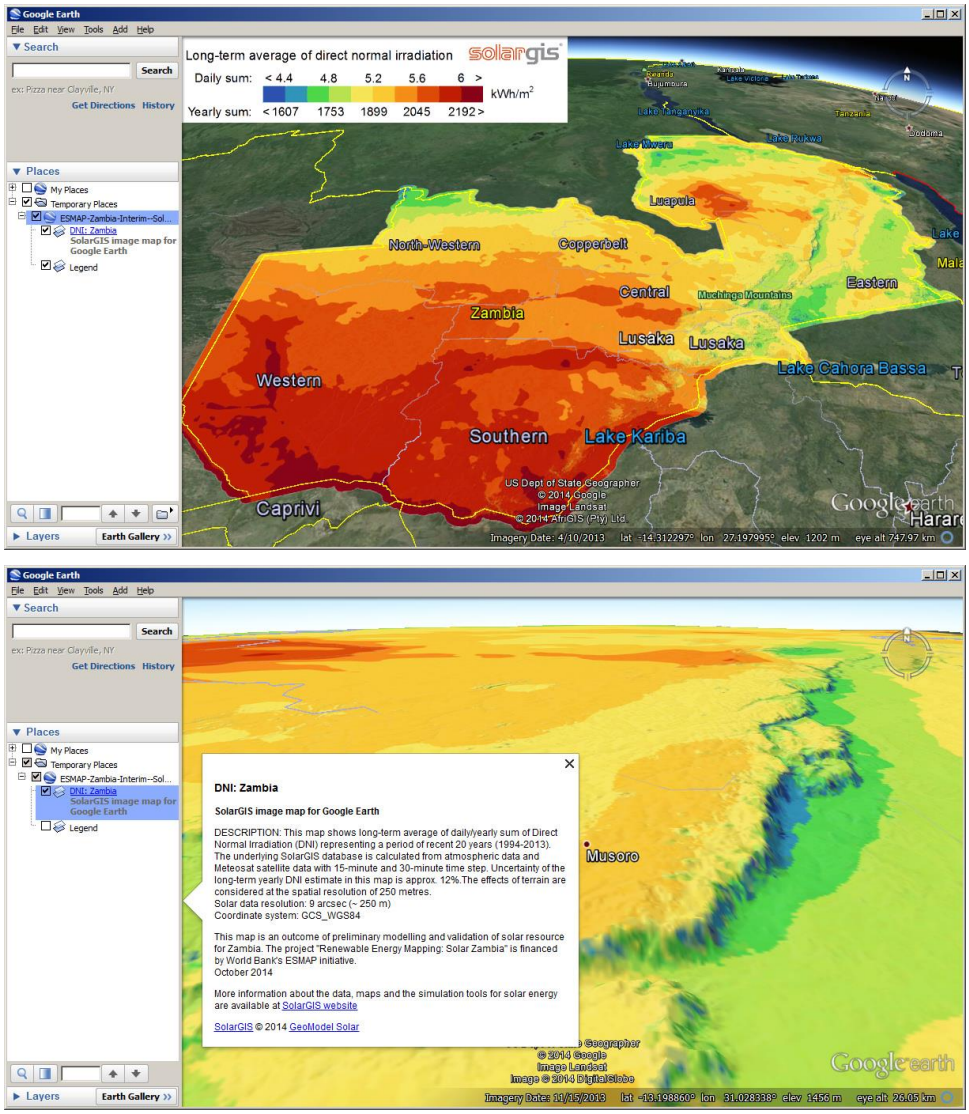

Fig. 11.4: Screenshot of DNI data displayed in Google Earth application

11.3 Site-specific data for eleven representative sites

For demonstration of climate diversity eleven representative sites were selected. Position of these sites was selected to coincide with meteo stations positions to obtain comparative data sets for further analysis. Representative sites are summarised in Tab. 11.7 and their position is marked in Fig. 11.5.

Tab. 11.7: Selected representative sites

ID	Name	Site manager	Province	Latitude	Longitude
1	Copperbelt	ZARI-ZMD	Copperbelt	-12.61417	28.14749
2	Chilanga	ZARI-ZMD	Lusaka	-15.54831	28.24822
3	Kabwe	ZARI-ZMD	Central	-14.39515	28.49444
4	Longe	ZARI	Western	-14.83966	24.93186
5	Lusaka	UNZA Agri	Lusaka	-15.39495	28.33711
6	Mansa	ZARI-ZMD	Luapula	-11.23868	28.95298
7	Mazabuka	ZARI-ZMD	Southern	-15.77720	27.92143
8	Misamfu	ZARI-ZMD	Northern	-10.17260	31.22314
9	Mochipapa	ZARI-ZMD	Southern	-16.83822	27.07028
10	Msekera	ZARI-ZMD	Eastern	-13.64610	32.56311
11	Mutanda	ZARI	Northwest	-12.42361	26.21528

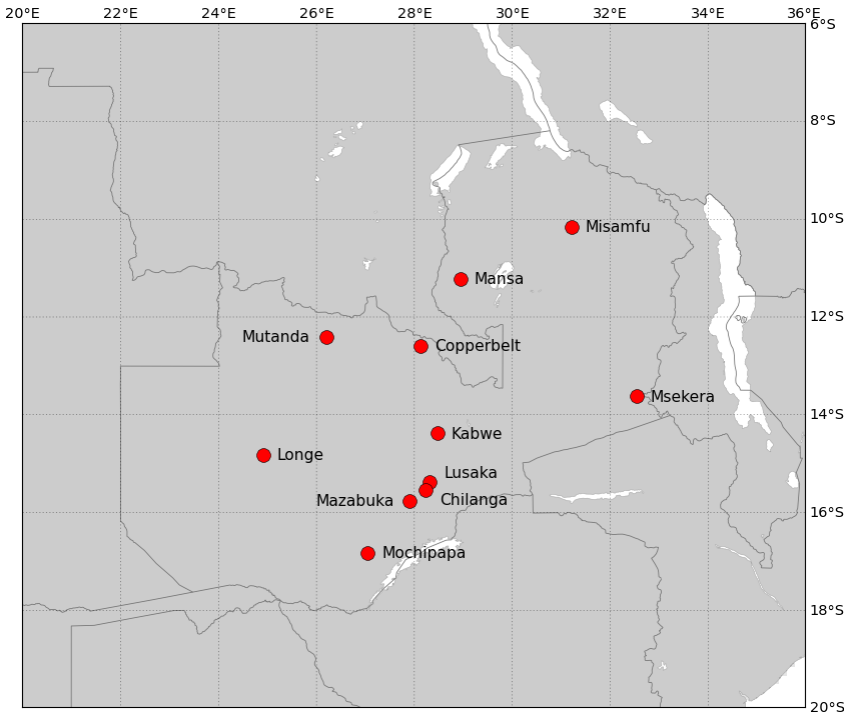

Fig. 11.5: Position of selected representative sites in Zambia

11.3.1 Multiyear Time Series

Time representation: full period of 1994 − 2013

Time step: hourly and monthly summaries

Time series represent 20 full years and they include the following parameters:

- Direct Normal Irradiation, DNI [Wh/m^2]
- Global Horizontal Irradiation, GHI [Wh/m^2]
- Diffuse Horizontal Irradiation, DIF [Wh/m^2]
- Global Tilted Irradiation, GTI [Wh/m^2] for optimally tilted PV modules facing North
- Azimuth and solar angle, SA and SE [°]
- Air temperature at 2 metres, TEMP [°C]
- Relative air humidity, RH [%]
- Wind speed at 10 metres, WS [m/s]
- Wind direction at 10 metres, WD [°]
- Atmospheric pressure, AP [hPa]

11.3.2 Typical Meteorological Year (TMY) data

Delivery of the site-specific TMY (Typical Meteorological Year) data is described in detail in Chapter 3.5.

Time representation: synthesis of 1994 − 2013

Time step: hourly summaries

Time series represent 20 full years and they include the following parameters:

- Global horizontal irradiance, GHI [W/m^2]
- Direct normal irradiance, DNI [W/m^2]
- Diffuse horizontal irradiance, DIF [W/m^2]
- Azimuth and solar angle, SA and SE [°]
- Air temperature at 2 metres, TEMP [°C]
- Wet bulb temperature, WBT [°C]
- Relative humidity, RH [%]
- Wind speed at 10 metres, WS [m/s]
- Wind direction at 10 metres, WD [°]
- Atmospheric pressure, AP [°]

12 METAINFORMATION

Metainformation for GIS data

- Global Horizontal Irradiation; longterm annual and monthly sums
- Direct Normal Irradiation; longterm annual and monthly sums
- Diffuse Horizontal Irradiation; longterm annual and monthly sums
- Global Tilted Irradiation (at optimum tilt); longterm annual and monthly sums
- Optimum tilt
- Photovoltaic electricity output for c-Si fixed-mounted modules, optimally tilted Northwards; longterm annual and monthly sums
- Air Temperature, Longterm (diurnal) annual and monthly averages
- Interannual variability of Global Horizontal Irradiation
- Interannual variability of Direct Normal Irradiation
- Interannual variability of Global Irradiation at optimum tilt
- Terrain elevation
- Terrain slope
- Terrain azimuth

Metainformation for GeoTIFF/KML image data

- Map of Global Horizontal Irradiation (GHI)
- Map of Direct Normal Irradiation (DNI)
- Map of photovoltaic electricity output for c-Si fixed-mounted modules, optimally tilted Northwards
- Map of terrain elevation
- Map of air temperature

13 LIST OF FIGURES

14 LIST OF TABLES

15 REFERENCES

[1] Perez R., Cebecauer T., Suri M., 2014. Semi-Empirical Satellite Models. In Kleissl J. (ed.) Solar Energy Forecasting and Resource Assessment. Academic press.

[2] Cebecauer T., Šúri M., Perez R., High performance MSG satellite model for operational solar energy applications. ASES National Solar Conference, Phoenix, USA, 2010.

[3] Cebecauer T., Suri M., Gueymard C., Uncertainty sources in satellite-derived Direct Normal Irradiance: How can prediction accuracy be improved globally? Proceedings of the SolarPACES Conference, Granada, Spain, 20-23 Sept 2011.

[4] Šúri M., Cebecauer T., 2014. Satellite-based solar resource data: Model validation statistics versus user's uncertainty. ASES SOLAR 2014 Conference, San Francisco, 7-9 July 2014.

[5] Ineichen P., A broadband simplified version of the Solis clear sky model, 2008. Solar Energy, 82, 8, 758-762.

[6] Morcrette J., Boucher O., Jones L., Salmond D., Bechtold P., Beljaars A., Benedetti A., Bonet A., Kaiser J.W., Razinger M., Schulz M., Serrar S., Simmons A.J., Sofiev M., Suttie M., Tompkins A., Uncht A., GEMS-AER team, 2009. Aerosol analysis and forecast in the ECMWF Integrated Forecast System. Part I: Forward modelling. Journal of Geophysical Research, 114.

[7] Benedictow A. et al. 2012. Validation report of the MACC reanalysis of global atmospheric composition: Period 2003-2010, MACC-II Deliverable D_83.1.

[8] Cebecauer T., Šúri M., 2010. Accuracy improvements of satellite-derived solar resource based on GEMS re-analysis aerosols. Conference SolarPACES 2010, September 2010, Perpignan, France.

[9] Cebecauer T., Perez R., Suri M., Comparing performance of SolarGIS and SUNY satellite models using monthly and daily aerosol data. Proceedings of the ISES Solar World Congress 2011, 28 August – 2 September 2011, Kassel, Germany.

[10] Climate Forecast System Reanalysis (CSFR), NOAA. http://cfs.ncep.noaa.gov/cfsr/

[11] Global Forecast System (GFS), NOAA. http://www.emc.ncep.noaa.gov/index.php?branch=GFS

[12] Meteosat satellites MFG and MSG, EUMETSAT. http://www.eumetsat.int/website/home/Satellites/CurrentSatellites/Meteosat/index.html

[13] Hammer A., Heinemann D., Hoyer C., Kuhlemann R., Lorenz E., Müller R., Beyer H.G., 2003. Solar energy assessment using remote sensing technologies. Rem. Sens. Environ., 86, 423-432.

[14] Perez R., Ineichen P., Maxwell E., Seals R. and Zelenka A., 1992. Dynamic global-to-direct irradiance conversion models. ASHRAE Transactions-Research Series, pp. 354-369.

[15] Perez, R., Seals R., Ineichen P., Stewart R., Menicucci D., 1987. A new simplified version of the Perez diffuse irradiance model for tilted surfaces. Solar Energy, 39, 221-232.

[16] Ruiz-Arias J. A., Cebecauer T., Tovar-Pescador J., Šúri M., Spatial disaggregation of satellite-derived irradiance using a high-resolution digital elevation model. Solar Energy, 84, 1644-1657, 2010.

[17] AERONET: NASA Aerosol Robotic Network. http://aeronet.gsfc.nasa.gov/

[18] Cebecauer T., Šúri M., 2012. Correction of Satellite-Derived DNI Time Series Using Locally-Resolved Aerosol Data.. Proceedings of the SolarPACES Conference, Marrakech, Morocco, September 2012.

[19] WMO, 2008. Guide to Meteorological Instruments and Methods of Observation, 7th ed., Rapport WMO-No.8. http://www.wmo.int/pages/prog/gcos/documents/gruanmanuals/CIMO/CIMO_Guide-7th_Edition-2008.pdf

[20] ISO, 1990. Solar Energy — Specification and Classification of Instruments for Measuring Hemispherical Solar and Direct Solar Radiation. Standard ISO 9060:1990.

[21] NREL, 1993. User's Manual for SERI_QC Software-Assessing the Quality of Solar Radiation Data. NREL/TP-463-5608. Golden, CO: National Renewable Energy Laboratory.

[22] Geiger M., Diabaté L., Ménard L., Wald L., 2002. A web service for controlling the quality of measurements of global solar irradiation. Solar Energy, 73, 475-480.

[23] Long C.N., Dutton E.G., 2002. BSRN Global Network recommended QC tests, V2.0. Rapport technique BSRN. http://epic.awi.de/30083/1/BSRN_recommended_QC_tests_V2.pdf

[24] Long C.N., Shi Y., 2008. An automated quality assessment and control algorithm for surface radiation measurements. Open Atmos. Sci. J., 2, 23-37.

[25] Younes S., Claywell R. and Munner T, 2005. Quality control of solar radiation data: Present status and proposed new approaches. Solar Energy 30, 1533-1549.

[26] Rymes M.D., Myers D.R., 2001. Mean preserving algorithm for smoothly interpolating averaged data. Solar Energy, 71, 225-231.

[27] Lundström L., 2012. Weather data for building simulation: New actual weather files for North Europe combining observed weather and modeled solar radiation. Projet de Maîtrise, Mälardalen Univ., Suède. http://mdh.diva-portal.org/smash/get/diva2:574999/FULLTEXT01

[28] Cebecauer T., Suri M., 2014. Typical Meteorological Year data: SolarGIS approach. Energy Proceedia, International Conference on Concentrating Solar Power and Chemical Energy Systems, SolarPACES 2014, in press.

[29] CFSV2 model. http://www.nco.ncep.noaa.gov/pmb/products/CFSv2/

[30] The Weather Research & Forecasting Model, WRF. http://www.wrf-model.org/

[31] King D.L., Boyson W.E. and Kratochvil J.A., Photovoltaic array performance model, SAND2004-3535, Sandia National Laboratories, 2004.

[32] Huld T., Šúri M., Dunlop E.D., Geographical variation of the conversion efficiency of crystalline silicon photovoltaic modules in Europe. Progress in Photovoltaics: Research and Applications, 16, 595-607, 2008.

[33] Huld T., Gottschalg R., Beyer H. G., Topic M., Mapping the performance of PV modules, effects of module type and data averaging, Solar Energy, 84, 2, 324-338, 2010.

[34] Huld T., Friesen G., Skoczek A., Kenny R.P., Sample T., Field M., Dunlop E.D., 2011. A power-rating model for crystalline silicon PV modules. Solar Energy Materials and Solar Cells, 95, 12, 3359-3369.

[35] Skoczek A., Sample T., Dunlop E. D., The results of performance measurements of field-aged crystalline silicon photovoltaic modules, Progress in Photovoltaics: Research and Applications, 17, 227-240, 2009.

[36] Martin N., Ruiz J.M. Calculation of the PV modules angular losses under field conditions by means of an analytical model. Solar Energy Material and Solar Cells, 70, 25–38, 2001.

[37] The German Energy Society, 2008: Planning and Installing Photovoltaic Systems. A guide for installers, architects and engineers. Second edition. Earthscan, London, Sterling VA.

[38] Šúri M., Cebecauer T., Skoczek A., 2011. SolarGIS: Solar Data And Online Applications For PV Planning And Performance Assessment. 26th European Photovoltaics Solar Energy Conference, September 2011, Hamburg, Germany.

[39] Lohmann S., Schillings C., Mayer B., Meyer R., 2006. Longterm variability of solar direct and global radiation derived from ISCCP data and comparison with reanalysis data, Solar Energy, 80, 11, 1390-1401.

[40] Gueymard C., Solar resource e assessment for CSP and CPV. Leonardo Energy webinar, 2010. http://www.leonardo-energy.org/webfm_send/4601

16 ABOUT GEOMODEL SOLAR

Primary business of GeoModel Solar is in providing support to the site qualification, planning, financing and operation of solar energy systems. We are committed to increase efficiency and reliability of solar technology by expert consultancy and access to our databases and customer-oriented services.

The Company builds on 25 years of expertise in geoinformatics and environmental modelling, and 14 years in solar energy and photovoltaics. We strive for development and operation of new generation high-resolution quality-assessed global databases with focus on solar resource and energy-related weather parameters. We are developing simulation, management and control tools, map products, and services for fast access to high quality information needed for system planning, performance assessment, forecasting and management of distributed power generation.

Members of the team have long-term experience in R&D and are active in the activities of International Energy Agency, Solar Heating and Cooling Program, Task 46 Solar Resource Assessment and Forecasting.

GeoModel Solar operates a set of online services, integrated within SolarGIS® information system, which includes data, maps, software, and geoinformation services for solar energy.

http://geomodelsolar.eu http://solargis.info

ISO 9001
LL-C (Certification)

GeoModel Solar is ISO 9001:2008 certified company for quality management.